

**Simulation Techniques for Thermal Storage Coupled to
Cogeneration/Trigenaration Systems.**

BY

LUCA ROMANO

B.S., Polytechnic of Milan, Milan, Italy, 2016

THESIS

Submitted as partial fulfillment of the requirements
for the degree of Master of Science in Mechanical Engineering
in the Graduate College of the
University of Illinois at Chicago, 2018

Chicago, Illinois

Defense Committee:

William A. Ryan, Chair and Advisor

Michael J. Scott

Marco C. Masoero, Polytechnic of Turin

ACKNOWLEDGMENTS

Firstly, I would like to thank Prof. William A. Ryan for the support and guidance provided during the development of this thesis.

I would also like to extend my appreciation to Prof. Marco C. Masoero for the assistance given and the professionalism which characterizes him.

A personal thanks goes to Mrs. Lynn Thomas, for the daily effort and patience shown in the course of my exchange program.

Most importantly I must express my gratitude to my mother Michela and my father Daniele, always by my side ready to support me. A special thought goes to my little sister Caterina for her constant inspiration and goodness of hearth.

Finally, I would like to thank my friends for making my stay in Chicago much more pleasurable. The warmth that everybody has shown has made up for all the cold winter days.

LR

TABLE OF CONTENTS

<u>CHAPTER</u>		<u>PAGE</u>
1	THE HOSPITAL	1
1.1	The Standard Adopted	2
1.2	The Base Model	3
1.3	Energy Consumption Profiles	7
1.3.1	Electric Consumption	10
1.3.2	Thermal Consumption	12
1.3.3	Fuel Consumption	17
2	THE GAS TURBINE	20
2.1	Cycle and Characteristic	21
2.2	Partial Load Operations	26
2.3	Modeling the Turbine in eQuest [®]	28
2.3.1	Partial Load Ratio over Heat Input Ratio	29
2.3.2	External Air Temperature over Capacity	34
3	THE COMBINED HEAT AND POWER PLANT	38
3.1	Overview of the Technology	38
3.1.1	Energy Fluxes Involved in the Process	41
3.1.2	Operating Strategy of the Plant	43
3.2	Modeling a CHP System in eQuest [®]	46
3.3	Thermal and Electrical Analysis	49
3.4	Efficiency Analysis	54
3.4.1	Total CHP System Efficiency	55
3.4.2	FERC Efficiency Standard	56
3.4.3	Percentage Reduction in Source Energy Consumption	57
3.4.4	Performance of the CHP System	61
4	THE COMBINED COOLING, HEATING AND POWER PLANT.	64
4.1	The Absorption Chiller	65
4.2	Modeling the Absorption chiller in eQuest [®]	70
4.2.1	Influence of the Chilled Water Temperature	71
4.2.2	Influence of the Condenser Temperature	77
4.2.3	Partial Load Performance	81
4.3	Layout of the Plant	83
4.4	Sizing of the Plant	86
4.5	Improvements in Source Energy Consumption	89
4.6	Efficiency Analysis	93

TABLE OF CONTENTS (continued)

<u>CHAPTER</u>		<u>PAGE</u>
5	THE THERMAL ENERGY STORAGE	98
5.1	Benefits of TES	99
5.2	Basic Principle of TES	100
5.3	Evaluation Process	102
5.3.1	Technical Criteria	103
5.3.2	Energetic Criteria	103
5.3.3	Sizing Criteria	104
5.3.4	Economic Criteria	104
5.4	Coupling TES to the CHP system	105
5.4.1	Thermal Losses	109
5.4.2	Supply and Demand Mismatch	117
5.4.3	Sizing of the TES	124
5.4.4	Benefits to the CHP System	130
5.5	Coupling TES to the CCHP system	134
5.5.1	Supply and Demand Mismatch	135
5.5.2	Sizing of the TES	141
5.5.3	Benefits to the CCHP System	143
6	CONCLUSIONS	147
	APPENDICES	154
	Appendix A	155
	Appendix B	160
	Appendix C	163
	Appendix D	165
	CITED LITERATURE	166
	VITA	169

LIST OF TABLES

<u>TABLE</u>		<u>PAGE</u>
I	MAIN PARAMETERS IN THE HOSPITAL LAYOUT.	4
II	ENERGY CONSUMPTION FOR THE <i>BASE MODEL</i> PROTO- TYPE HOSPITAL.	9
III	SUMMARY OF INSTALLED CHP SITES AND CAPACITY BY PRIME MOVER IN THE U.S.	39
IV	MONTHLY ELECTRIC PRODUCTION [MWH] OF A CHP PLANT BY INSTALLED TURBINE SIZE.	50
V	PERFORMANCE OF THE CHP BY INSTALLED TURBINE SIZE	61
VI	HOURS AT FULL LOAD OF DIFFERENT GAS TURBINE SIZE.	63
VII	INSTALLED ABSORPTION CHILLER SIZES.	90
VIII	REDUCTION IN ELECTRIC PEAK DEMAND: COMPARISON BETWEEN A CHP AND A CCHP SYSTEM.	90
IX	VARIATION IN ELECTRICITY CONSUMPTION [MWH]: COM- PARISON BETWEEN A CHP AND A CCHP SYSTEM.	91
X	VARIATION IN FUEL CONSUMPTION [MBTU]: COMPARI- SON BETWEEN A CHP AND A CCHP SYSTEM.	93
XI	PERFORMANCE OF THE CCHP BY INSTALLED TURBINE SIZE.	96
XII	THERMAL CAPACITIES AT 68 °F OF SOME COMMON TES MATERIALS.	107
XIII	DIFFERENT SIZES OF TES MODELS.	108
XIV	THERMAL CONDUCTIVITY OF DIFFERENT MATERIALS.	110
XV	HEAT LOSS COEFFICIENTS FOR DIFFERENT TES MODELS.	117
XVI	RELATIONSHIP BETWEEN CONSUMPTION AND SUPPLY FOR HEATING AND ELECTRICITY WORKING CONDITIONS.	121
XVII	VALUES OF DM AND ESTIMATED PRSEC FOR DIFFERENT SIZES OF CHP SYTEMS INTEGRATED WITH AND IDEAL TES FACILITY.	123
XVIII	FIRST STEP OPTIMIZATION PROCESS, OPTIMAL ENGINE SIZE FOR A <i>MODEL 3</i> TES FACILITY IN A CHP FACILITY. . .	126
XIX	SECOND STEP OPTIMIZATION PROCESS, OPTIMAL TES SIZE FOR A 700 KW GAS TURBINE IN A CHP FACILITY. . . .	127
XX	SECOND STEP OPTIMIZATION PROCESS, TES EFFICIENCY VALUES FOR A 700 KW GAS TURBINE IN A CHP FACILITY.	128
XXI	THIRD STEP OPTIMIZATION PROCESS, OPTIMAL ENGINE SIZE FOR A <i>MODEL 2</i> TES FACILITY IN A CHP FACILITY. . .	129
XXII	COMPARISON OF CHP OVER TES-CHP IN TERMS OF EF- FICIENCIES AND ENERGY CONSUMPTION.	131

LIST OF TABLES (continued)

<u>TABLE</u>		<u>PAGE</u>
XXIII	INSTALLED ABSORPTION CHILLER SIZES FOR THE CCHP PLANT WITH DIFFERENT TES CAPACITY.	135
XXIV	RELATIONSHIP BETWEEN CONSUMPTION AND SUPPLY FOR HEATING, COOLING AND ELECTRICITY WORKING CONDITIONS.	137
XXV	VALUES OF DM AND ESTIMATED PRSEC FOR DIFFERENT SIZES OF CCHP SYTEMS INTEGRATED WITH AND IDEAL TES FACILITY.	140
XXVI	FIRST STEP OPTIMIZATION PROCESS, OPTIMAL ENGINE SIZE FOR A <i>MODEL 3</i> TES FACILITY IN A CCHP SYSTEM. .	142
XXVII	SECOND STEP OPTIMIZATION PROCESS, OPTIMAL TES SIZE FOR A 900 KW GAS TURBINE IN A CCHP SYSTEM. . .	142
XXVIII	THIRD STEP OPTIMIZATION PROCESS, OPTIMAL ENGINE SIZE FOR A <i>MODEL 5</i> TES FACILITY IN A CCHP SYSTEM. .	142
XXIX	COMPARISON OF CCHP OVER TES-CCHP IN TERMS OF PERFORMANCE AND ENERGY CONSUMPTION.	144
XXX	COMPARISON OF THE PERFORMANCE IN THE FOUR DIFFERENT OPTIMAL LAYOUTS.	153

LIST OF FIGURES

<u>FIGURE</u>		<u>PAGE</u>
1	3D rendering of the prototype hospital.	5
2	Layout of the VAV HVAC system for the <i>base model</i>	6
3	Layout of the <i>base model</i> plant.	8
4	Annual electric consumption - <i>base model</i>	10
5	Monthly electric consumption - <i>base model</i>	11
6	Electric duration curve - <i>base model</i>	12
7	Annual thermal consumption (heat) - <i>base model</i>	13
8	Monthly thermal consumption (heat) - <i>base model</i>	14
9	Thermal duration curve (heat) - <i>base model</i>	15
10	Annual thermal consumption (cold) - <i>base model</i>	16
11	Monthly thermal consumption (cold) - <i>base model</i>	16
12	Annual fuel consumption - <i>base model</i>	18
13	Monthly fuel consumption - <i>base model</i>	19
14	Joule-Bryton thermodynamic cycle.	22
15	Gas turbine layout.	23
16	Gas turbine performance - Percentage increase in CO emission vs Partial Load Ratio.	28
17	Gas turbine performance - Efficiency vs. Partial Load Ratio - SOLAR model.	31
18	Gas turbine performance - Heat Input Ratio vs. Partial Load Ratio - comparison between SOLAR model and eQuest model.	33
19	Gas turbine performance - Capacity vs. External Air Temperature - comparison between SOLAR model and eQuest model.	36
20	Scheme of a CHP system and overall efficiency.	40
21	Energy fluxes involved in the CHP system.	42
22	CHP growth in the U.S. Hospitals.	44
23	eQuest [®] layout of the CHP plant.	47
24	Monthly electricity production of a 700 kW CHP plant.	50
25	Monthly electricity production of a 1300 kW CHP plant.	51
26	Comparison of turbine's fuel consumption between a 700 kW and a 1300 kW CHP layout.	52
27	Amount of <i>Recovered Heat</i> and <i>Wasted Recovered Heat</i> of a 700 kW CHP plant.	53
28	Amount of <i>Recovered Heat</i> and <i>Wasted Recovered Heat</i> of a 1300 kW CHP plant.	54
29	Absorption chiller layout.	67
30	Absorption chiller performance - Capacity Percentage vs Chilled Wa- ter Temperature - comparison between YORK model and eQuest model.	72

LIST OF FIGURES (continued)

<u>FIGURE</u>		<u>PAGE</u>
31	Absorption chiller performance - Fuel Consumption vs Chilled Water Temperature - YORK model.	74
32	Absorption chiller performance - COP Percentage vs Chilled Water Temperature - comparison between YORK model and eQuest model.	75
33	Absorption chiller performance - COP vs Chilled Water Temperature - comparison between YORK model and eQuest model.	76
34	Absorption chiller performance - COP Percentage vs Condenser Temperature - YORK model.	78
35	Absorption chiller performance - COP vs Condenser Temperature - comparison between YORK model and eQuest model.	80
36	Absorption chiller performance - Capacity Percentage vs Condenser Temperature - YORK model.	81
37	Absorption chiller performance - COP vs Partial Load Ratio - comparison between YORK model and eQuest model.	82
38	eQuest [®] layout of the CCHP plant.	84
39	CCHP system working scheme.	86
40	Thermal energy consumption of the hospital - <i>base model</i>	87
41	Efficiency loss due to the improper management of the absorption chiller.	88
42	Charging, storage, discharging phases in a general TES system.	102
43	Temperature and heat flow during conductive heat transfer.	109
44	Temperature and velocity near a surface during convective heat transfer.	112
45	Surface of the TES affected by conductive and convective heat transfer.	114
46	Trend of the PRSEC in function of the DM for a CHP system adopting FEL strategy.	122
47	Comparison of the amount of <i>Recovered Heat</i> between CHP and TES-CHP system, both with a 700 kW turbine.	132
48	Comparison of boiler fuel consumption between CHP and TES-CHP system, both with a 700 kW turbine.	133
49	Trend of the PRSEC in function of the DM and r for a CCHP system adopting FEL strategy.	138
50	Influence of TES volume over percentage of <i>Recovered Heat</i> for different CHP sizes.	148
51	Influence of TES volume over PRSEC for different CHP sizes.	149
52	Influence of TES volume over percentage of <i>Recovered Heat</i> for different CCHP sizes.	151
53	Influence of TES volume over PRSEC for different CCHP sizes.	152

LIST OF ABBREVIATIONS

eQuest	Quick Energy Simulation Tool
ASHRAE	American Society of Heating, Refrigerating, and Air-Conditioning Engineers
PRSEC	Percentage Reduction in Source Energy Consump- tion
CI	Critical Infrastructure
DOE	U.S. Department of Energy
NREL	National Renewable Energy Laboratory
MOB	Medical Office Building
HVAC	Heating, Ventilation, and Air Conditioning
VAV	Variable Air Volume
CHP	Combined Heat and Power
CCHP	Combined Cooling, Heating, and Power
CCGT	Combined Cycle Gas Turbine
PLR	Partial Load Ratio
HIR	Heat Input Ratio
ISO	International Organization for Standards

LIST OF ABBREVIATIONS (continued)

TES	Thermal Energy Storage
WHRS	Waste Heat Recovery System
HRSG	Heat Recovery Steam Generator
EPA	U.S. Environmental Protection Agency
WRH	Wasted Recoverable Heat
FTL	Following Thermal Load
FEL	Following Electrical Load
HPR	Heat to Power Ratio
RFCW	Reliability First Corporation/West
GHG	Green House Gasses
CAP	Criteria Air Pollutant
FERC	Federal Energy Regulatory Commission
ANSI	American National Standard Institute
ARI	Air Conditioning and Refrigeration Institute
NGCC	Natural Gas Combined Cycle
COP	Coefficient Of Performance
CWT	Chilled Water Temperature
DM	Degree of Mismatch
DM_{CRI}	Critical Degree of Mismatch

SUMMARY

The objective of this thesis is to study and compare different plant layouts for the fulfillment of the energy needs of an hospital facility located in Chicago, IL. A cogeneration and a trigeneration plant, driven by a gas turbine, were modeled and analyzed using a simulation software called eQuest[®] (QUick Energy Simulation Tool). In particular, the benefits of the introduction of a hot thermal storage system was evaluated and discussed.

Partial improvements to the ASHRAE Standard 90.1-2004 ([6] [7]) prototype hospital model were introduced in order to guarantee the achievement of the required design conditions, enabling every section of the structure to reach the intended temperature.

An upgrade of the eQuest[®] model describing the gas turbine was introduced. In particular, the new model brought an improvement in the efficiency of the equipment at partial load conditions. Various turbine sizes were studied (from 600 kW to 1,300 kW) in terms of energy output and wasted products. Among various performance parameters, the percentage reduction in source energy consumption (PRSEC) was considered for the optimal sizing of the plant, since it was the one better describing the overall performance of the system. In the cogeneration system, the highest value of PRSEC reached 19.0%, resulted from the operation of a 700 kW turbine. This system enabled a better utilization of the source energy compared to a traditional separated generation system, in particular, it permitted a reduction in the boiler's fuel consumption due to the exploitation of the heat coming from the exhaust gasses of the turbine.

Moreover a trigeneration plant was analyzed. In this second case, like in the previous, the

SUMMARY (continued)

heating needs of the hospital were satisfied by the recovery of the heat coming from the prime mover, in addition the cooling loads were partially fulfilled by an absorption chiller driven by the exhaust gasses of the turbine. To guarantee the best accuracy of the results, an improvement in the absorption chiller model was implemented starting from the technical sheet of the *Millennium YIA*TM, manufactured by *YORK*[®] [4] [18] [19]. The same turbine sizes considered in the cogeneration plant were investigated. It emerged that a 800 kW gas turbine was able to reach the highest value of PRSEC of 22.7%. Major improvements in the performance resulted in a lower electricity consumption and electricity peak demand. Furthermore, especially during warmer months, the introduction of the absorption chiller guaranteed a better usage of the waste heat deriving from the turbine.

To conclude the analysis, the effects of the introduction of a hot thermal storage were evaluated in both types of plant's layouts. A fully mixed water tank model was created and implemented in eQuest[®] starting from the information provided by *Advance Tank, Co.* [29]. Various capacities were studied ranging from 11,800 gal to 53,000 gal. For both types of plant a feasibility study and an optimal sizing procedure was elaborated.

In the cogeneration system, a 14,000 gal tank paired to a 700 kW turbine enabled to reach a value of PRSEC of 20.3%, resulting in an improvement of 1.3% compared to the case of a cogeneration plant without storage. The major benefit introduced by the use of the tank resulted in lower boiler's fuel consumption due to an increment of the recovered heat used for heating purposes.

Much more evident were the benefits brought by the thermal storage in the case of a tri-

SUMMARY (continued)

generation layout. In fact, it resulted in an increase of the size of the prime mover compared to the original layout (from 800 kW to 900 kW). In particular, a reduction in overall electricity consumption and total fuel consumption was observed. These benefits must be attributed to a higher availability of recovered heat, which also resulted in a more extensive use of the absorption chiller. A 39,500 gal tank coupled to a 900 kW turbine allowed to have a 25.1% PRSEC, 2.4% higher than a 800 kW trigeneration plant.

CHAPTER 1

THE HOSPITAL

This thesis presents several technological solutions in order to satisfy the energy loads of a health care facility located in Chicago, IL.

Fours different solutions are analyzed and compared:

- Cogeneration system;
- Trigeneration system;
- Cogeneration system with a thermal energy storage option;
- Trigeneration system with a thermal energy storage option.

Every system is compared to the *base model* of the hospital, in order to understand its advantages in terms of efficiency and overall energy consumption. In this initial chapter, the definition of the *base model* will be given, together with the profile of the energy load requested by the facility.

Hospitals, unlike other commercial buildings, are characterized by a continuous request of electrical and thermal energy: 7 days a week, 24 hours a day. This, together with the relatively high and prolonged loads, makes their energy consumption 2.5 times higher than average commercial building of the same size [1].

Furthermore, health care facilities are classified as Critical Infrastructure (CI). The CI are those networks, assets and facilities which, if not properly operated, could result in a dramatic

negative impact on the national security, economic or public health safety [2]. This means that the uninterrupted supply of electricity assumes vital importance in order to prevent the occurrence of tragic scenarios.

Engineers during the past years have worked to find alternative and more reliable solutions compared to the purchase of the electricity from the grid. Hence, the development of *on-site* power production has experienced substantial improvements. Cogeneration and trigeneration systems have become more trustworthy and efficient, thanks to the adoption of newer technologies (fuel-cells [3], absorption chillers [4], microturbine and organic rankine cycles [5]).

1.1 The Standard Adopted

The analysis of the health care facility has been conducted through the use of eQuest[®], a simulation software developed by the U.S. Department of Energy (DOE). The model prototype for the hospital is the result of the implementation on eQuest[®] of the design addressed by the National Renewable Energy Laboratory (NREL). This model has already been validated in previous works, and has undergone further improvements [4].

The guidelines for the definition of the prototype hospital are the result of DOE support to the development of commercial building energy codes and standards. The Commercial Buildings Group at NREL developed the model of the hospital and its technical support document under the direction of the U.S. Department of Energy Building Technologies Program. The study was meant to document the analysis performed and the resulting design guidance that will enable to achieve energy savings of 50% over ASHRAE Standard 90.1-2004. This report also documents in detail the modeling methods used to demonstrate that the design recommendations meet or

exceed the 50% energy savings goal [6].

ASHRAE Standard 90.1 (Energy Standard for Buildings Except Low-Rise Residential Buildings) is a US standard providing the minimum accepted requirements for the design of energy efficient buildings. The analyzed building categories cover a wide range of buildings typologies although there are some exemption, such as the low-rise residential buildings[7].

Starting from the ASHRAE Standard 90.1 and NREL data, the implementation of the hospital model on eQuest[®] has been possible [6] [7].

The information for the correct simulation of the prototype facility include:

- Building internal layout description;
- Building shell description;
- Internal loads;
- Occupation and equipment schedules;
- Lighting schedules;
- Heating, ventilating and air conditioning information;
- Service water heating.

This prototype will be referred as the *base model* throughout the development of this study.

1.2 The Base Model

The *base model* has a total surface of 527,000 ft^2 (49,000 m^2). This surface is divided in two main buildings: the hospital space (427,000 ft^2 divided into seven stories) and the medical office building (MOB) (100,000 ft^2 divided into five stories). A 3D rendering of the hospital

TABLE I: MAIN PARAMETERS IN THE HOSPITAL LAYOUT.

Parameter	Value	
Total Area	527,000 <i>ft</i> ²	48,960 <i>m</i> ²
Hospital Space Area	427,000 <i>ft</i> ²	39,670 <i>m</i> ²
MOB Floor Area	100,000 <i>ft</i> ²	9,290 <i>m</i> ²
Floor-to-Floor Height	10.00 <i>ft</i>	3.05 <i>m</i>
Number of Floors - Hospital	7	
Number of Floors - MOB	5	

is illustrated in Figure 1. Table I summarizes the major parameters of the hospital's layout.

The facility is located in Chicago, IL. The climate zone has been defined as 6A by ASHRAE 169-2006 (cold-humid climate) [8].

No standard information regarding the fenestration area was found, so a 40% fraction of fenestration to gross wall area is assumed.

The frame of the prototype's structure is made of steel, with an arrangement of the roof with insulation above deck. All the spaces of the facility are considered to operate with the same schedule:

- Hospital space 24/7;
- Medical office building from 7:00 am to 5:00 pm;
- Extended hours from 5:00 am to midnight.

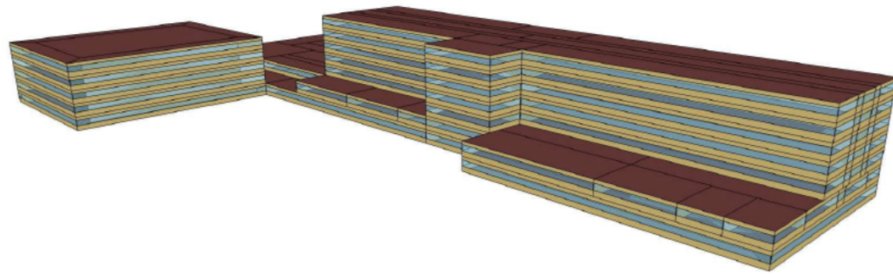


Figure 1: 3D rendering of the prototype hospital.

Each room and space has its specific occupancy.

Base model heating, ventilation, and air conditioning (HVAC) equipment consists of central air handling units, chillers, boilers, chilled and hot water air handling unit coils and terminal units with hot water reheat coils, as shown in Figure 2. This configuration is specific for the *base model*, the introduction of alternative technologies (e.g. cogeneration, trigeneration, thermal storage) will be discussed in future chapters. Improvements to the prototype hospital were introduced in previous works in order to fix some discrepancies between the data provided by the thermostats in each space and their actual design temperature [4]. This issue derived from the interaction of the thermal load with some default parameters in the eQuest[®] HVAC system properties. In order to identify the areas affected by the temperature mismatch the structure was divided in 9 *spaces*, characterized by the same conditions and managed by the same HVAC system. The different spaces are listed as follows:

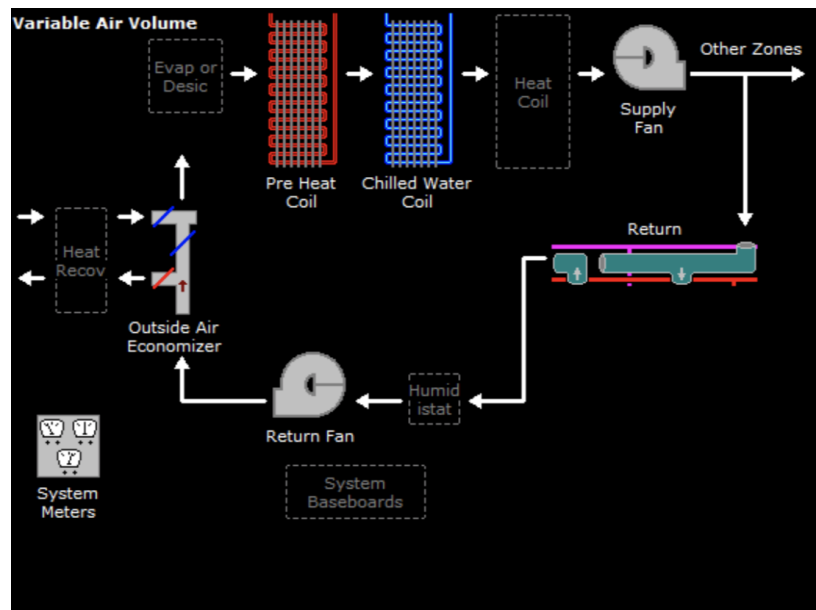


Figure 2: Layout of the VAV HVAC system for the *base model*.

- MOB - Medical office building, five stories building;
- PT - Patient Tower, five stories (from third to seventh floor);
- BLD3 - Building 3, two stories;
- BLD4 - Building 4, two stories;
- BLD5 - Building 5, one story;
- BLD6 - Building 6, two stories;
- BLD7 - Building 7, three stories;
- BLD8 - Building 8, one story;

- BLD9 - Building 9, two stories (located below the PT).

The problem was easily solved by the introduction of the following upgrades:

- **Introduction of pre-heat coils:** in each of the variable air volume (VAV) HVAC systems, pre-heat coils have been manually implemented. This allowed the proper operation of the system especially in winter months, when the temperature of the air may drop below the freezing point of water causing damages to the cold deck coils;
- **Increase of the *Reheat Delta T* of the coils re-heat coils:** to satisfy the requirement about the inlet temperature of the supply air, the *Reheat Delta T* has been increased from 30 °F to 50 °F[9]. This parameter represents the maximum increase in temperature for supply air passing through the reheat coils;
- **Increment of the sizing ratio:** this parameter represents a multiplier of the program-calculated values of air flow rate and coil size. This value has been modified from 1 to 1.15, resulting in an oversizing of 15% of the entire system. This final improvement was applied only to those spaces that still had issues with the reaching of the proper design conditions (PT, MOB, BLD4, BLD6, BLD7, and BLD9).

Thanks to these major improvements, the temperature in every space resulted equal to the design one.

1.3 Energy Consumption Profiles

The layout of the *base model* plant is shown in Figure 3.

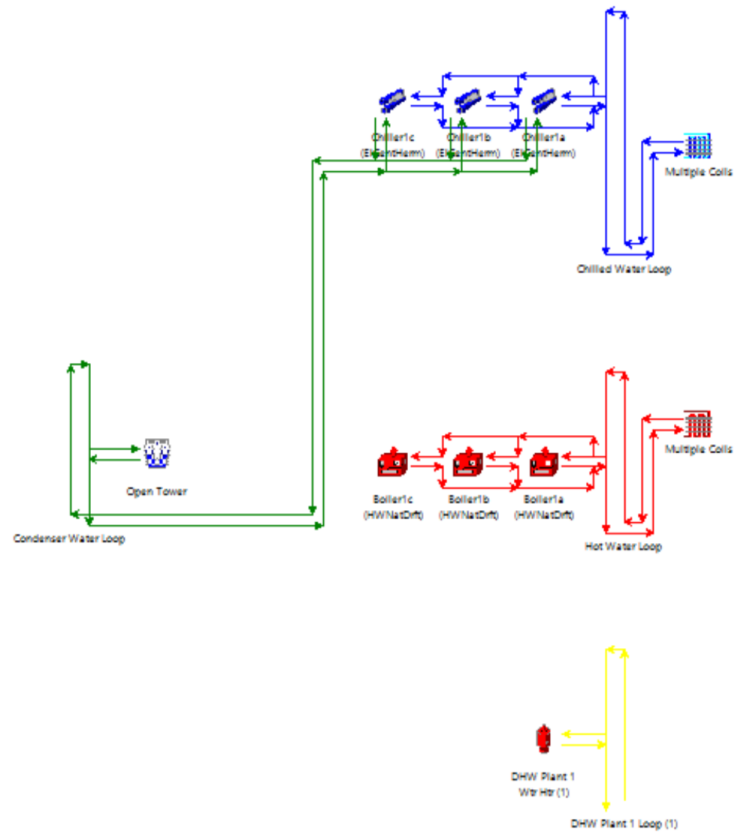


Figure 3: Layout of the *base model* plant.

Three gas driven boilers are connected to the *Space Heating Hot Water loop* in order to fulfill the space heating request of the facility. The *Domestic Hot Water loop* is connected to a water heater, which is also driven by natural gas. On the other hand, the *Chilled Water loop*, accountable for the cooling loads requested by the hospital, is driven by three electric chillers.

Hence, the need of a *Condenser Water loop*, to properly operate the electric chillers.

No power generator is modeled in the *base model* layout, therefore the electricity is withdrawn directly from the grid. Furthermore, the thermal load is satisfied by the combustion of natural gas.

The study of the consumption profiles has been accomplished through a detailed simulation with eQuest[®]. The outputs were given on hourly, monthly or annual basis. The post processing was of fundamental importance in order to understand the *base model's* energy profiles and compare them with the alternative systems developed in this thesis. A summary of the energy consumption of the hospital is given in Table II.

TABLE II: ENERGY CONSUMPTION FOR THE *BASE MODEL* PROTOTYPE HOSPITAL.

Period	Electric Consumption [MWh]	Thermal Consumption (Heat) [MBTU]	Thermal Consumption (Cold) [MBTU]	Fuel Consumption [MBTU]
January	774.5	6,105.1	117.1	7,402.5
February	699.8	5,401.5	115.4	6,521.2
March	775.3	4,813.7	119.8	5,812.3
April	773.4	3,069.0	198.3	3,634.8
May	860.3	2,101.4	1,550.4	2,708.1
June	916.1	1,791.8	2,967.6	2,157.7
July	1,016.7	1,799.6	4,002.6	2,232.4
August	1,014.0	1,758.3	3,956.8	2,227.1
September	861.3	1,746.2	2,011.2	2,223.9
October	808.4	2,183.5	417.8	2,877.5
November	740.8	3,382.9	116.2	4,609.8
December	774.6	5,670.6	118.5	6,960.3
ANNUAL	10,015.2	39,823.6	15,691.7	49,367.6

1.3.1 Electric Consumption

The annual electric consumption on hourly bases is depicted in Figure 4.

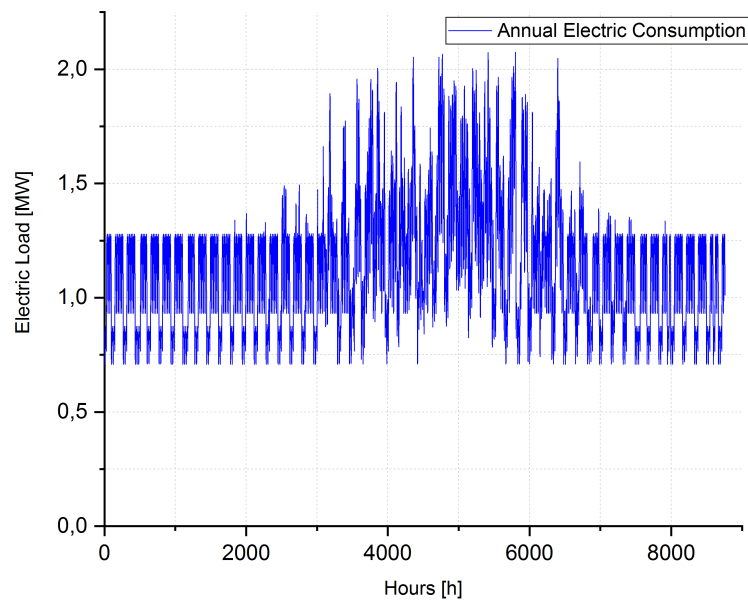


Figure 4: Annual electric consumption - *base model*.

It is possible to observe that, beside the daily fluctuation due to the occupancy of the structure and the recurring usage of electric equipment, the electric consumption profile during warmer months is significantly higher. This is caused by an increase of the cooling loads required

by the facility, which relies on electric chillers. For a better perception of the monthly value of electric consumption, Figure 5 was generated.

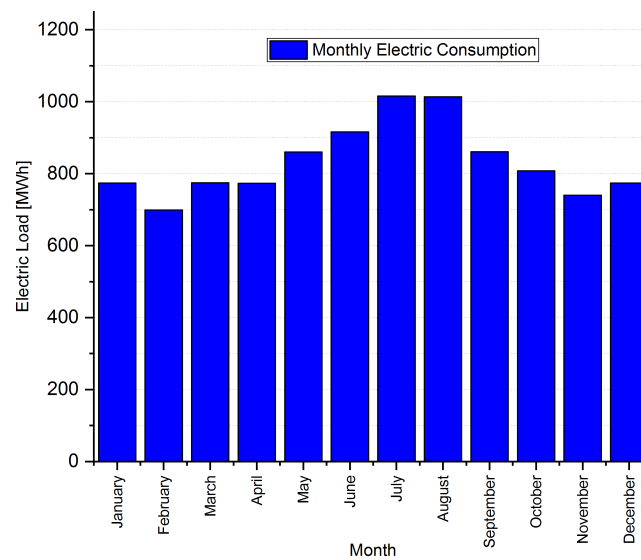


Figure 5: Monthly electric consumption - *base model*.

Furthermore, a load duration curve was represented in Figure 6. This type of curve is necessary to establish the magnitude of the peak load (2.0745 MW) and the number of hours during which a certain load persists. It is particularly useful in the sizing of the generator: the higher its capacity, the higher will be the number of hours it will work in partial load conditions.

On the opposite, the lower its capacity, the greater will be the number of hours it will work in full load conditions.

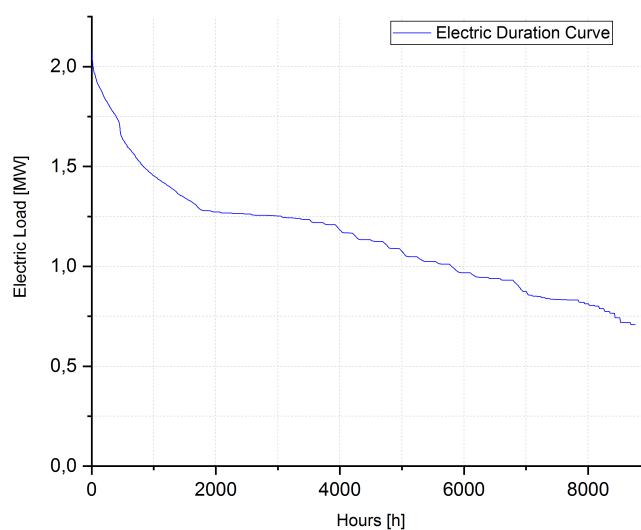


Figure 6: Electric duration curve - *base model*.

1.3.2 Thermal Consumption

The heating thermal consumption of the health care facility is comprehensive of the hot water requested by the *Domestic Hot Water loop* and by the *Space Heating loop*. The annual profile is presented in Figure 7.

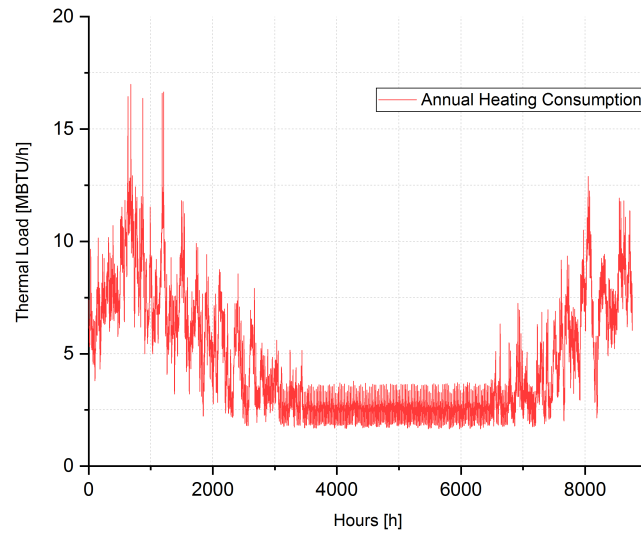


Figure 7: Annual thermal consumption (heat) - *base model*.

It is noted that this profile presents the opposite trend compared to the annual electric profile. The reason is the same as in the previous case. Obviously, the hot thermal consumption reaches its maximum during colder months, in which the heating system works at full load in order to satisfy the needs of the facility.

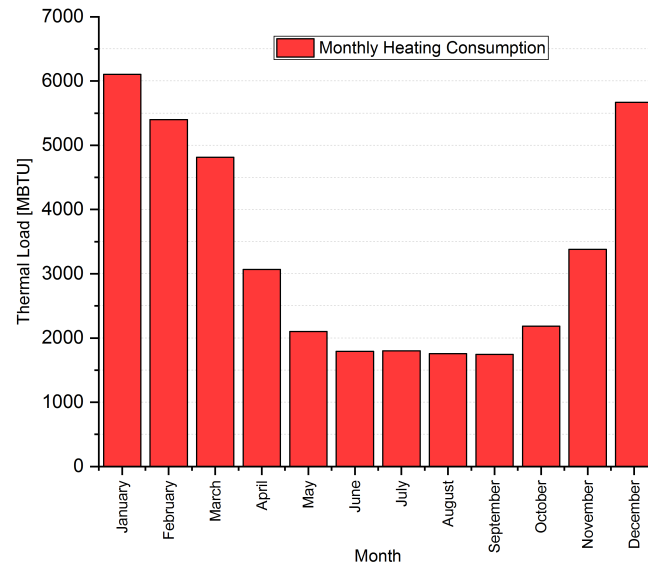


Figure 8: Monthly thermal consumption (heat) - *base model*.

The monthly heating thermal loads are illustrated in Figure 8. Moreover, the thermal duration curve is shown in Figure 9.

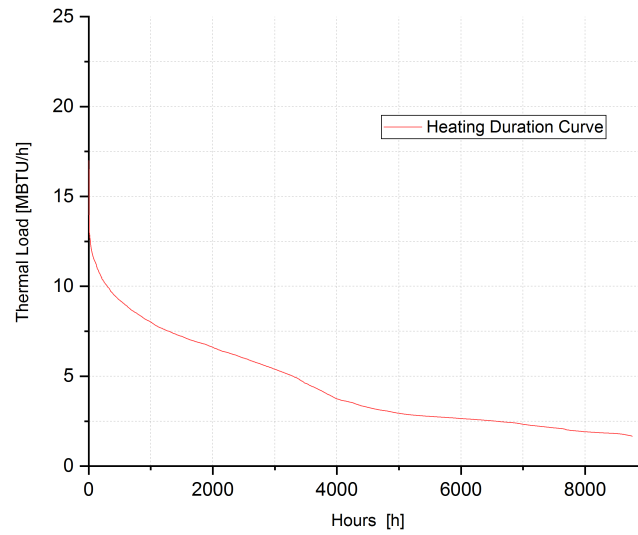


Figure 9: Thermal duration curve (heat) - *base model*.

Looking at the annual cooling consumption (Figure 10) and at its monthly trend (Figure 11) it is possible to understand the electric load profile.

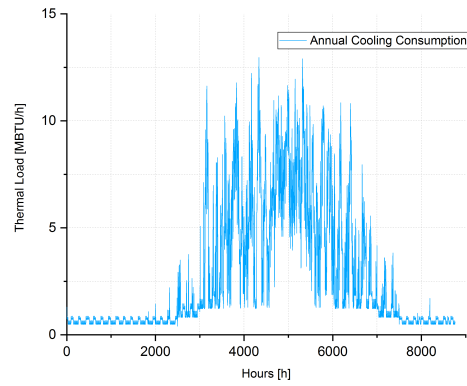


Figure 10: Annual thermal consumption (cold) - *base model*.

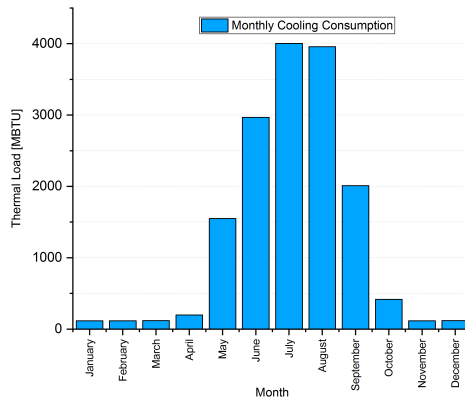


Figure 11: Monthly thermal consumption (cold) - *base model*.

1.3.3 Fuel Consumption

The analysis of the thermal load of the hospital has been addressed by a complementary study of the fuel consumption. The main reason is that the amount of fuel burned, rather than the heat request, takes into account the efficiency of the conversion system (e. g. gas boilers). Furthermore, the fuel consumption takes into account the expenditure of other miscellaneous equipment (e. g. laundry, kitchen) in addition to the hot water requested for space heating and domestic use.

Therefore, the fuel consumption is affected not only by the request of heat, but also by the efficiency of the equipment adopted in order to satisfy that demand.

This characteristic is of primary importance if comparing two diverse technical solutions, with different component's efficiencies.

In Figure 12 it is shown the annual fuel consumption.

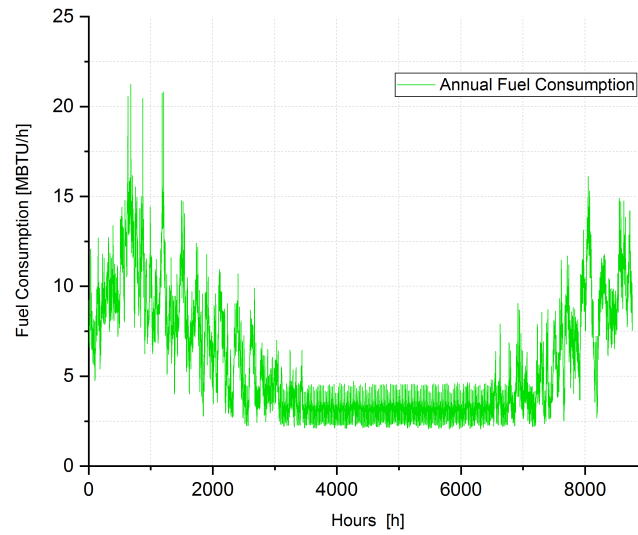


Figure 12: Annual fuel consumption - *base model*.

Certainly the fuel consumption assumes the same profile as the thermal load. The monthly fuel consumption is represented in Figure 13.

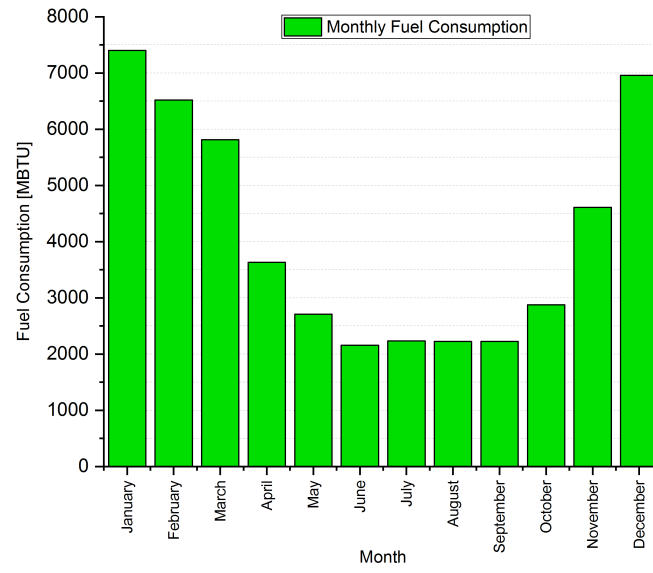


Figure 13: Monthly fuel consumption - *base model*.

CHAPTER 2

THE GAS TURBINE

The gas turbine is a rotary mechanical device which produces mechanical energy through the internal combustion of fuel. A detailed explanation of the working principle and performance of this devices has been provided in this chapter. Furthermore, an improved eQuest[®] model was elaborated starting from the study of currently available gas turbines.

This kind of technology has numerous applications, although the one analyzed in this work refers to the production of electricity, in which the mechanical output produced by the turbine is used by an electric generator.

In the past decades the employment of this technology in the power production industry has drastically increased. Currently, the sizes available on the market range from 500 kW to more than 300 MW. Smaller sizes can be found down to 25 kW, but they are referred to as micro turbines [13].

Gas turbines can be used in different layouts: only-electricity production solutions, or more complex generation plants in which the waste product can be successfully recovered in order to satisfy other needs of the facility beside the electric one, or to produce extra power. Example can be found in cogeneration systems, trigeneration systems, or combined cycle plants.

This diverse layouts will not affect the working principle of the gas turbine, which will remain the same. In particular, cogeneration and trigeneration plants include an heat recovery system in order to exploit the thermal energy of the exhaust gases produced by the turbine. If

the plant is capable of directly producing heat together with electric power it will be referred as combined heat and power (CHP), if it is also able to produce cold thermal energy it will be referred as combined cooling heating and power (CCHP). A detailed explanation of these technologies has been provided in Chapter 3 and Chapter 4, respectively.

On the other hand, the Combined Cycle Gas Turbines (CCGT) route the waste heat from the gas turbine into a steam turbine to produce extra electric power. This configuration has allowed this technology to reach electrical efficiencies of around 60%, much higher compared to the ones of single cycle gas turbines, which remain close to 30%.

In the following section a detailed explanation of the working principle of this technology has been given.

2.1 Cycle and Characteristic

The reference thermodynamic cycle for gas turbine is the *Joule-Brayton* cycle. In its ideal form it's composed of two *isobaric* (constant pressure) and two *isentropic* (constant entropy) transformations, as shown in Figure 14. The Joule- Brayton cycle is performed using a compressor, a combustion chamber, and an expansion turbine.

It is composed of four phases:

- Isentropic compression;
- Isobaric heating;
- Isentropic expansion;
- Isobaric cooling.

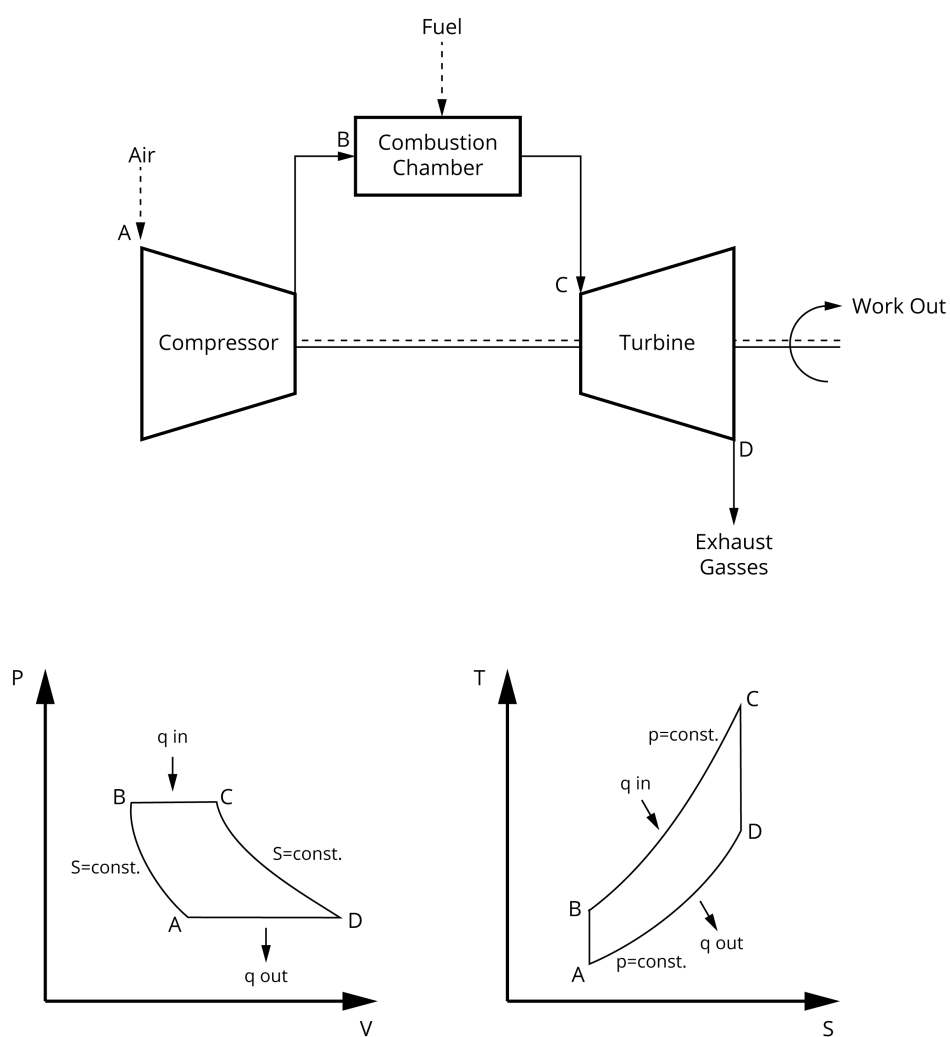


Figure 14: Joule-Bryton thermodynamic cycle.

The compressor increases the external air pressure to the feeding pressure of the combustion chamber. The external air temperature is then raised up by the combustion process occurring in the combustion chamber. The resulting fluid, which is the product of the combustion process (exhaust gasses), enters the expansion turbine.

The expansion turbine shown in Figure 15 is divided into two elements. The first one is the gas producer, where the mechanical power output drives the compressor. The second one is the power turbine, whose power production drives the electric generator. Therefore, the

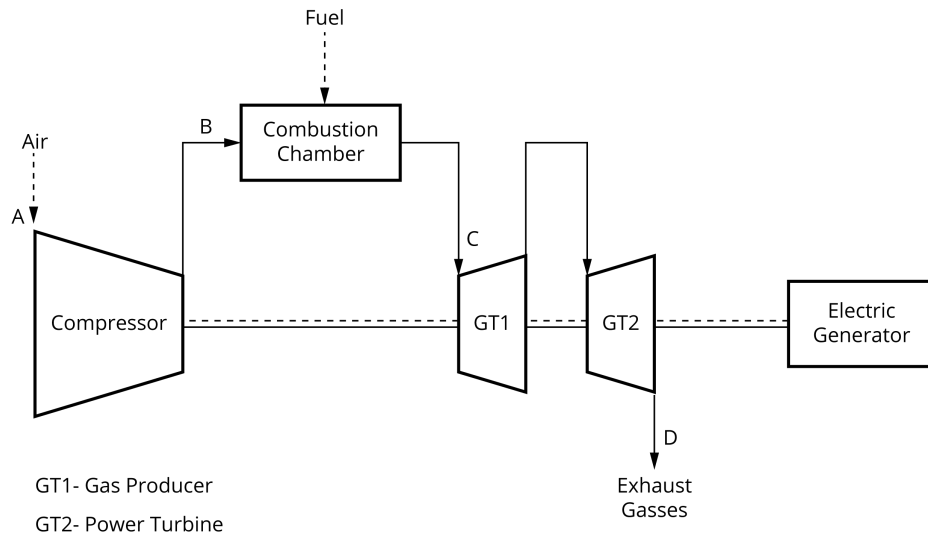


Figure 15: Gas turbine layout.

expansion work of the exhaust gases is transformed into shaft work. The produced shaft work

is necessary to move the electric generator, as well as to drive the compressor. Once the fluid has completed the expansion process, it is brought back to atmospheric conditions.

The aforementioned Joule-Bryton cycle is the ideal one, which means that the following assumptions were considered:

- Closed cycle: the mass flow rate is constant through every component;
- The fluid considered is a perfect gas, specific heat (c_p) is constant;
- Ideal components, no irreversible transformations;
- No heat loss towards the external environment.

For the purpose of this work it was considered sufficient the analysis of the ideal cycle. The objective was the proper understanding of which and how the thermodynamic parameters involved in the process influence the performance of the gas turbine. After the establishment of relationships that drive the efficiency of this technology, actual gas turbine's parameters will be taken into account.

Further variations of the Joule-Bryton cycle have been developed during the years, each aiming at some efficiency improvements (e. g. reheating strategies, intercooling strategies). Although, the study of this alternatives goes beyond the development of a single stage gas turbine model in eQuest[®].

The efficiency of the ideal cycle shown in Figure 14, is calculated through the following equation:

$$\eta = 1 - \frac{T_D}{T_C} = 1 - \frac{1}{\rho^{\frac{\gamma-1}{\gamma}}} \quad (2.1)$$

- η Efficiency of the system;
- T_D Outlet temperature of the exhaust from the power producer section of the turbine ;
- T_C Inlet temperature of the exhaust in the gas generator section of the turbine;
- ρ Pressure ratio of the turbine ($\rho = \frac{p_C}{p_D}$);
- γ Air specific heat ratio.

Looking at Equation 2.1, a direct dependence between the efficiency and the increase of the temperature T_C is shown. T_C represents the absolute temperature of the exhaust gas at the inlet of the turbine's gas producer section. Consequently, it is obvious that one of the main challenges in increasing the performance of these devices has been connected to the need of operating the turbine at the highest possible temperature. The main constraints are connected to the reliance of the blade material, which has to be capable to tolerate the high temperatures. By increasing both, the gas temperature at the gas producer inlet, and the pressure ratio of the equipment, it is possible to improve the efficiency. Therefore, the trend adopted by manufacturers in enhancing performance has been in the direction of increasing both temperatures and pressures.

Another important information can be obtained analyzing Equation 2.1. Gas turbines off-design operation, and thus power output management, is obtained by reducing the amount of fuel burnt in the combustion chamber. This management strategy has a direct effect on the inlet temperature of gases in the expansion turbine and thus on the values of the efficiency achievable during partial load operation. This information will represent an important factor when choosing the proper turbine size during the design phase of the energy production plant.

Oversizing the gas turbine will result in undesired effects, if this choice implies the need to run the equipment at partial load for a considerable number of hours per year.

2.2 Partial Load Operations

In some cases, the user has the necessity of adjusting the output power produced by the gas turbine. This is obtained by reducing the fuel flow entering the combustion chamber, which represents the quantity of heat that enters the process from point B to point C (Figure 14). This fuel reduction results in a decrease in temperature of the inlet gas in the expansion turbine (T_C). Since the temperature of the inlet gas in the expansion turbine is directly proportional to the work produced by the expansion turbine, a reduction of T_C leads to a lower amount of work output.

Under the simplifying assumption of an ideal machinery, the expression of the output power produced by the gas turbine is presented by the following equation (the adopted notation refers to Figure 14):

$$P = (G_a + G_f) \cdot l_t - G_a \cdot l_c \quad (2.2)$$

$$= (G_a + G_f) \cdot c_p \cdot (T_C - T_D) - G_a \cdot c_p \cdot (T_B - T_A) = \quad (2.3)$$

$$= (G_a + G_f) \cdot c_p \cdot T_C \cdot \left(1 - \frac{T_D}{T_C}\right) - G_a \cdot c_p \cdot T_A \cdot \left(\frac{T_B}{T_A} - 1\right) = \quad (2.4)$$

$$= (G_a + G_f) \cdot c_p \cdot T_C \cdot \left(1 - \left(\frac{p_C}{p_D}\right)^{\frac{1-\gamma}{\gamma}}\right) - G_a \cdot c_p \cdot T_A \cdot \left(\left(\frac{p_B}{p_A}\right)^{\frac{\gamma-1}{\gamma}} - 1\right) = \quad (2.5)$$

$$= (G_a + G_f) \cdot c_p \cdot T_C \cdot \left(1 - (\beta_t)^{\frac{1-\gamma}{\gamma}}\right) - G_a \cdot c_p \cdot T_A \cdot \left((\beta_c)^{\frac{\gamma-1}{\gamma}} - 1\right) = \quad (2.6)$$

$$= (G_a \cdot c_p) \cdot \left(\left(\frac{1 + \alpha}{\alpha} \right) \cdot T_C \cdot \left(1 - (\beta_t)^{\frac{1-\gamma}{\gamma}} \right) - T_A \cdot \left((\beta_c)^{\frac{\gamma-1}{\gamma}} - 1 \right) \right) \quad (2.7)$$

- P Power output from the gas turbine;
- l_t Work produced by the gas turbine;
- l_c Work required by the compressor;
- G_a Air mass flow rate;
- G_f Fuel mass flow rate;
- c_p Specific heat (constant pressure);
- β_t Pressure ratio of the turbine ($\beta_t = \frac{p_C}{p_D}$);
- β_c Pressure ratio of the compressor ($\beta_c = \frac{p_B}{p_A}$);
- γ Air specific heat ratio;
- α Air to fuel ratio ($\alpha = \frac{G_a}{G_f}$).

It is possible to observe that a reduction of T_C lowers the power output of the turbine (P). Unfortunately, as seen in Equation 2.1, a drop of T_C also results in the worsening of the system's efficiency. Therefore, in partial load conditions the gas turbine has a poor performance compared to the one at full load conditions.

Moreover, taking into account also environmental issues, the amount of pollutants emitted by the gas turbine is generally increased at part load conditions. The effect is stronger when the Partial Load Ratio (PLR), which is the ratio between the produced power to the design

one, approaches half of the load and below. Figure 16 illustrates the percentage increase in carbon monoxide (CO) emission when the gas turbine works in partial load conditions.

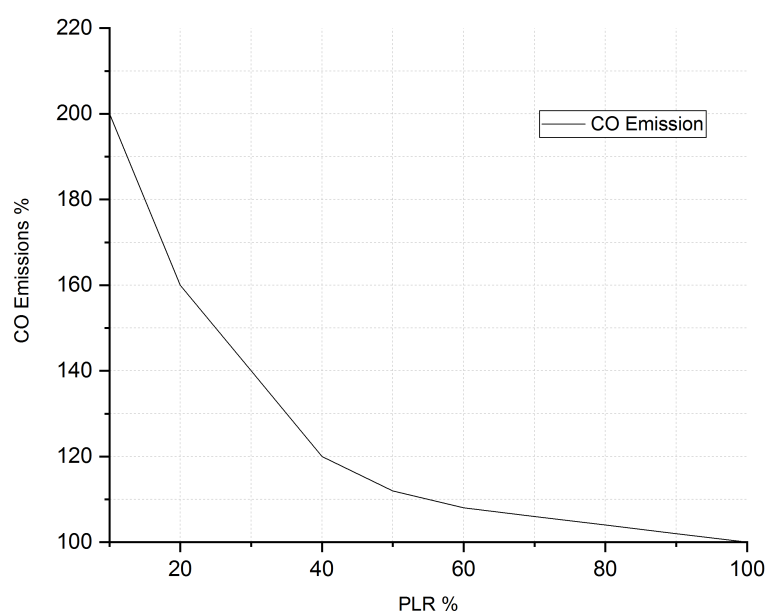


Figure 16: Gas turbine performance - Percentage increase in CO emission vs Partial Load Ratio.

2.3 Modeling the Turbine in eQuest[®]

eQuest[®] needs a model to describe the behavior of the gas turbine and properly define the power output and fuel consumption of the equipment during its operation in the framework of

the cogeneration and trigeneration plant analyzed in Chapter 3 and Chapter 4.

In particular the software requires the definition of three curves:

- *Heat input ratio* in function of the *partial load ratio*;
- *Exhaust heath recovery* in function of the *partial load ratio*;
- *Capacity* in function of the *heat input ratio*.

In the following sections, an improved model of these curves will be assessed. Starting from the technical data given by *SOLAR*[®], an up to date equipment has been created and implemented in eQuest[®] [10] [11]. Previous efforts have produced a revision of the gas turbine model found on eQuest[®] [4], although some basic information were found to be missing.

Problems were encountered in the definition of the *Heat Input Ratio* (HIR) over *partial load ratio* curve, and in the effect of *capacity* over the HIR. In fact, a deep analysis of the output provided by the software, has demonstrated that what is wrongly referred as the capacity over heat input ratio curve, is actually the relationship describing the influence of *external temperature* on the *efficiency*.

No additional improvements were made to the exhaust heat recovery curve, therefore the standard eQuest[®] curve was maintained.

A detailed set of instructions regarding the modeling and upgrade of the gas turbine in eQuest[®] has been attached in Appendix A.

2.3.1 Partial Load Ratio over Heat Input Ratio

The updated model has been created through the analysis of the technical data of the Taurus[™] 60 manufactured by *SOLAR*[®]. The Taurus[™] 60 has been adopted despite its large

capacity (5 MW), which is considered excessive for the need of the health care facility. The main reason relies in the fact that this turbine represents the latest technology available on the market, and has much better performances compared to smaller turbine such as the Saturn™ 20 (1 MW).

Even though the Saturn™ 20 has a more suitable size for the application needed, its efficiency is out of date compared to the present market standards. In Figure 17 it is possible to see a comparison between the eQuest® model and the updated one, in terms of efficiency over PLR [10] [11]. At full load condition the improved model approaches an efficiency of around 30% while the previous one remains below 20%.

The PLR ranges between 10% to 100%: the lower limit is the result of manufacturer's prescription about the minimum required power output to safely operate the equipment.

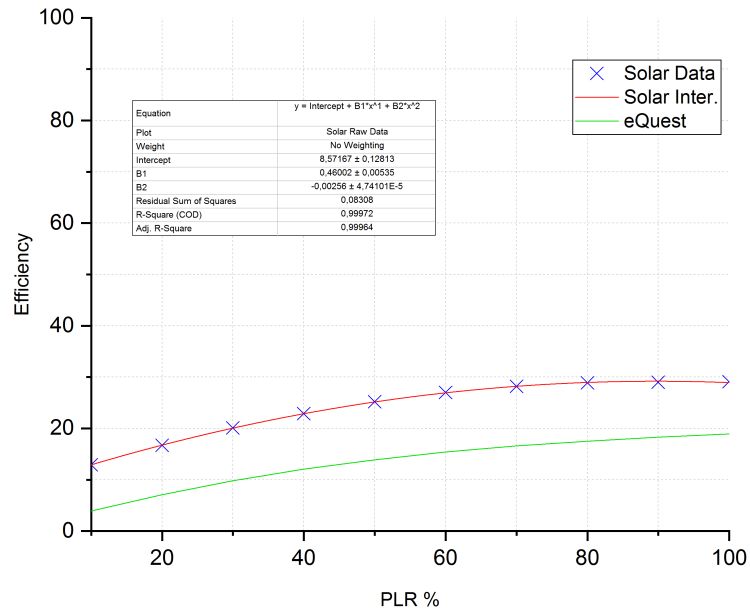


Figure 17: Gas turbine performance - Efficiency vs. Partial Load Ratio - SOLAR model.

Starting from the creation of this curve, the relationship between PLR and the HIR required by eQuest[®] was easily calculated.

The definition of the partial load ratio is given by the following equation:

$$PLR = \frac{\text{Power Currently Developed } [P_C]}{\text{Power at Full Load } [P_{FL}]} = \% \text{ Full Load} \quad (2.8)$$

Moreover, the definition of the heat input ratio is given by:

$$HIR = \frac{\text{Heat Currently Supplied}}{\text{Heat Supplied at Full Load}} = \frac{\frac{P_C}{\eta_C}}{\frac{P_{FL}}{\eta_{FL}}} = \eta_{FL} \cdot \frac{P_C}{P_{FL} \cdot \eta_C} = \eta_{FL} \cdot \frac{PLR}{\eta_C} \quad (2.9)$$

- η_C Efficiency at current condition;
- η_{FL} Efficiency at full load.

Combining the data obtained in Figure 17 with Equation 2.9 it is possible to obtain the values of HIR in function of PLR, as shown in Figure 18.

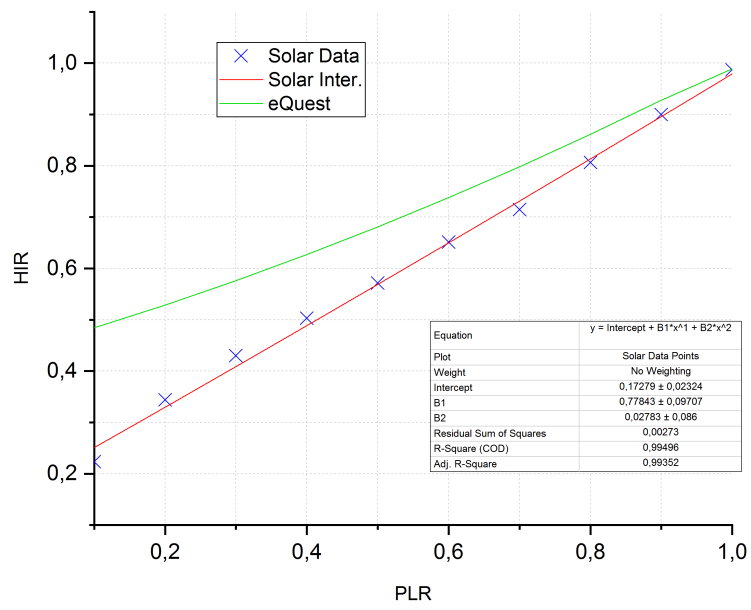


Figure 18: Gas turbine performance - Heat Input Ratio vs. Partial Load Ratio - comparison between SOLAR model and eQuest model.

The software needs an input curve in the following form:

$$HIR = a + bx + cx^2 \rightarrow x = PLR \quad (2.10)$$

A new quadratic approximation (Equation 2.11) has been obtained through an interpolation process of the experimental data in order to replace the standard eQuest[®] relationship (Equation 2.12).

$$HIR_{Solar} = 0.1728 + 0.7784 x + 0.0278 x^2 \quad (2.11)$$

$$HIR_{eQuest} = 0.443 + 0.3974 x + 0.1569 x^2 \quad (2.12)$$

2.3.2 External Air Temperature over Capacity

To better describe the behavior of the gas turbine, the software requires also a model defining the relation between the external air temperature and the performance of the equipment. As already mentioned, despite the fact that the software demands an input curve called *capacity in function of HIR*, it actually wants a curve describing the influence of air temperature over the capacity.

The external conditions, both in terms of pressure and temperature, associated to the operation of a gas turbine have a strong influence on the produced power and also on the overall efficiency. Because of the fixed installation of the equipment this study does not deal with the effect of atmospheric pressure on the performance.

When an increase in the inlet air temperature occurs, both the produced power and the efficiency of the equipment are negatively affected. The causes of this reduced performance are linked with two main factors. The first factor is the reduction of the gas mass flow rate through the equipment (this occurs because the density of air decrease when its temperature increases). The second underlying factor for the efficiency drop is the increase of work per air mass unit

required by the compressor. For a fixed pressure ratio of the compressor, the work required is proportional to the inlet air temperature. Looking at Equation 2.7, it is possible to understand how increasing T_A , the net power output (P) decreases.

These effects have led to the establishment of fixed and widely accepted reference conditions to evaluate gas turbine performances. The reference condition fixed by the International Organization for Standards (ISO) consists of an outdoor pressure equal to the pressure at the sea level (101.325 [Pa]) and an ambient temperature equal to 59 °F [12].

As an example of the correlation provided by the manufacturer, when the external temperature reaches 100 °F, power output can be reduced to 90% of the power output estimated following the ISO standard. On the other hand, by reducing the inlet temperature to about 50 °F, the net power output rises up to 105% of the power output estimated following the ISO standard.

The comparison between the eQuest[®] default model and the *SOLAR*[®] one is shown in Figure 19.

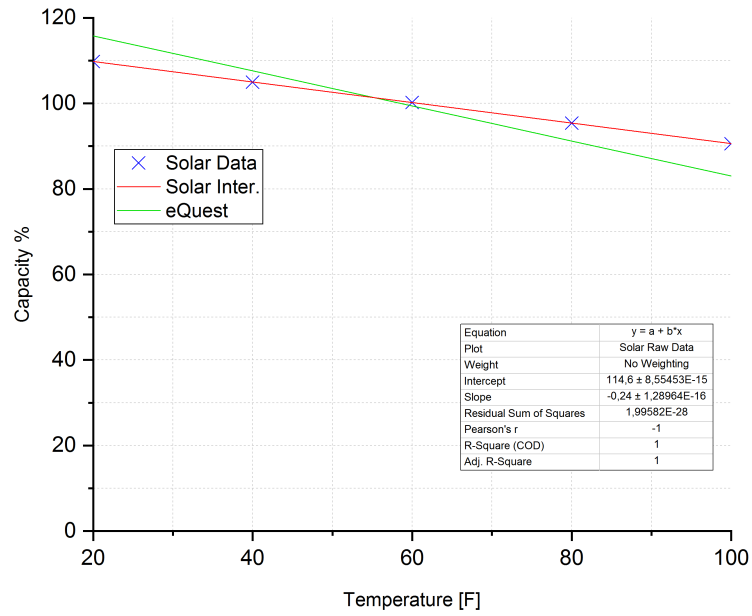


Figure 19: Gas turbine performance - Capacity vs. External Air Temperature - comparison between SOLAR model and eQuest model.

The trend of the eQuest[®] standard definition is steeper than the one of the improved model, which has a less marked sensitivity to the changes of ambient conditions.

The software requires an equation in the following form:

$$Cap.\% = a + b x \longrightarrow x = \text{External Temperature} \quad (2.13)$$

An updated linear relationship is evaluated in Equation 2.14 in order to replace the standard one existing in eQuest[®] (Equation 2.15).

$$Cap.\%_{Solar} = 114.6 - 0.24 x \quad (2.14)$$

$$Cap.\%_{eQuest} = 124 - 0.41 x \quad (2.15)$$

The improved model of the gas turbine represents the foundation for the plant layouts developed in Chapter 3 and Chapter 4, ensuring more realistic and accurate results.

CHAPTER 3

THE COMBINED HEAT AND POWER PLANT

The following chapter will provide a detailed characterization of the CHP technology, and an efficiency analysis of this system related to the electrical and thermal loads of the health care facility. Moreover, the introduction of a Thermal Energy Storage (TES) device will be discussed in Section 5.4, including the potential energy savings and efficiency improvement this equipment could bring to the plant.

3.1 Overview of the Technology

Combined heat and power systems are one of the most efficient solutions to generate electric power and simultaneously produce thermal energy using a single prime mover. While the on-site power production aims to meet the electric load of the user, the heat released during this process can be successfully exploited to satisfy the requested thermal energy. Industrial applications such as factories with a large and steady thermal and electric loads are the main focus of the CHP application and represent the largest share of installed capacity as of today. However, commercial buildings, such as hospitals, universities, hotels, could benefit from this technology since they need a considerable amount of hot water and heat.

Even if it is not the objective of this thesis to analyze each system based on its prime mover, Table III provides a brief summary of the installed capacity across the United States [13]. The classification of a CHP system can vary widely based on the kind of technologies

TABLE III: SUMMARY OF INSTALLED CHP SITES AND CAPACITY BY PRIME MOVER IN THE U.S.

Prime Mover	Sites	Share of Sites	Capacity [MW]	Share of Capacity
Reciprocating Engine	2,194	51.9%	2,288	22.7%
Gas Turbine	667	15.8%	53,320	64.0%
Boiler/Steam Turbine	734	17.4%	26,741	32.1%
Microturbine	355	8.4%	78	0.1%
Fuel Cell	155	3.7%	84	0.1%
Other	121	2.9%	806	1.0%
Total	4,226	100.0%	83,317	100.0%

being used in the system, although it is possible to identify some key components and features that differentiate it from a traditional plant, as shown in Figure 20.

The main element is the *prime mover*, which is the engine that converts chemical fuel into mechanical energy to drive the *generator*, whose job is to transform mechanical energy to electric power. During the conversion process that takes place into the prime mover, the fuel is burned (only in the case of heat engines) and heat is produced. Part of this heat is used for the final electricity production, while the majority of it is exhausted from the process and needs to be recovered. Through the *Waste Heat Recovery System* (WHRS) made of one or more heat exchangers this waste heat is recycled and converted in order to satisfy the thermal loads of the user. A set of *equipment controls* ensure that all the components function properly together.

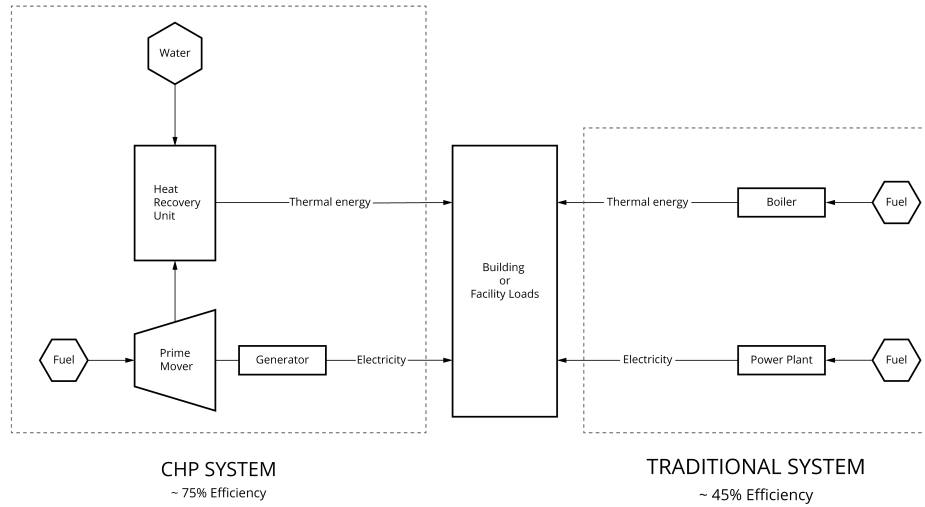


Figure 20: Scheme of a CHP system and overall efficiency.

As it is clear, the key factor that enables this technology to be so efficient and competitive on the market is the proper recovery of the exhaust gasses which represent 60 to 80% of the energy content of the burned fuel. In the case of a gas turbine, exhaust heat is commonly used as a direct source for hot water production. In other applications, the recovered heat could be used for the production of steam, with the help of a Heat Recovery Steam Generator (HRSG).

Some of the major direct benefits provided by the correct implementation of a CHP system were provided in a report elaborated by a partnership between the U.S. Environmental Protection Agency (EPA) and the U.S. Department of Energy in 2017 [13]. These benefits are listed as follows:

- **Efficiency benefits:** CHP requires a lower quantity of fuel to produce a specific energy output compared to a traditional system. Moreover, it avoids transmission and distribution losses which occur when electric power travels along the grid;
- **Environmental benefits:** due to a lower amount of burned fuel, as well as the overall better efficiency of the system, CHP has a reduced value of greenhouse gases emissions and other air pollutants;
- **Economic benefits:** because of its enhanced performance, CHP can provide a valuable solution in cost saving operations, as well as providing a protection against electricity rate increase;
- **Reliability benefits:** CHP is an on-site generation resource and can be designed to support continued operations in the event of a disaster or grid disruption.

3.1.1 Energy Fluxes Involved in the Process

In order to properly proceed with the description and analysis of the system, major importance is given to the definition of the energy fluxes throughout the process. A detailed scheme of the system is provided in Figure 21.

During the conversion process that takes place in the prime mover the *fuel* is transformed in *mechanical energy*, that will be converted into *electrical energy* by the generator. During this operation part of the heat is inevitably lost towards the external environment. This flux is called *Wasted Heat* and takes into account all those inefficiencies of the WHRS that wouldn't allow the complete recovery of the heat produced by the turbine. On the opposite, the amount

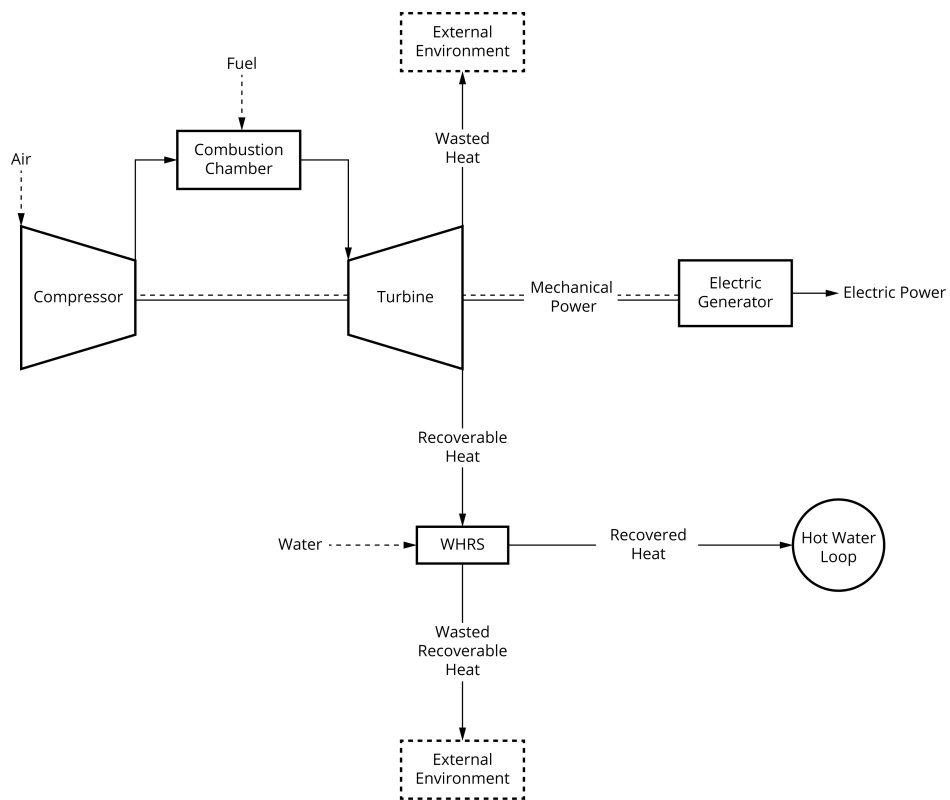


Figure 21: Energy fluxes involved in the CHP system.

of heat that can be exploited by the WHRS is called *Recoverable Heat*. This amount of thermal energy is ideally available to meet the thermal load of the user, although, the actual quantity of heat that can be used by the facility is called *Recovered Heat*.

The amount of *Recovered Heat* is strictly related to the efficiency of the heat exchangers, the thermodynamic constraints of the system (e. g. temperature of the hot water loop) and the profile of the thermal energy requested. In particular, this last one dictates the amount of heat needed by the user and therefore recovered. If the user consumption is drastically lower than the *Recoverable Heat*, then, part of the latter, will be wasted and will never turn into a thermal source exploited by the facility. This quantity will be addressed as *Wasted Recoverable Heat* (WRH), and represents the amount of energy originally available from the exhaust gases of the prime mover, but never requested by the hospital. The WRH must not to be confused with the *Wasted Heat*, which is dumped into the external environment due to inefficiencies of the plant, that does not allow its recovery. The WRH will assume a key role during the study of the system's efficiency and the eventual implementation of a TES device.

3.1.2 Operating Strategy of the Plant

Health care facilities represent a particularly suited facility for the installation of a CHP system. Their continuous and large loads allows them to achieve high efficiencies of roughly 80% throughout the majority of the year. This is supported by the increment of installed CHP capacity in the U.S hospitals during the years, as shown in Figure 22[14]. The operation strategy adopted by the system must be discussed, before continuing with the analysis of plant's

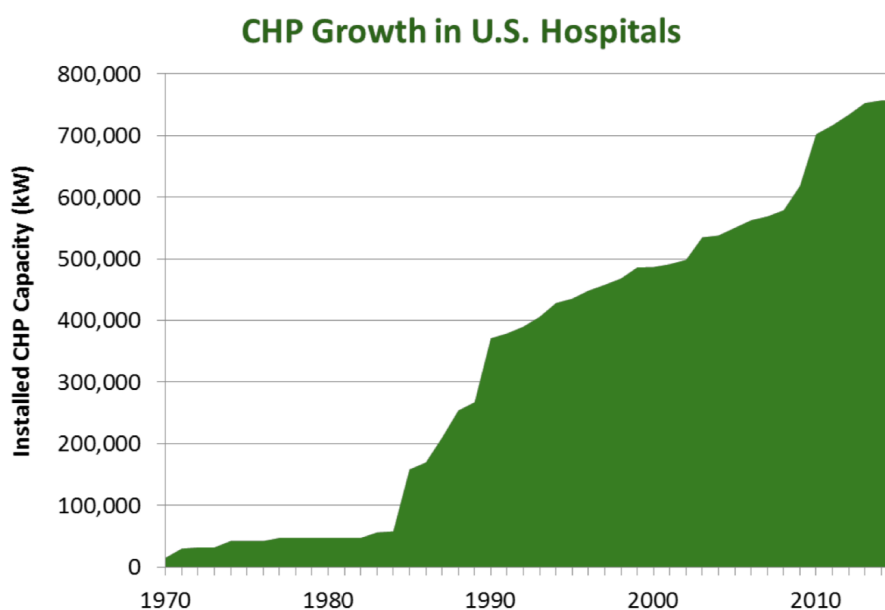


Figure 22: CHP growth in the U.S. Hospitals.

layout. A cogeneration technology can follow two main operational strategies, depending on the primary load the user would like to satisfy:

- **Following Thermal Load (FTL):** the system is designed to fulfill the thermal load of the facility, and the production of electricity is considered to be a secondary output in order to reduce the purchased power from the grid;
- **Following Electrical Load (FEL):** the system is designed to fulfill the electrical load of the facility and the heat produced is considered to be a secondary output in order to reduce the fuel consumption by the boilers.

The main factor used to determine which strategy to follow is the *Heat to Power Ratio* (HPR).

This quantity is defined as follows:

$$HPR = \frac{\text{Heat Consumption [MWh]}}{\text{Power Consumption [MWh]}} \quad (3.1)$$

In the case studied and in the majority of the health care facilities, the power consumption is much higher than the heating one, especially during summer months, when the hot energy requested by the user drops drastically. This leads to the logical conclusion of adopting a FEL strategy. Furthermore, since the prime mover adopted by the plant is a gas turbine, the plant should work in full load conditions as long as possible. As already mentioned in 2.2, this kind of technology has a drastic decrease in efficiency if working in partial load. A FTL strategy, given the fluctuating nature of the thermal load, would not allow full load operations of the turbine, unless an undersized equipment is adopted. Moreover, considering the electricity produced as a primary output, FEL operation will lead to an increase of the economic benefit in a scenario characterized by growing rates of primary sources[15].

FEL operation increases the reliability of the power supply. In case of power outage, co-generation and trigeneration plants will continue to operate steadily since they do not rely on the operation of the grid. The resilience and reliability of the system are a primary concern in health care facilities, since a power interruption could result in catastrophic consequences. Traditional system depend on emergency generators in case of blackouts, such as diesel engines. This generators are often useful for short term electricity production, but cannot assure an

extended period of service, since they have a limited amount of fuel storage.

During calamities, cogeneration and trigeneration systems could result in an optimal solution to keep the facility running as demonstrated during hurricane Harvey in September 2017 [21].

3.2 Modeling a CHP System in eQuest[®]

In order to properly analyze the efficiency and the feasibility of a cogeneration plant integrated in the prototype hospital a series of simulations were performed in order to obtain the thermal and electrical outputs produced by the system. The layout modeled on eQuest[®] is shown in Figure 23, no information regarding the prime mover and the *Heat Recovery loop* appears in the scheme.

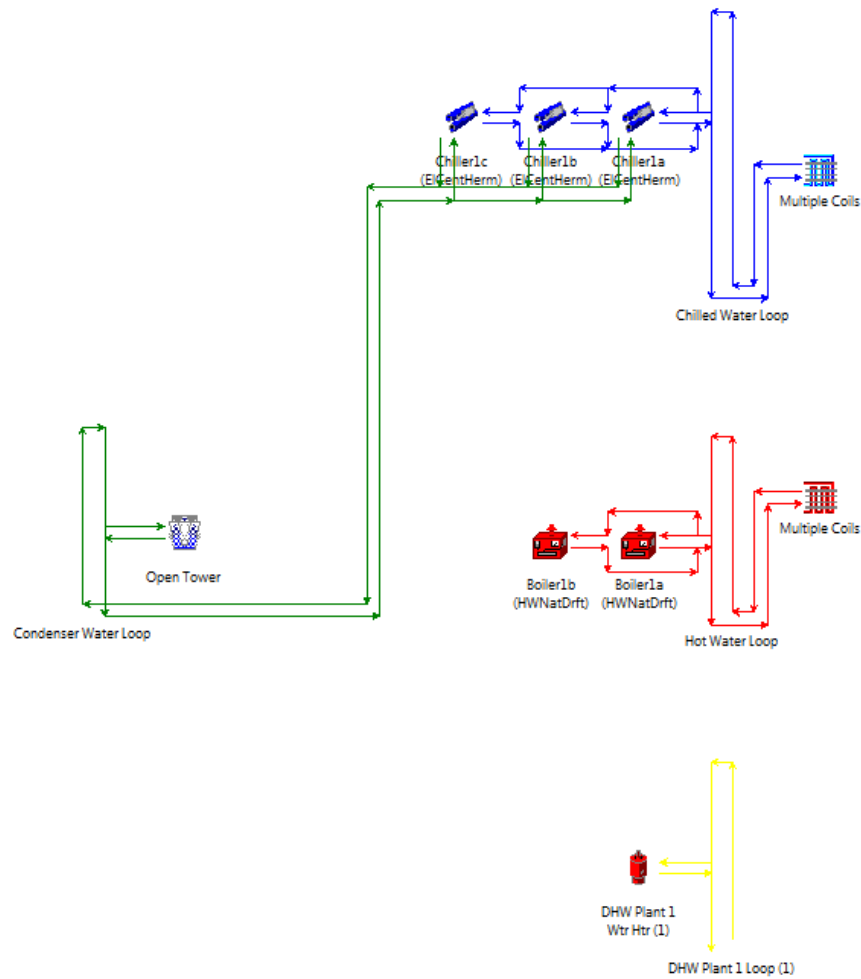


Figure 23: eQuest[®] layout of the CHP plant.

The software proved to be essential in the realization of this thesis, although a simplifying assumption had to be made. The heating load and the domestic hot water load were considered as one. In order to allow that, the *Domestic Hot Water loop* was attached to the *Space Heating*

Hot Water loop as a miscellaneous load (the definition of the *Domestic Hot Water loop* and *Space Heating Hot Water loop* were provided in Section 1.3). This simplification does not affect the total value of the thermal load, but drastically facilitate the modeling of the plant. The reason relies on the fact that the software does not allow the user to attach multiple loops to the *Heat Recovery loop* of the prime mover. So instead of attaching it to both, the *Space Heating Hot Water loop* and the *Domestic Hot Water loop*, the *Heat Recovery loop* has been connected only to the first one. The domestic hot water load was incorporated in the space heating load with the resulting procedure. Using Equation 3.2, the domestic hot water process load was calculated:

$$Q = G \rho c \Delta T \quad (3.2)$$

- Q domestic hot water process load;
- G domestic hot water process flow;
- ρ water density;
- c water specific heat;
- ΔT temperature difference between T_{in} and T_{out} .

The temperature of the water entering the *Domestic Hot Water loop*, T_{in} is considered to be 45 °F, while the T_{out} is assumed to be 125 °F. The so computed process load was resembled as miscellaneous load in the *Space Heating Hot Water loop*.

Even adopting this strategy, eQuest[®] still needs the creation of a *Domestic Hot Water loop* in which the capacity of the boiler has been set to zero.

Finally, the cooling load represented by the *Cold Water loop*, is satisfied by the introduction of an electric chiller (COP=4.0). A detailed description of the steps needed by the user to implement a CHP system in eQuest[®] is reported in Appendix A.

3.3 Thermal and Electrical Analysis

Depending on the size of the turbine adopted, various scenarios have been observed.

The general outcome can be summarized as follows, increasing the size of the prime mover generates the following results:

- Increase of the electricity produced and resulting in a reduction of the purchased power;
- Increase in the fuel consumption of the prime mover;
- Longer periods operating in partial load conditions, which means worse efficiency;
- Higher amount of *Recovered Heat*, which brings down the fuel consumption of the boilers.

The monthly production of electricity is shown in Figure 24 (700 kW) and in Figure 25. A general overview of the trend can be understood by comparing the 700 kW layout over the 1,300 kW one. A more detailed analysis of the electricity production of every analyzed turbine's capacity is provided in Table IV.

TABLE IV: MONTHLY ELECTRIC PRODUCTION [MWH] OF A CHP PLANT BY INSTALLED TURBINE SIZE.

Period	<i>Base M.</i>	600	700	800	900	1,000	1,100	1,200	1,300
January	774.5	446.1	521.5	592.3	648.6	695.2	733.0	763.1	775.2
February	700.2	403.7	470.3	535.1	585.2	628.7	662.3	689.4	700.1
March	775.3	446.7	521.4	592.8	648.7	695.1	732.8	762.1	775.4
April	773.4	431.0	503.8	572.7	630.4	680.1	719.2	750.5	767.2
May	860.3	441.4	515.1	586.5	651.9	707.6	754.0	792.2	817.4
June	916.1	420.8	490.7	559.2	626.7	687.8	740.4	784.2	820.1
July	1,016.7	431.6	503.4	574.4	646.3	714.7	774.5	826.2	870.4
August	1,014.0	432.3	505.1	576.0	645.3	709.0	766.2	817.1	862.1
September	861.3	425.2	496.9	564.2	625.5	681.1	727.0	765.8	794.9
October	808.4	445.5	519.5	590.1	653.2	707.0	748.3	781.2	800.1
November	740.8	432.2	504.8	572.3	625.5	668.2	701.0	728.8	740.2
December	774.6	446.6	521.3	592.2	648.8	695.2	733.0	763.8	775.4
ANNUAL	10,015.2	5,200.2	6,066.9	6,906.4	7,630.8	8,266.2	8,788.8	9,220.5	9,495.7

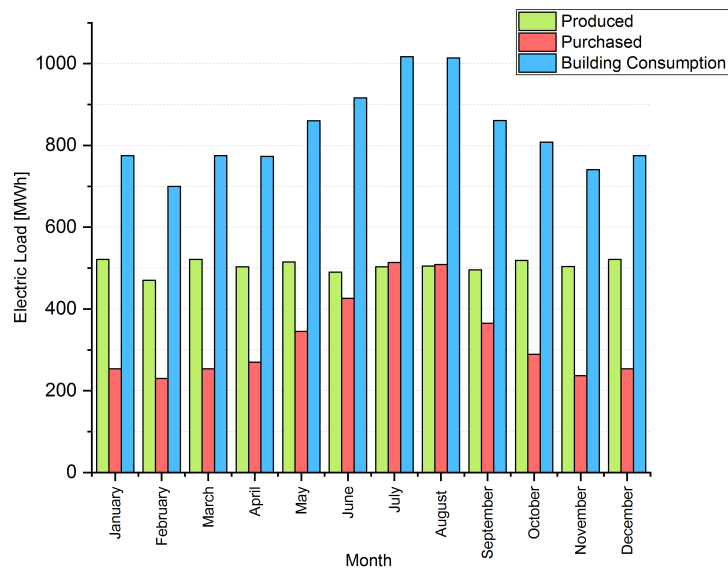


Figure 24: Monthly electricity production of a 700 kW CHP plant.

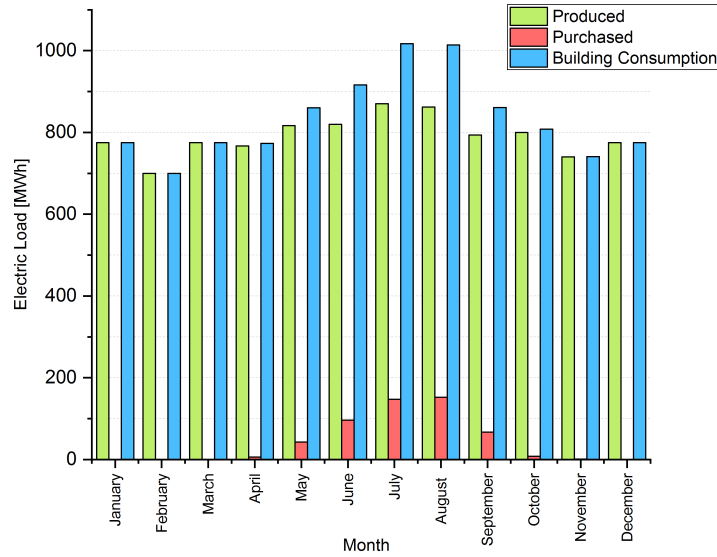


Figure 25: Monthly electricity production of a 1300 kW CHP plant.

A comparison between the prime turbine's fuel consumption is illustrated in Figure 26. It is possible to see how a 1,300 kW layout burns twice the amount of fuel than a 700 kW one. This last one reflects a more constant trend due to the fact that it runs always at full load conditions. On the other hand, the 1,300 kW is affected by a longer period of partial load operations, especially during colder months (when the need of electricity by the electric chillers is roughly zero). This brings down the performance of the system, resulting in an higher consumption of fuel during those months, despite the lower electric output.

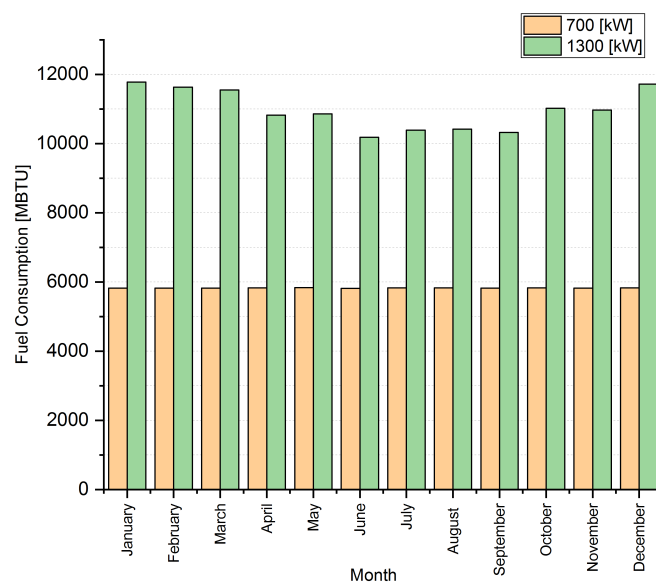


Figure 26: Comparison of turbine’s fuel consumption between a 700 kW and a 1300 kW CHP layout.

In Figure 27 and Figure 28 the amount of *Recovered Heat* of a 700 kW and a 1,300 kW plant is respectively highlighted.

It is evident how the operation of a larger turbine enables to use a much higher quantity of exploited heat. Although, this positive effect comes at a cost: larger prime movers require bigger quantities of fuel. Since, most of the *Recoverable Heat* is wasted during warmer periods, this extra expense of fuel does not always seem convenient.

The following Section will provide detailed information on the overall efficiency and performance of the system, properly addressing this problem.

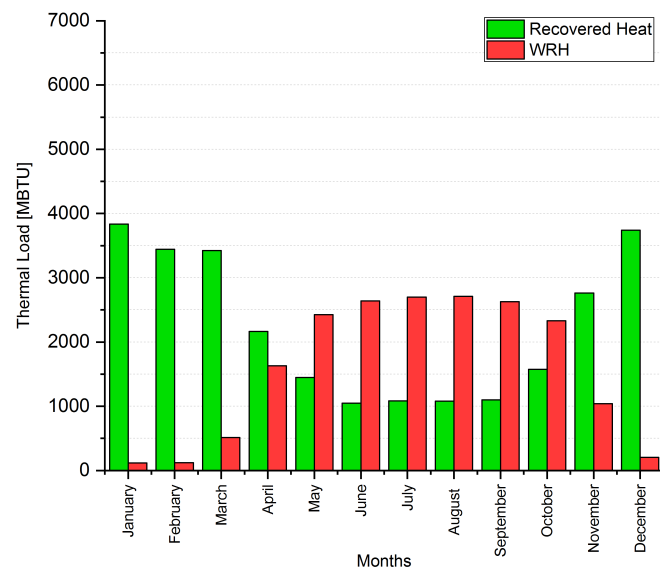


Figure 27: Amount of *Recovered Heat* and *Wasted Recovered Heat* of a 700 kW CHP plant.

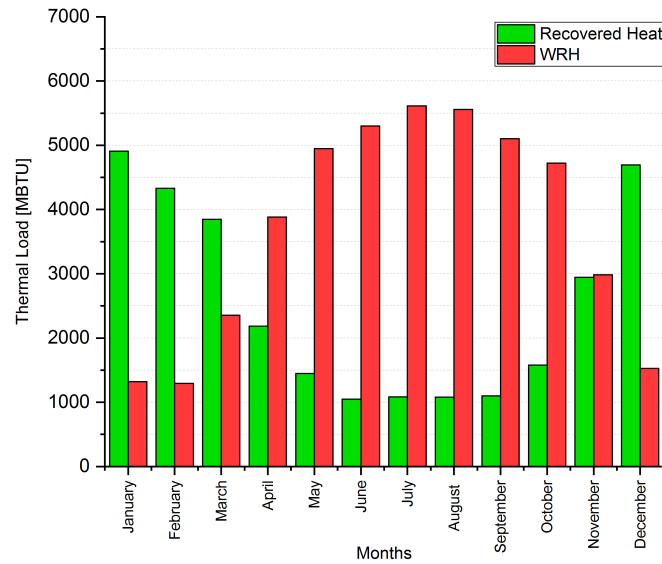


Figure 28: Amount of *Recovered Heat* and *Wasted Recovered Heat* of a 1300 kW CHP plant.

3.4 Efficiency Analysis

The efficiency definition adopted in this thesis can assume different meaning depending on the importance given to the heat and electricity output of the system.

In this work, two main definition were adopted:

- **Total CHP system efficiency;**
- **FERC efficiency standard.**

In terms of thermodynamics and consequently on the market, the electric power is considered to be a more valuable energy than the thermal one. More precisely, depending on the thermo-

dynamic evaluation of the energy, the ratio of the value between the two can vary drastically. If we consider the first law of thermodynamics, the importance given to thermal energy is equal to the one given to electricity. While considering the second law, the value of electricity is extremely higher than the one of the heat, especially if a low temperature thermal source is used (low exergy).

These different evaluations have brought numerous experts to develop different methods of calculating the efficiency.

3.4.1 Total CHP System Efficiency

The total CHP system efficiency attributes the same importance to the heat recovered from the exhaust gasses and the electricity produced.

The definition is given as follows:

$$\eta_{CHP} = \frac{E_{PM} + Q_{rec.}}{F_{PM}} \quad (3.3)$$

- E_{PM} Electrical energy produced by the prime mover;
- $Q_{rec.}$ Thermal energy recovered;
- F_{PM} Prime mover fuel consumption.

Clearly, the aforementioned efficiency strictly depends on the amount of heat recovered by the plant.

This amount is dictated by two main parameters, the exhaust gasses temperature (WHRS inlet temperature) and the HRSG temperature (only if steam is produced) or, like in the case

studied, the requested temperature of the heated fluid (WHRS exit temperature).

The first parameter is a function of the pressure ratio and the inlet gas temperature of the expansion section of the turbine. Typical exhaust temperatures are in the range of 850 to 950 °F. With a fixed WHRS exit temperature, the higher the temperature of the gasses exiting the turbine, the higher will be the amount of recoverable energy. Correspondingly, assuming a constant temperature for the exhaust gasses, the lower is the WHRS exit temperature the higher will be the efficiency of the system. Usually, WHRS units are designed to recover roughly 80% of the maximum energy recoverable from the plant according to the temperature values of the exchanging fluid. In the *Space Heating Hot Water loop* the inlet temperature of the water was assumed to be 45 °F and the exit temperature 170 °F.

It has been noticed that during partial load operations of the plant, the CHP efficiency does not drop drastically. This is mainly due to the fact that even if the electric efficiency of the turbine decreases, with a consequent decline of the power output, the heat available for recovery increases. This leads to an increment of the recovered thermal energy, which is particularly beneficial to those applications requesting a substantial amount of heat.

3.4.2 FERC Efficiency Standard

The FERC standard efficiency was introduced in 1978 by the *Public Utilities Regulatory Policies Act*. This definition allots greater importance to the electric power produced (compared

to the CHP efficiency) by halving the value of thermal energy recovered.

The FERC efficiency standard is given by the following formula:

$$\eta_{FERC} = \frac{E_{PM} + \frac{Q_{rec.}}{2}}{F_{PM}} \quad (3.4)$$

- E_{PM} Electrical energy produced by the prime mover;
- $Q_{rec.}$ Thermal energy recovered;
- F_{PM} Prime mover fuel consumption.

Using the FERC definition of efficiency, the partial load operations of the plant have a greater negative impact on the final value of the overall performance of the system.

3.4.3 Percentage Reduction in Source Energy Consumption

The *Percentage Reduction in Source Energy Consumption* (PRSEC), represents a way to calculate the decline in source energy consumption by comparing a conventional system (Section 1.3) with the CHP plant analyzed. The conventional system is connected to the electric grid in order to satisfy its electric loads and uses natural gas driven boiler to fulfill the thermal request.

The PRSEC is expressed below:

$$PRSEC = \frac{SE_{CONV} - SE_{CHP}}{SE_{CONV}} \quad (3.5)$$

$$PRSEC = 1 - \frac{SE_{CHP}}{SE_{CONV}} \quad (3.6)$$

- SE_{CONV} Source energy consumption of a conventional system;

- SE_{CHP} Source energy consumption of a CHP system.

In order to estimate the source energy consumption, it was adopted the AN- SI/ASHRAE Standard 105-2014: Standard Methods of Determining, Expressing and Comparing Building Energy Performance and Greenhouse Gas Emissions [22]. This standard is largely accepted, and provides important conversion factors which take into account the various energy sources used. Starting from the various types of energy consumption resource of the hospital, and multiplying it by the conversion factor reported in the standard, it is possible to evaluate the energy source. In this study, the following conversion factors were considered:

- 3.29 for the electricity;
- 1.09 for the natural gas.

These factors are heavily influenced by the geographical location where the energy is produced and consumed. Depending on the different regions, the efficiency of the production and the efficiency of the energy grids must be considered. Illinois is part of the so-called *Reliability First Corporation/West* (RFCW) region, one of the 22 different ones in which the country is divided.

It has to be noticed that the PRSEC index is not only influenced by the components of the CHP system itself, but by every component of the system that requires energy, such as boilers and chillers. The numerator is calculated as the sum of the source energy consumption of the boilers, of the prime mover (gas turbine) and the cost of the electricity purchased from the grid in order to meet the hospital's load. On the denominator, the *base model* is considered, which adopts a conventional system (buying electricity from the grid to fulfill the electrical load, and

burning natural gas in the boilers to produce the thermal energy required).

Following this approach the reduction of source energy consumption can be calculated as follows:

$$PRSEC = 1 - \frac{[SE_{F.B.} + SE_{F.P.M.} + SE_{E.P.}]_{CHP}}{[SE_{F.B.} + SE_{E.P.}]_{CONV}} \quad (3.7)$$

$$PRSEC = 1 - \frac{[F_B \cdot AF_{NG} + F_{PM} \cdot AF_{NG} + E_{pur.} \cdot AF_E]_{CHP}}{[F_B \cdot AF_{NG} + E_{pur.} \cdot AF_E]_{CONV}} \quad (3.8)$$

- $SE_{F.B.}$ Source energy consumption associated with fuel for boilers;
- $SE_{F.P.M.}$ Source energy consumption associated with fuel for the prime mover;
- $SE_{E.P.}$ Source energy consumption associated with the electricity purchased;
- F_B Fuel consumption of the boilers;
- F_{PM} Fuel consumption of the prime mover;
- $E_{pur.}$ Electricity purchased from the grid;
- AF_{NG} ASHRAE conversion factor for natural gas;
- AF_E ASHRAE conversion factor for electricity.

A second index of the PRSEC has been calculated, referred as the *Gas Turbine - Percentage Reduction Source Energy Consumption* ($PRSEC_{GT}$). In this second case the focus was shifted from the overall system to the specific prime mover used by the CHP. This approach is intended

to decouple the performance of the system itself, from the efficiency of other equipment (e.g. boilers, chillers). Equation 3.7 becomes:

$$PRSEC_{GT} = 1 - \frac{[SE_{F.P.M.}]_{CHP}}{[SE_{Q_{rec.}} + SE_{E_{P.M.}}]_{CONV}} \quad (3.9)$$

$$PRSEC_{GT} = 1 - \frac{[F_{PM} \cdot AF_{NG}]_{CHP}}{[F_B \cdot AF_{NG} + E_{PM} \cdot AF_E]_{CONV}} \quad (3.10)$$

$$PRSEC_{GT} = 1 - \frac{[F_{PM} \cdot AF_{NG}]_{CHP}}{[\frac{Q_{rec.}}{\eta_B} \cdot AF_{NG} + E_{PM} \cdot AF_E]_{CONV}} \quad (3.11)$$

- $SE_{F.P.M.}$ Source energy consumption associated with fuel for the prime mover;
- $SE_{Q_{rec.}}$ Source energy consumption associated with fuel consumption to replace $Q_{rec.}$;
- $SE_{E_{P.M.}}$ Source energy associated with the electricity produced by the gas turbine;
- F_{PM} Fuel consumption of the prime mover;
- F_B Fuel consumption of the boilers to replace the recovered heat $Q_{rec.}$;
- E_{PM} Electricity produced by the prime mover;
- $Q_{rec.}$ Heat recovered by the CHP system;
- η_B Average efficiency of the boilers;
- AF_{NG} ASHRAE conversion factor for natural gas;
- AF_E ASHRAE conversion factor for electricity.

With the introduction of this parameters it is possible to develop a detailed analysis of the performance of the cogeneration system.

3.4.4 Performance of the CHP System

Table V shows the main parameters involved in the efficiency analysis and the various values of the indexes mentioned in the prior section depending on the installed gas turbine's size. The definition of the abbreviations adopted in Table V is given in Appendix D.

TABLE V: PERFORMANCE OF THE CHP BY INSTALLED TURBINE SIZE

Size [kW]	F_B [MBTU]	F_{PM} [MBTU]	$Q_{rec.}$ [MBTU]	E_{PM} [MWh]	$E_{pur.}$ [MWh]	η_{CHP}	η_{FERC}	PRSEC	PRSEC _{GT}
600	14,829.1	59,922.6	24,788.3	5,200.2	4,814.8	70.9%	50.3%	18.4%	29.1%
700	12,921.9	69,908.7	26,707.3	6,066.9	3,948.1	67.8%	48.7%	19.0%	27.0%
800	12,759.8	79,978.5	28,101.8	6,906.4	3,108.6	64.6%	47.0%	18.2%	24.7%
900	12,639.7	90,321.6	28,917.2	7,630.8	2,384.2	60.8%	44.8%	16.3%	21.2%
1,000	11,976.4	100,585.6	29,453.3	8,266.2	1,749.8	57.3%	42.7%	14.3%	17.5%
1,100	11,516.8	110,781.6	29,797.3	8,788.8	1,226.2	53.9%	40.5%	11.5%	13.2%
1,200	11,219.4	120,718.2	30,038.5	9,220.5	794.5	50.9%	38.5%	8.1%	8.8%
1,300	11,033.8	130,642.1	30,180.6	9,495.7	519.2	47.9%	36.3%	3.5%	3.5%

Taking a look at Table V it is possible to see how a 700 kW gas turbine reaches the highest value of PRSEC among the different installed capacities, which results in the largest savings

achievable in terms of source energy. While, referring to the $PRSEC_{GT}$, a 600 kW turbine reflects the best performances.

The fact that these two different indexes reflect optimal results for different installed capacities relies on their definition. They refer to different portion of the system, although both of them are strongly affected by the following parameters:

- number of hours the turbine works at full load conditions (efficiency of the turbine);
- the amount of WRH;
- the amount of *Recovered Heat*;
- the electricity produced.

Both, the 600 and 700 kW turbines have the same amount of hours operating at full load, as shown in Table VI. Although, using the $PRSEC_{GT}$ approach, the fact that the 600 kW size has a lower amount of WRH, makes it a better solution in terms of performance. While, looking at the whole system, the fact that the 700 kW has a higher amount of electricity produced and recovered heat, allows it to reduce the cost (in terms of source energy) of the electricity purchased from the grid.

TABLE VI: HOURS AT FULL LOAD OF DIFFERENT GAS TURBINE SIZE.

Size [kW]	600	700	800	900	1,000	1,100	1,200	1,300
Full Load Hours [h]	8,760	8,760	8,172	6,880	5,798	4,771	3,950	1,699

Generally, increasing the size of the prime mover, reflects an increment in the number of hours in which the equipment operates in partial load conditions, reducing its electrical efficiency, thus the performance of the entire system. Nevertheless, the bigger the size, the higher is the amount of WRH with respect to the amount of *Recovered Heat* which means a worst exploitation of the heat source.

CHAPTER 4

THE COMBINED COOLING, HEATING AND POWER PLANT.

A combined cooling, heating and power plant, also called trigeneration plant, works similarly to a CHP system. In fact the main difference is based on the double benefit provided by the heat recovered from the exhaust gasses. The first one, just as in a cogeneration system, is the production of thermal energy to feed the heating system of the facility. Secondly, the trigeneration plant is capable of producing cold water through the use of chilling technologies (e. g. absorption chillers) that rely on the use of the hot thermal energy recovered by the system.

The production of cold water, combined with the production of hot thermal energy and electricity, allows a trigeneration system to partially satisfy every energy demand of the user. A better management and exploitation of the primary energy source, grants CCHP plants to reach remarkable performances.

The overall efficiency of a trigeneration plant lies around 85%, much higher compared to traditional power production plants, which usually do not exceed 40% [16]. An exception is represented by Natural Gas Combined Cycle plants (NGCC), which however can only reach efficiency standards near 60%, still lower than cogeneration and trigeneration plants [17].

The layout of a CCHP plant is similar to the one of a CHP plant, with an increased complexity in the cooling system due to the introduction of absorption chillers. Therefore, the need of a detailed explanation on the working principle and characteristic of this technology is

required. Furthermore, an improved eQuest[®] model for the implementation of this device will be presented in the following section, based on a previous study [4].

4.1 The Absorption Chiller

Absorption chillers are a specific kind of refrigeration machinery that represent a valuable alternative to electric compression chillers. In fact, their operation cycle is based on the usage of a hot source in order to produce cold thermal energy.

This technology removes thermal energy from the refrigerating water through the evaporation of a low-temperature and low-pressure fluid. Since the equipment has to perform a continuous operation, it is necessary to bring the vapor back to the liquid phase. An absorption chiller performs this action relying on a thermo-chemical process rather than the traditional vapor cycle, which relies on the electric compressor.

The working fluid involved in the process is a mixture of two substances: the *absorbent* and the *refrigerant*.

The prerequisites are that these two substances must dissolve into each other and that, reversely, they can be separated by a simple process. Only two pairs of substances have been widely used by absorption chilling technologies:

- $H_2O - LiBr$: a mixture in which water is used as the refrigerant and lithium bromide ($LiBr$) serves as absorbent;
- $H_2O - NH_3$: a mixture in which water is used as absorbent, while ammonia (NH_3) is the refrigerant.

In order to properly understand the working principle of the absorption chiller, three physical concepts must be explained (for the description of the technology a $H_2O - LiBr$ mixture will be considered):

- Considering the water phase diagram, water can evaporate at 40 °F if at a very low pressure, as the one in the absorption chamber (840 [Pa]);
- Lithium bromide is a salt in a liquid form, which attracts vapor water molecules. The higher is the percentage of refrigerant dissolved into the mixture, the lower will be the absorption capability of the absorbent;
- When H_2O and $LiBr$ are mixed together, it is possible to separate them by applying heat. Doing so, the water will evaporate, while the heavier $LiBr$ particles will precipitate.

As illustrated in Figure 29, a single stage absorption chiller is made of four components:

- Generator, connected to a high temperature thermal energy reservoir (e.g. waste heat from the prime mover);
- Condenser, connected to an intermediate temperature thermal energy reservoir (e.g. external environment, cooling tower);
- Evaporator, connected to the low temperature source (the water that needs to be refrigerated);
- Absorber.

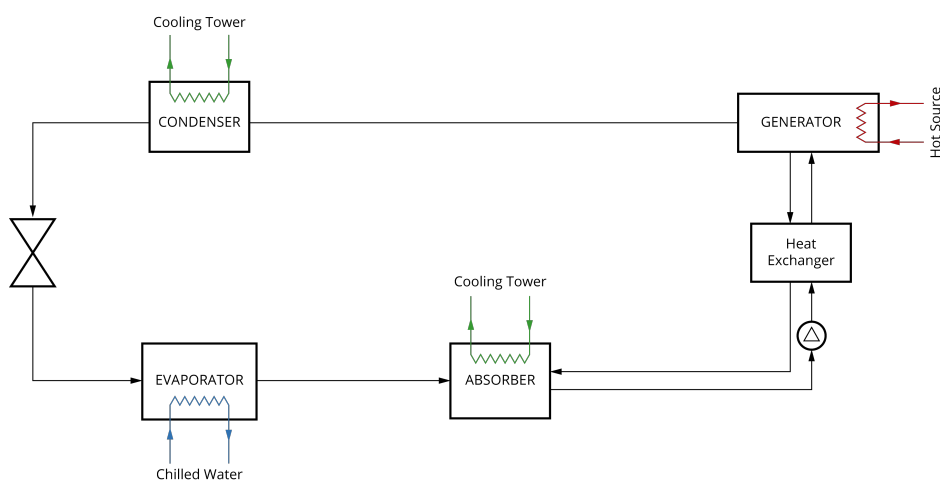


Figure 29: Absorption chiller layout.

Starting from the generator, the mixture of $H_2O - LiBr$ is heated using the thermal energy coming from the hot energy reservoir (e. g. *Recovered Heat* from the turbine). The mixture evaporates, separating the water vapor from the lithium bromide particles.

The vapor enters the condenser, where it condenses due to the cooling effect provided by the *condenser water* which runs through the cooling tower. The refrigerant water obtained in the condenser enters the evaporator. In the evaporator, which is maintained at a very low pressure, the water is sprayed on the coils in which the *chilled water* runs. Thanks to the low-pressure environment the refrigerant water is forced to evaporate, subtracting thermal energy to the chilled water, which consequently lowers its temperature (beneficial effect).

The low-temperature water vapor enters the absorber in order to regenerate the original

$H_2O - LiBr$ mixture. In fact, the high concentration $LiBr$ solution absorbs the water vapor particles coming from the evaporator. This strong attractions between H_2O and $LiBr$ is what helps maintaining the very low pressure conditions inside the evaporator. As mentioned earlier, the higher will be the concentration of lithium bromide particles, the stronger this attraction will be.

The heat produced during the regeneration process is rejected, meanwhile the liquid mixture of $H_2O - LiBr$, which is collected at the base of the absorber, is ready to be pumped back to the generator.

For the sake of clarity, a parallel loop established between the generator and the absorber has the function to bring the high concentration lithium bromide fluid from the generator to the absorber, to enable the regeneration process. In the case of a double stage absorption chiller additional steps are required to complete the process, however this technology will not be discussed in this thesis.

Double stage absorption chillers are usually more complex in terms of components, but run on higher performances. However, due to specific economic and thermodynamic constraint, they were not considered for the realization of the trigeneration facility.

The efficiency of this equipment, as in every kind of chiller technology, is evaluated through the use of the Coefficient Of Performance (COP). Depending on the literature or the technical

sheet of the component, the COP can assume two different definitions.

The first one is the *thermal* COP, defined by the following equation:

$$COP_T = \frac{Q_-}{Q_+} \quad (4.1)$$

- Q_- Amount of heat removed by the low temperature source;
- Q_+ Amount of heat provided to the generator.

The second connotation it can assume is the *electrical* COP, given by the following:

$$COP_E = \frac{Q_-}{Q_+} \quad (4.2)$$

- Q_- Amount of heat removed by the low temperature source;
- Q_+ Amount of work to perform the cycle.

Typical values of COP_T for single effect absorption chillers vary between 0.6-0.8.

Higher values can be achieved using a double effect chiller, reaching a thermal COP of around 1.0-1.2. Despite the better performance, double effect absorption chiller was not examined in the layout of the CCHP plant. The reason relies on the higher investment cost of this equipment, and the higher temperature required by the hot thermal source connected to the generator.

Emphasis must be placed on the fact that the COP_T of single effect absorption chiller is much lower than the one of electric chillers (4.0-8.0). However, while electric chillers run on electricity (considered the most valuable source available), absorption chillers use waste heat

(which has a value close to zero, considering the temperature level and the fact that it's a waste product).

In the following section, it will be explained how to properly model a single effect absorption chiller in eQuest[®] and the kind of upgrades performed by Cicciarella in his past thesis [4].

4.2 Modeling the Absorption chiller in eQuest[®]

The necessity of improving the standard model provided by the software represents a key point in order to obtain accurate results during the analysis of the performance of the trigeneration system.

To implement the single stage absorption chiller, eQuest[®] requires the definition of five main curves:

- *Capacity percentage* in function of the *chilled water temperature*;
- *COP percentage* in function of the *chilled water temperature*;
- *COP* in function of the *condenser temperature*;
- *Capacity percentage* in function of the *condenser temperature*;
- *COP percentage* over the *partial load ratio*.

The *capacity percentage* represents the percentage of cooling capacity available and is defined as the ratio of the capacity in a specific condition over the design capacity. Similarly, the *COP percentage* is the ratio of the COP in a particular condition over the design COP.

Furthermore, the *chilled water temperature* (CWT) refers to the temperature of the cold

water source needed by the user (it's set by the user). On the other hand, the *condenser temperature* is strictly linked to the external ambient temperature, under the simplifying assumption of constant rejected thermal energy operated by the cooling tower. The curves appearing in the following section were elaborated through the analysis of the technical specifications of the *Millennium YIA*™, manufactured by *YORK*® [18] [19]. A detailed set of instructions has been provided in Appendix B in order to correctly model the absorption chiller in eQuest®.

4.2.1 Influence of the Chilled Water Temperature

The CWT has a strong significance in the performance of the chiller. As shown in Figure 30, a decrease in temperature lowers the capacity percentage of the equipment. This is related to a decrease of the evaporator temperature.

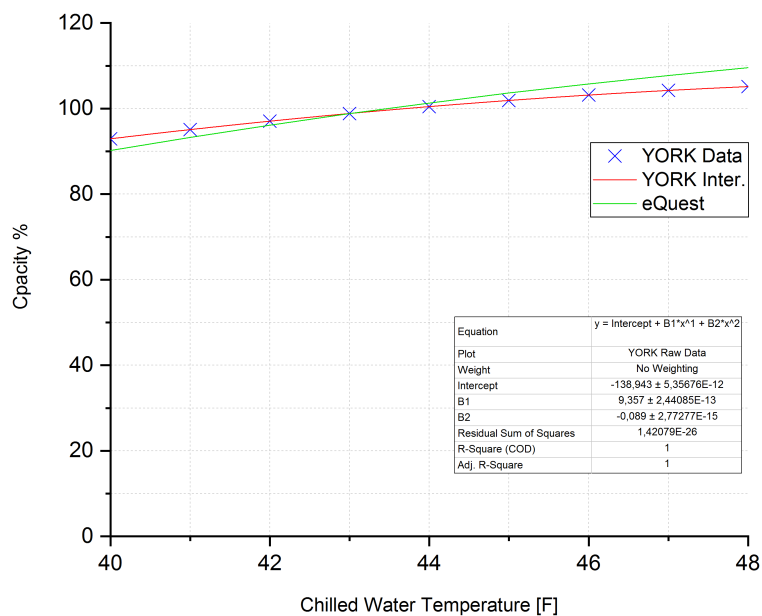


Figure 30: Absorption chiller performance - Capacity Percentage vs Chilled Water Temperature - comparison between YORK model and eQuest model.

It is possible to observe that 100% of the capacity is reached when the CWT is at 44 °F (at a constant condenser temperature of 85 °F). These values are imposed by the ARI 550/590 standard; therefore, the curve was normalized adopting these reference values (CWT 44 °F, condenser temperature 85 °F) [20]. The steepness of the curve reflects a major influence of the

CWT over the percentage capacity for the previous eQuest[®] model. The improved relationship is represented by Equation 4.3 which replaces the previous one, Equation 4.4.

$$Cap\%_{YORK} = -0.089 x^2 + 9.357 x - 138.943 \longrightarrow x = CWT \quad (4.3)$$

$$Cap\%_{eQuest} = -0.089 x^2 + 10.247 x - 177.261 \longrightarrow x = CWT \quad (4.4)$$

YORK[®] does not provide information about the influence of CWT over the COP percentage, although it does provide a relationship between the CWT and the fuel consumption percentage, as shown in Figure 31.

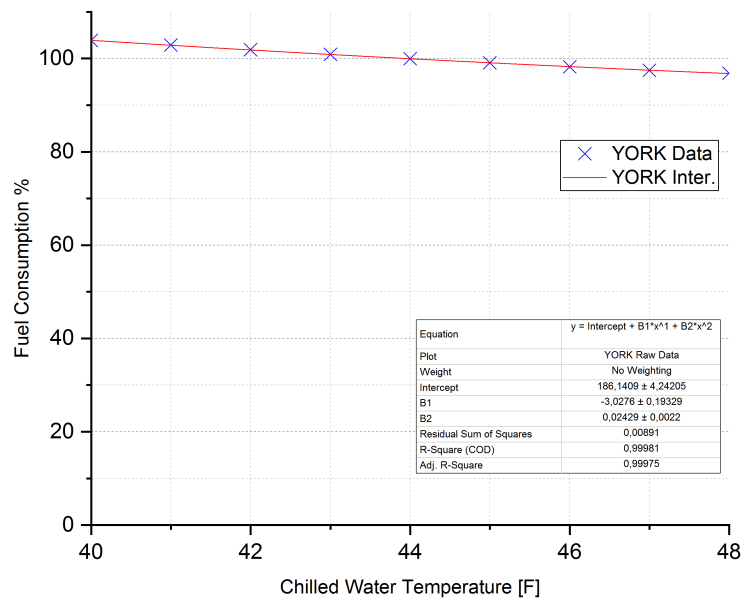


Figure 31: Absorption chiller performance - Fuel Consumption vs Chilled Water Temperature
- YORK model.

Combining the information on the effect of CWT over the capacity percentage and the fuel consumption percentage it is possible to model the values of COP percentage according to the CWT.

$$COP\% = \frac{COP}{COP_{des}} = \frac{\frac{Cooling\ Capacity}{Fuel\ Consumption}}{COP_{des}} = \frac{(Cool. Cap)_{des} \cdot Cap\%}{(Fuel\ Cons.)_{des} \cdot Fuel\ Cons.\%} = \quad (4.5)$$

$$COP\% = \frac{COP_{des} \cdot \frac{Cap.\%}{Fuel\ Cons.\%}}{COP_{des}} = \frac{Cap.\%}{Fuel\ Cons.\%} \quad (4.6)$$

The curve representing the COP percentage variation with respect to the CWT is illustrated in Figure 32. Equation 4.7 replaces Equation 4.8.

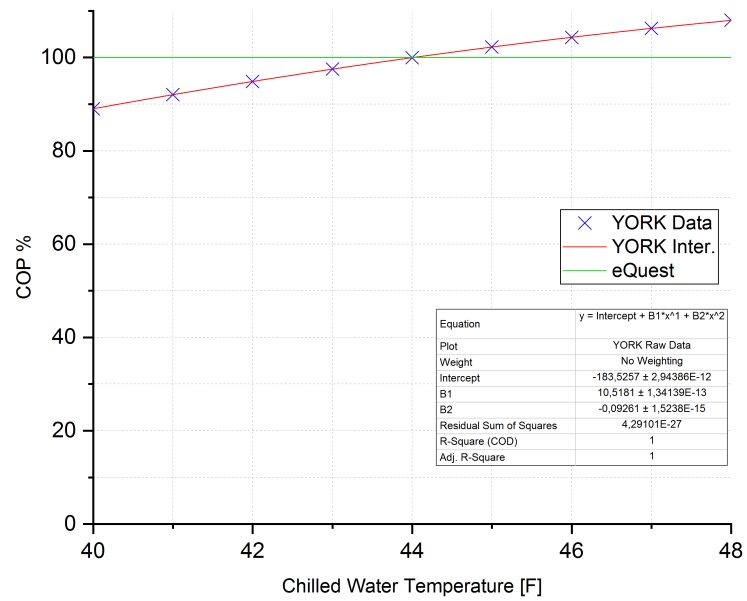


Figure 32: Absorption chiller performance - COP Percentage vs Chilled Water Temperature - comparison between YORK model and eQuest model.

$$COP\%_{YORK} = -0.093 x^2 + 10.518 x - 183.526 \longrightarrow x = CWT \quad (4.7)$$

$$COP\%_{eQuest} = 100 \quad (4.8)$$

The COP at the design condition of the *Millennium YIA*™ is 0.75, while the one modeled in eQuest® is 0.65. Figure 33 shows a comparison between the two models. The previous model considered the COP percentage independent from the variation of CWT.

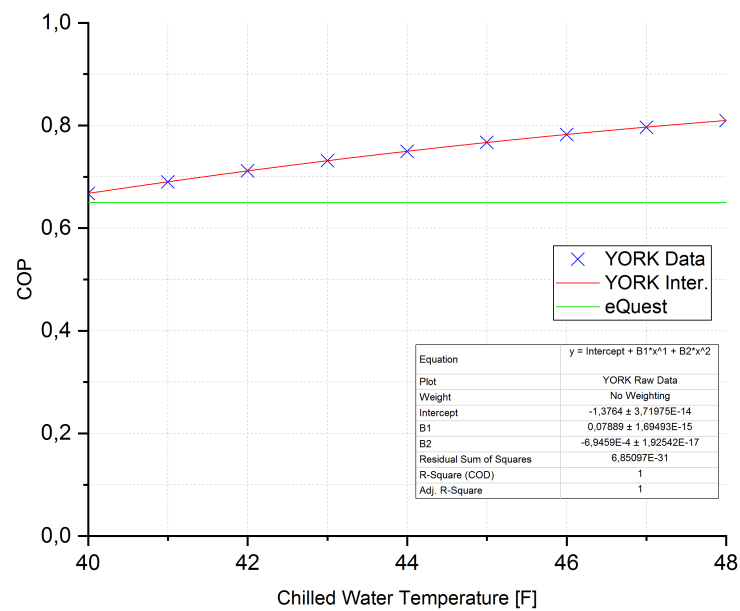


Figure 33: Absorption chiller performance - COP vs Chilled Water Temperature - comparison between YORK model and eQuest model.

Even though a detailed analysis of the effect of CWT over the performance of the chiller was elaborated, a basic assumption was made. The CWT requested by the user is constantly 44 °F. This means that the curves were normalized assuming 100% of cooling capacity and COP at 44 °F, following ARI 550/590 standard.

4.2.2 Influence of the Condenser Temperature

The manufacturer provided a curve representing the relationship between the condenser temperature and the COP percentage, Figure 34. This data was obtained maintaining a constant CWT of 44 °F.

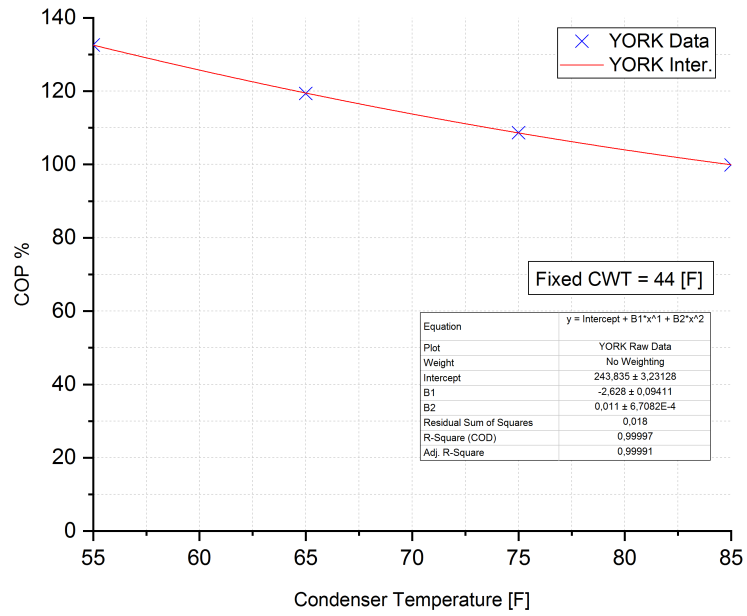


Figure 34: Absorption chiller performance - COP Percentage vs Condenser Temperature - YORK model.

The equation describing the behavior modeled in Figure 34 is the following:

$$COP\%_{YORK} = 0.011x^2 - 2.628x + 243.835 \rightarrow x = \text{Condenser } T. \quad (4.9)$$

Obviously, the 100% of the COP is obtained with a condenser temperature of 85 °F (ARI 550/590 standard). A comparison between the updated model and the eQuest[®] one is shown in Figure 35. Indeed Equation 4.10 substitutes Equation 4.11.

$$COP_{YORK} = 9e-5 x^2 - 0.021 x + 1.898 \longrightarrow x = \text{Condenser } T. \quad (4.10)$$

$$COP_{eQuest} = -2e-5 x^2 - 0.003 x + 1.054 \longrightarrow x = \text{Condenser } T. \quad (4.11)$$

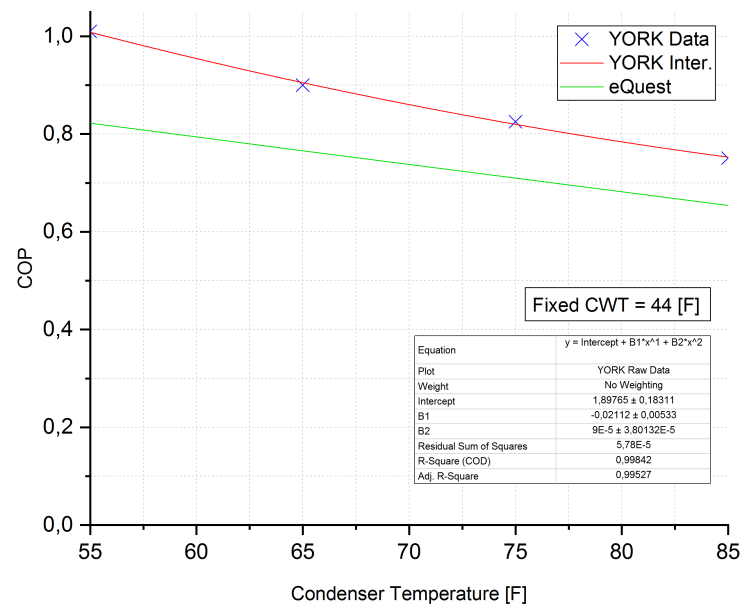


Figure 35: Absorption chiller performance - COP vs Condenser Temperature - comparison between YORK model and eQuest model.

In Figure 36 it is demonstrated the effect of the condenser temperature variation over the cooling capacity.

$$Cap\%_{YORK} = -1e-3x^2 - 0.692x + 165,928 \rightarrow x = Condenser\ T. \quad (4.12)$$

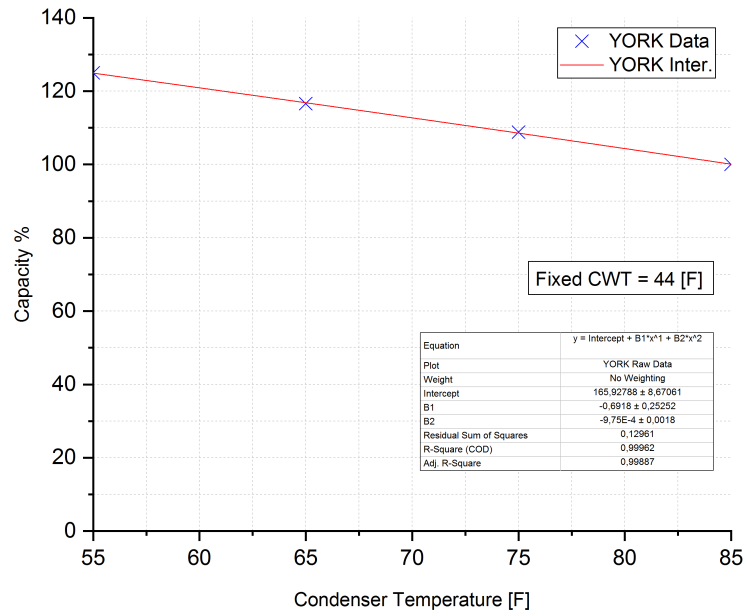


Figure 36: Absorption chiller performance - Capacity Percentage vs Condenser Temperature - YORK model.

4.2.3 Partial Load Performance

A main role in the convenience of the implementation of this equipment is represented by its performance in off-design conditions. In fact, the relationship between the PLR and the COP needs to be analyzed.

In the layout of the CCHP plant the absorption chiller will be ran by the *Wasted Recovered Heat* connected to the *Space Heating Hot Water loop*. This means that the availability of

recovered thermal energy will not always be granted, since the prime mover is adopting a FEL strategy. Furthermore, the cooling needs of the building are not always constant.

Therefore, the importance of having an absorption chiller that behaves properly also in partial load conditions assumes a primary concern.

The model describing the COP in function of the PLR is provided in Figure 37.

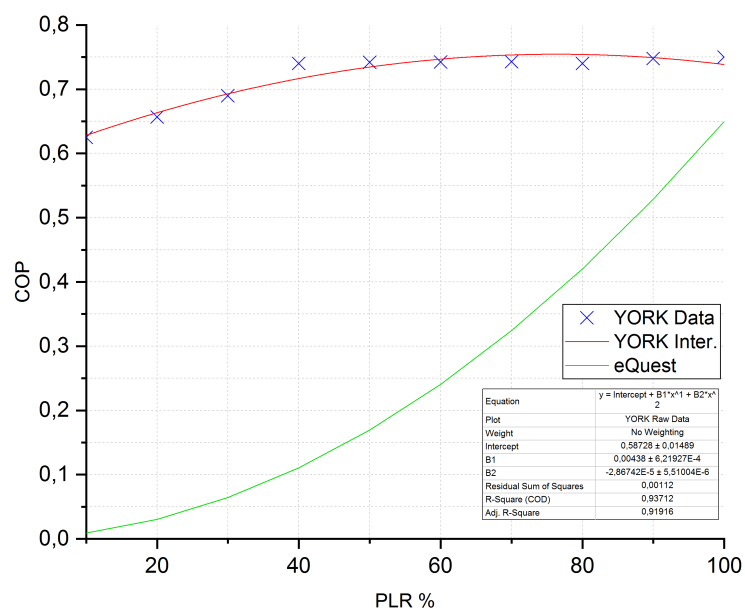


Figure 37: Absorption chiller performance - COP vs Partial Load Ratio - comparison between YORK model and eQuest model.

The *Millennium YIA*TM shows a drastic improvement in partial load conditions compared to the eQuest[®] model. This analysis encourages the implementation of this technology to satisfy the significant cooling load during warmer months. Equation 4.13 replaces Equation 4.14.

$$COP_{YORK} = -3e-5 x^2 + 0.004 x + 0.587 \longrightarrow x = PLR \quad (4.13)$$

$$COP_{eQuest} = 6e-5 x^2 + 0.001 x + 3e-5 \longrightarrow x = PLR \quad (4.14)$$

4.3 Layout of the Plant

The layout of the CCHP plant is similar to the one of the CHP plant studied in Chapter 3. An increased complexity regards the adoption of the single stage absorption chiller in the *Cold Water loop*.

The same considerations regarding the creation of the CHP plant are valid for the trigeneration system. The definition of the energy fluxes given in Section 3.1.1 remains unchanged, as well as the operating strategy of the plant (Section 3.1.2) and the merging of the *Domestic Hot Water loop* into the *Space Heating Hot Water loop* (Section 3.2).

Figure 38 shows the layout of the plant on eQuest[®].

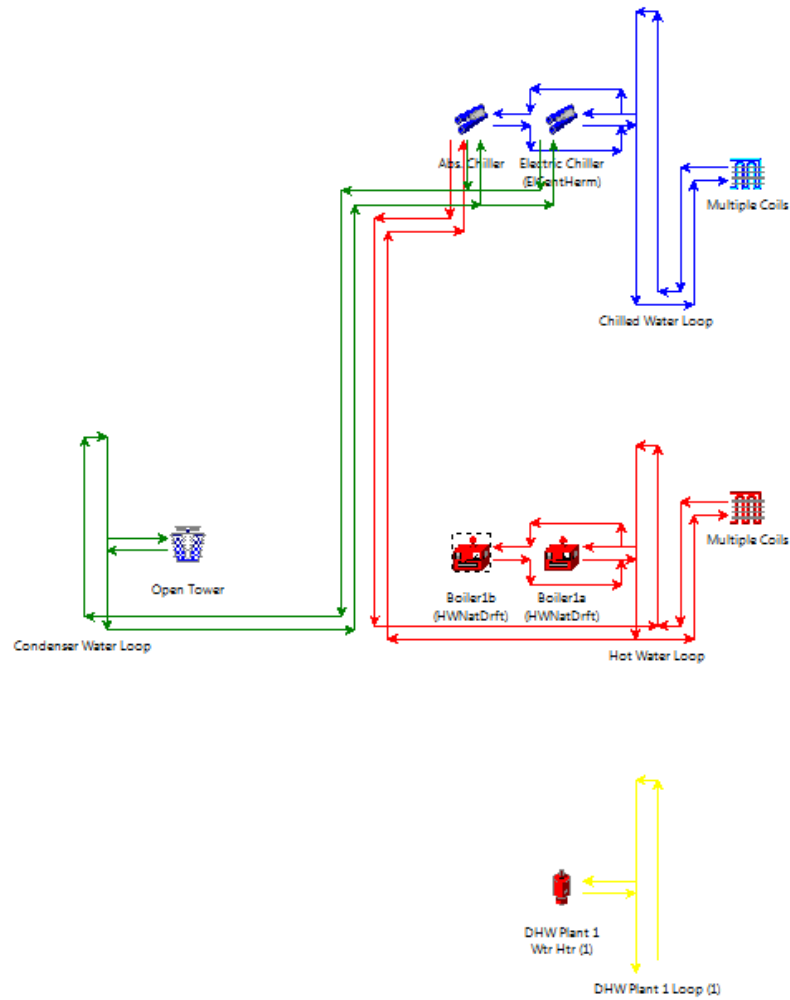


Figure 38: eQuest[®] layout of the CCHP plant.

The prime mover, which is not illustrated, is considered to be a gas turbine. The absorption chiller is connected to the *Space Heating Hot Water loop* in order to receive the hot thermal

energy recovered from the exhaust gasses. Furthermore, the chiller is connected to a cooling tower, for the discharge of the heat produced during the process, and obviously, it is integrated into the *Cold Water loop* to provide its cooling effect. An electric chiller is introduced as a backup in case the lack of *Recovered Heat* would not enable the proper functioning of the absorption chiller, or during the peak cooling loads, which cannot be solely fulfilled by a single chiller.

Through the introduction of a control system, the plant was imposed to prioritize the use of the absorption chiller over the electric one.

No additional changes were made to the heating system, beside the ones already mentioned in the introduction of the CHP plant (Section 3.2), which were the establishment of the *Heat Recovery loop*, and the merging of the *Domestic Hot Water loop* into the *Space Heating Hot Water loop*. Figure 39 illustrate a logical scheme in which are clearly depicted the benefits provided by the introduction of a CCHP plant in terms of energy production (cold, hot, and power).

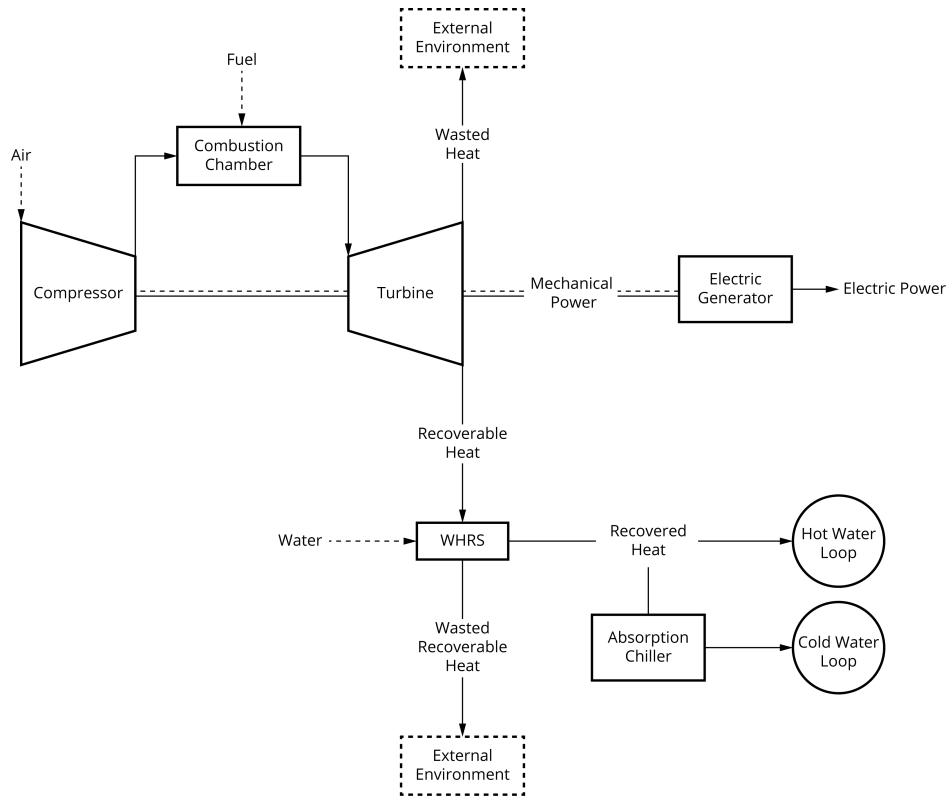


Figure 39: CCHP system working scheme.

4.4 Sizing of the Plant

The correct sizing of the plant should satisfy most of the thermal load requested by the health care facility. Figure 40 shows that the heat demand is mainly during colder months, while it drops drastically during warmer months. On the opposite, the cooling energy consumption is high during warmer months, while its almost null during the cold ones. The introduction of an absorption chiller allows a better exploitation of the WRH, through the

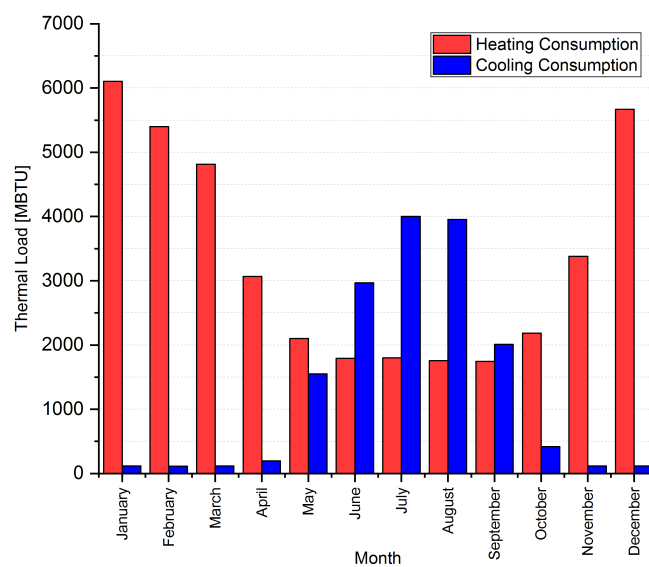


Figure 40: Thermal energy consumption of the hospital - *base model*.

fulfillment of the cold thermal energy needs of the hospital.

The same range of turbine sizes analyzed in Chapter 3 was considered (from 600 kW to 1,300 kW). A problem was encountered in the correct sizing of the chiller, which resulted in a significant increase in the fuel consumption of the boiler connected to the *Space Heating Hot Water loop*. The reason was strictly connected to the improper management of the absorption chiller control system, regulated by eQuest[®].

Despite the lack of *Recovered Heat* (hot source for the absorption chiller), which should have prevented the functioning of the chiller, the software prioritized the use of this equipment over the electric one. Doing so, the system was forced to produce hot water through the use of the

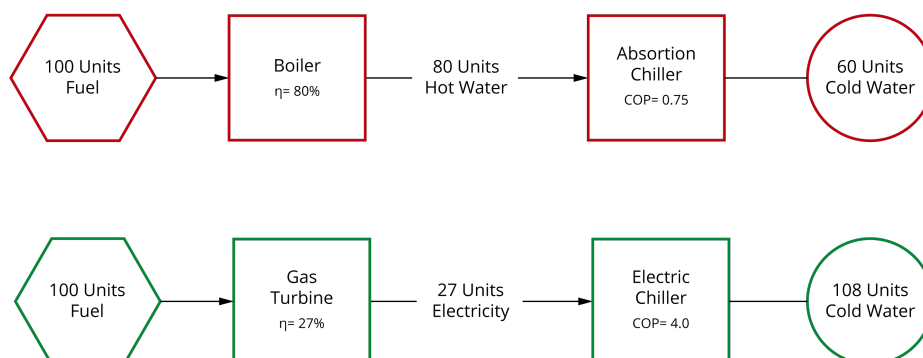


Figure 41: Efficiency loss due to the improper management of the absorption chiller.

boiler, in order to allow the operation of the absorption chiller.

This management strategy represents a significant reduction in terms of efficiency if compared to a solution where the absorption chiller is sized accordingly to the *Recovered Heat* available. The comparison of the performance between a system using exclusively an absorption chiller and one using a combination of absorption and electric chillers is represented in Figure 41. For a correct operation of the system, the absorption chiller should be used until the entire amount of *Recoverable Heat* available has been turned into *Recovered Heat*. Once the *Recovered Heat* has been entirely exploited, the electric chiller should cover the rest of the user's request.

For this reason, a correct sizing procedure of the absorption chiller must be evaluated. An empiric approach has been adopted, based on the analysis of the boiler's fuel consumption, and the amount WRH coming from the cogeneration system (it represents the heat source allocated to the operation of the absorption chiller in the case of a trigeneration plant).

For instance, the fuel consumption of the boilers should not increase in comparison to the case of a CHP plant, in fact the introduction of the absorption chiller shall not cause this negative effect. Various sizes of chillers were tested, if an higher fuel usage was noted, the chiller's capacity was decreased. On the other hand, starting from the maximum and minimum values of WRH (highly fluctuating values) generated by the cogeneration plant during the summer months, an increment of the absorption chiller's capacity was provided in order to correctly recover most of the WRH.

The final results are summarized in Table VII, culminating in a trade-off between the fully exploitation of the *Recoverable Heat*, and an unchanged boiler's consumption profile.

The introduction of thermal energy storage in the plant, will allow a reduction in the fluctuation of the WRH as well as increasing its amount, enabling a minor increment in the chiller's size (Section 5.5).

4.5 Improvements in Source Energy Consumption

The implementation of a CCHP plant focuses on the need of fulfilling every load requested by the facility: heating, cooling, and electric power.

Compared to the CHP facility, the main difference relies in the introduction of the absorption chiller in the cooling system. The implementation of this technology is intended to satisfy part of the cooling load of the hospital, resulting in a lower utilization of the electric chiller, especially during summer months (electric peak demand period). This has produced a decrease of peak electricity consumption of the facility, and, in general an overall reduction of the power consumption. Table VIII summarizes the reduction in electricity peak consumption in

TABLE VII: INSTALLED ABSORPTION CHILLER SIZES.

Size [kW]	WRH Availability (min / max) [MBTU/h]	Est. Chill. Cap. (min / max) [MBTU/h]	Installed Chiller Cap. [MBTU/h]	Installed Chiller Cap. [tons]
600	2.0 / 3.0	1.6 / 2.4	1.8	150
700	2.7 / 3.7	2.2 / 3.0	2.7	225
800	3.6 / 4.4	2.9 / 3.5	3.2	267
900	4.0 / 5.0	3.2 / 4.0	3.6	300
1,000	4.9 / 5.8	3.9 / 4.6	4.0	333
1,100	5.6 / 6.6	4.5 / 5.3	4.5	375
1,200	6.0 / 7.0	4.8 / 5.6	5.0	417
1,300	7.0 / 9.0	5.6 / 7.2	5.8	483

TABLE VIII: REDUCTION IN ELECTRIC PEAK DEMAND: COMPARISON BETWEEN A CHP AND A CCHP SYSTEM.

Size [kW]	Abs. Chiller Size [tons]	Elec. Peak Demand CHP [MW]	Elec. Peak Demand CCHP [MW]	Percentage Reduction
600	150	1.52	1.44	5.3%
700	225	1.43	1.33	7.0%
800	250	1.34	1.23	8.2%
900	300	1.25	1.13	9.6%
1,000	333	1.15	1.03	10.4%
1,100	367	1.06	0.93	12.3%
1,200	416	0.97	0.83	14.4%
1,300	483	0.88	0.6	31.8%

TABLE IX: VARIATION IN ELECTRICITY CONSUMPTION [MWH]: COMPARISON BETWEEN A CHP AND A CCHP SYSTEM.

Size [kW]	CHP Plant			CCHP Plant		
	Produced	Purchased	Total	Produced	Purchased	Total
600	5,200	4,185	10,015	5,200	4,225	9,425
700	6,066	3,949	10,015	6,059	3,361	9,420
800	6,906	3,109	10,015	6,847	2,533	9,379
900	7,630	2,385	10,015	7,517	1,815	9,368
1,000	8,266	1,750	10,015	8,081	1,284	9,365
1,100	8,788	1,227	10,015	8,552	809	9,361
1,200	9,220	795	10,015	8,941	412	9,352
1,300	9,495	520	10,015	9,141	209	9,349

comparison to the CHP plant. Increasing the capacity of the turbine, enables to have higher values of *Recoverable Heat*, therefore allows the installation of larger absorption chillers. The larger the size of the chiller (the lower the load that the electric chiller has to satisfy), the more evident is the decrease in the peak electric consumption. The reduction in the overall electricity consumption are shown in Table IX. The reduction of the electric consumption has multiple effects that need to be analyzed:

- Reduction in electricity consumption and demand resulting in an increased PLR operations for the gas turbine (especially for larger sizes);
- Reduced amount of electricity production, which means a reduced amount of *Recoverable Heat*;

- Increased PLR operation, decreasing the efficiency of the prime mover, and arising the amount of *Recoverable Heat*.

These effects have a different impact depending on the size of the gas turbine and the original operating conditions. In particular, smaller gas turbine (600 kW and 700 kW) will continue to work at full load conditions also in the CCHP plant configuration. This results in the same turbine fuel consumption compared to a cogeneration layout, and a slight increase of the boiler fuel consumption due to the operation of the absorption chiller (acceptable negative effect).

On the other hand, larger prime movers are affected by a reduction of the full-load working hours. From the study conducted on the gas turbine (Section 2.2), it was found that a lower PLR condition resulted in a lower efficiency of the equipment. This means an overall decline in the performance. A lower efficiency means an increased fuel consumption, assuming the same power output. Additionally, this decrease reflects a major quantity of wasted heat, which could have been exploited by the heating system during the colder months, and by the absorption chiller during the warmer period.

Furthermore, in larger turbines, the reduction of electricity demand obviously affected the fuel consumption of the prime mover, which eventually reduced its electricity output and its fuel consumption, balancing out the increment due to the worsening of the performance. The decrease of the overall fuel consumption of the prime mover compared to a cogeneration plant is summarized in Table X. Meanwhile, the fuel consumption of the gas boilers remained practically unchanged compared to the one of the CHP plant.

TABLE X: VARIATION IN FUEL CONSUMPTION [MBTU]: COMPARISON BETWEEN A CHP AND A CCHP SYSTEM.

Size [kW]	CHP Plant		CCHP Plant	
	Fuel Gas Turbine	Overall Fuel Consumption	Fuel Gas Turbine	Overall Fuel Consumption
600	59,922	74,752	59,922	75,865
700	69,908	82,829	69,807	83,199
800	79,978	92,738	79,195	91,900
900	90,321	102,960	88,695	101,312
1,000	100,585	112,561	97,938	109,832
1,100	110,781	122,297	107,405	119,132
1,200	120,718	131,938	116,717	128,468
1,300	130,642	141,675	125,562	136,916

4.6 Efficiency Analysis

Similarly to Section 3.4, a study was conducted in order to understand which layout brought the major improvement to the efficiency of the plant.

The introduction of the absorption chiller enabled the recovery of a larger quantity of heat. This quantity was mainly used by the heating system in colder months ($Q_{rec.}$, similarly to the CHP plant), while it was exploited by the cooling system during summer months ($Q_{abs.}$).

This extremely high value of *Recovered Heat* can be misleading in the interpretation of the efficiency of the plant. Especially during summer, the *Recovered Heat* contributes to the operation of the absorption chiller, which has a very low COP (0.75). This results in a much

lower quantity of cooling output, which will be referred as $Q_{abs.}$. In other words, during colder periods the $Q_{rec.}$ is entirely used by the heating system, while, during warmer months only 75% of the $Q_{rec.}$ is converted into cooling load.

Therefore, in the calculation of the parameters η_{CHP} and η_{FERC} the $Q_{rec.}$ (appearing in the numerator of Equation 3.3 and Equation 3.4) was considered made up of the entire *Recovered Heat* excluding the part that ended up feeding the absorption chiller, which was converted into $Q_{abs.}$.

The approach involving the analysis of the $PRSEC$ parameter (Equation 3.8) was maintained unvaried. A modification in the evaluation of the $PRSEC_{GT}$ was introduced in order to take into account the benefits provided by the CCHP system in terms of electricity reduction. Equation 3.11 was changed into the following:

$$PRSEC_{GT} = 1 - \frac{[SE_{F.PM.}]_{CCHP}}{[SE_{Q_{rec.}} + SE_{E_{PM.}} + SE_{Q_{abs.}}]_{CONV}} \quad (4.15)$$

$$PRSEC_{GT} = 1 - \frac{[F_{PM} \cdot AF_{NG}]_{CCHP}}{[F_B \cdot AF_{NG} + E_{PM} \cdot AF_E + E_{abs.} \cdot AF_E]_{CONV}} \quad (4.16)$$

$$PRSEC_{GT} = 1 - \frac{[F_{PM} \cdot AF_{NG}]_{CCHP}}{[\frac{Q_{rec.}}{\eta_B} \cdot AF_{NG} + E_{PM} \cdot AF_E + \frac{Q_{abs.}}{COP} \cdot AF_E]_{CONV}} \quad (4.17)$$

- $SE_{F.PM.}$ Source energy consumption associated with fuel for the prime mover;
- $SE_{Q_{rec.}}$ Source energy consumption associated with fuel consumption to replace $Q_{rec.}$;
- $SE_{E_{PM.}}$ Source energy associated with the electricity produced by the gas turbine;
- F_{PM} Fuel consumption of the prime mover;

- F_B Fuel consumption of the boilers to replace the recovered heat $Q_{rec.}$;
- E_{PM} Electricity produced by the prime mover;
- $E_{abs.}$ Electricity used to produce $Q_{abs.}$ with the electric chiller;
- $Q_{rec.}$ Heat recovered by the CCHP system (excluding the one for the absorption chillers);
- $Q_{abs.}$ Cooling load satisfied by the absorption chiller;
- η_B Average efficiency of the boilers;
- COP Average coefficient of performance of the electric chiller;
- AF_{NG} ASHRAE conversion factor for natural gas;
- AF_E ASHRAE conversion factor for electricity;

Assuming a boiler efficiency of 82% (same as in the cogeneration case) and an electric chiller COP of 4.0, the results are summarized in Table XI. The definition of the abbreviations adopted in Table XI is given in Appendix D.

TABLE XI: PERFORMANCE OF THE CCHP BY INSTALLED TURBINE SIZE.

Size [kW]	F_B [MBTU]	F_{PM} [MBTU]	$Q_{rec.}$ [MBTU]	E_{PM} [MWh]	$E_{pur.}$ [MWh]	η_{CCHP}	PRSEC	PRSEC _{GT}
600	15,942.1	59,922.3	24,779.5	5,200.2	4,225.8	73.6%	21.7%	33.8%
700	13,393.2	69,807.9	26,768.6	6,066.4	3,361.6	70.3%	22.6%	31.5%
800	12,706.5	79,195.7	28,099.1	6,906.1	2,533.9	67.2%	22.7%	29.4%
900	12,617.2	88,695.3	28,914.6	7,630.8	1,851.2	63.6%	21.0%	26.2%
1,000	11,894.7	97,938.3	29,450.2	8,266.3	1,284.7	60.1%	19.3%	22.7%
1100	11,726.5	107,405.6	29,793.1	8,788.9	809.1	56.7%	16.4%	18.6%
1,200	11,751.2	116,717.1	30,035.7	9,220.5	412.5	53.6%	12.9%	14.4%
1,300	11,354.2	125,562.4	30,177.6	9,495.8	209.2	50.5%	8.8%	9.4%

From the results shown in Table XI it is evident that a better exploitation of the source energy enables the trigeneration system to reach higher performance parameters compared to the cogeneration system (Table V).

The increment of the engine size results in a decrease of the overall efficiency of the system (η_{CCHP}). This is mainly because of the longer PLR periods for larger turbine's capacities, and due to the higher values of WRH. The larger the prime mover's size, the higher will be the fluctuation of the *Recoverable Heat* available, the harder will be its correct exploitation.

Although, it is evident that for larger turbines, the improvements in the values of *PRSEC*

and $PRSEC_{GT}$ are more evident if compared to the CHP plant. The reason relies in the fact that bigger turbines imply the use of larger absorption chillers, which resulted in a higher impact on the overall system electric consumption.

This favors the utilization of a larger turbine compared to the CHP system (700 kW). The 800 kW turbine enables to reach a value of PRSEC of 22.7%. Much higher in comparison to the optimal cogeneration plant that had a PRSEC of 19.0%.

CHAPTER 5

THE THERMAL ENERGY STORAGE

A *thermal energy storage* (TES) equipment is defined as a device capable of storing energy at high or low temperatures for later use, it's basically an energy "holding" for a later exploitation of the source [23]. The two most common ways in which this component stores energy involve modifying the temperature level of the substance used for the storage (sensible TES), or changing its phase (latent TES). This kind of technology has attracted increasing interest during the past years, due to the variety of thermal applications in which it can be used, such as space and water heating, cooling, and air conditioning.

TES becomes particularly useful in the case of a temporal mismatch between the building loads and the availability of the energy. In facilities and systems that rely on the recovery of waste heat, and in which the energy loads vary on daily bases, TES plays a fundamental role in terms of fuel savings and in the overall improvement of the system's efficiency.

As an example, if this technology is implemented into the CHP system studied in Chapter 3, it could be possible to store thermal energy when the quantity of *Recovered Heat* exceeds the building's consumption, and later use this energy when the *Recovered Heat* cannot meet the thermal loads requested.

5.1 Benefits of TES

Considering various studies conducted over the years, major benefits resulting from the application of this technology are listed below [23][24][25]:

- **Increasing generation capacity:** the installation of a TES system can improve the generation of thermal energy. The excess heat available during off-peak periods can be stored and used during on-peak hours. This benefit is particularly useful in the case of a CHP or CCHP plant adopting FEL strategy;
- **Enables better operation of a cogeneration/trigeneration plant:** if the plant is designed to follow the thermal load, it may happen that an excess of electricity is generated during periods of low power demand. By the addition of a TES, the thermal load can be met more easily, and the plant can be operated more steadily and efficiently;
- **Shift energy purchases at low-cost periods:** if the user is subject to temporally based energy rates, the storage of energy could be a useful strategy in order to shift energy purchase to a more convenient period, and use the stored energy when prices are higher;
- **Increase system reliability:** any form of energy storage improves the reliability of the system to which is applied;
- **Integration with other functions:** in fire protection applications, where water storage is mandatory, a water energy storage tank could be used with a double purpose;

- **Environmental benefits:** through a better exploitation of the energy, as well as an increase in the energy efficiency of the system, and a reduction in the peak load demand, TES can reduce *Green House Gasses* (GHG) and *Criteria Air Pollutant* (CAP) emissions.

5.2 Basic Principle of TES

In order to properly understand the process that enables a TES system to operate it is important to understand that the energy content of a substance strictly depends on its temperature. The higher the temperature, the higher the energy content is available. This basic concept is expressed by the following formula:

$$E = m c (T_2 - T_1) = \rho V c (T_2 - T_1) \quad (5.1)$$

- E Amount of energy required by a substance to go from T_1 to T_2 ;
- m Mass of the substance;
- c Specific heat of the substance;
- V Volume of the substance;
- ρ Density of the substance.

As already mentioned, TES technologies available on the market rely on two main types of strategies:

- Sensible heat storage;
- Latent heat storage.

The energy released by a material when its temperature is decreased, or the energy absorbed when its temperature is increased is called *sensible heat*. Considering this concept, the proper establishment of the operating temperatures, the size, and the substance adopted assume vital importance.

The correct understanding of *energy quality* assumes a key role in the proper design of the system: 1 kWh of energy can be stored by heating 1.1 tons (US) of water to 33.5 °F or by heating 22 lb of water to 186.8 °F. The higher the temperature, the higher the quality of energy contained in the substance due to the wider range of purposes that can be accomplished with the discharging of the system.

In general, parameters such as the space needed to install the TES system and the operating temperatures of the requested fluid are the main constraints to the design of this device.

Latent heat storage systems rely on the *latent heat*, which is associated with a change in the phase or state of the material, such as the *heat of fusion* which is required to melt paraffin wax or convert ice to water. However, latent heat storage systems have not been discussed, because the focus of this thesis falls on the adoption of a sensible heat storage system operated by water.

In recent years, another strategy adopted to store thermal energy was characterized by the use of reversible endothermic chemical reactions. Despite the fact that in some literature this is considered as a TES system, for the sake of clarity, in this work this technology has been considered as a chemical energy storage system, so it has not been treated.

Despite the difference in the meaning by which the thermal energy is stored, every storage

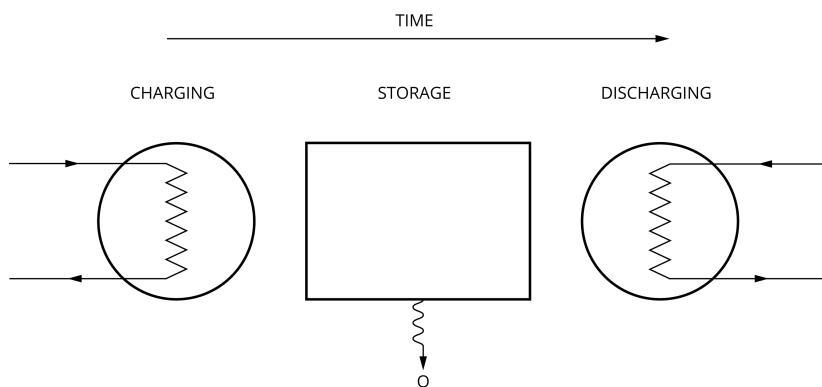


Figure 42: Charging, storage, discharging phases in a general TES system.

component undergoes the same process consisting in three different phases, as depicted in figure Figure 42:

- **Charge:** the heat flow enters the TES, increasing the amount of energy stored;
- **Storage:** the energy is properly preserved in the TES and a certain quantity of heat is lost towards the surrounding environment (in case of hot storage) or is gained by the TES (in case of cold storage);
- **Discharge:** the heat flow exits the TES, and contributes to the fulfillment of the thermal loads.

5.3 Evaluation Process

In order to allow the proper application of a thermal storage system into an existing facility, it is important to analyze different aspects affected by the integration of this equipment. Various

standards must undergo an assessment process (technical, energetic, sizing, and economic) to enable the correct design of the TES.

5.3.1 Technical Criteria

Even if technical criteria are specific to each kind of project, some basic ones are common to each application:

- Storage capacity and size;
- Storage strategy and application;
- Storage media used;
- Lifetime and material used for the construction;
- Installation constraints;
- Commercial availability.

To evaluate the feasibility of the installation, specific technical information must be acquired on the various types of storage (e. g. fully mixed tank, stratified tank, concrete tank, aquifer thermal storage) and their application (hot thermal storage or cold thermal storage). The size and capacity of the storage must reflect the commercially available dimensions and must respect the installation constraints such as the space needed for the installation.

5.3.2 Energetic Criteria

Key role in the evaluation of a TES system is the understanding of the impact that it has on the energy consumption and the overall efficiency of the plant. Depending on the system considered, the effects to be compared to the already existing plant are the following:

- Amount of source energy consumption;
- Maximum load and change in the electrical profile;
- Amount of stored energy;
- Efficiency of the TES;
- Efficiency of the plant;
- Thermal losses.

At some level, a properly designed TES system must produce a reduction of source energy consumption and decrease of the amount of hours the equipment of the facility operates at full load. This advantage could lead to a reduction in the sizing of certain equipment (if the TES partially satisfies the thermal load of the user, the boiler previously operated can be reduced in capacity), while increasing the capacity of others (a larger amount of *Recovered Heat* enable the operation of a larger absorption chiller).

5.3.3 Sizing Criteria

The correct sizing of the component still remains a matter of debate. As of today, a widely adopted sizing technique does not exist. In the development of this work a valuable method has been established, relying on a multi-criteria optimization strategy that focused on the energy savings and efficiency output of the system.

5.3.4 Economic Criteria

Strictly related to the energy savings achieved by the TES system are the economic criteria. In matter of fact, the economic evaluation justifies if every cost related to the TES (e. g.

investment, operation and maintenance) is acceptable compared to the savings produced. Some of the information considered are listed below:

- Investment cost;
- Operation and maintenance cost;
- Reduction of source energy consumption;
- Hourly loads for the peak day;
- Electricity demand charges and time-of-use costs;
- Financial incentives available.

In this thesis, the economic evaluation of the project will not be considered. This decision was taken for a simple reason, the economic analysis must be tailored on the client's characteristics. It may reach totally different conclusions depending on the type of energy contract the customer has (e. g. demand charges, time-of-use costs), and on the energy rates, which fluctuate daily. Therefore, in order to produce a generally accepted study of the benefits achievable by this technology, the focused remained on more technical aspects.

5.4 Coupling TES to the CHP system

The TES system implemented on the CHP plant already studied in Chapter 3 is a fully mixed tank using water as a storage media. The modeling technique and the sizing of the TES facility adopted will be discussed in this section. Moreover, the improvements in terms of energy savings and efficiency will be presented, with a specific comparison to the CHP plant without storage option. The fully mixed storage tank uses sensible heat to store energy: the amount of

stored energy is proportioned to the difference between the initial and the final temperature of the tank, the mass of the storage medium, and its heat capacity as explained in Equation 5.1.

Logically, the higher the specific heat and density of a substance, the better the ability to store thermal energy. Water has a bigger value of specific heat compared to other storage media, which makes it the most effective substance to operate in a range of temperatures required for building heating or cooling. On the other hand, rocks and ceramics, have a low value of specific heat, which is counterbalanced by a high value of density that enables them to operate through large temperature changes [26].

In Table XII are listed some of the thermal capacities of the most common materials used in TES applications. Water has the highest volumetric thermal capacity, is inexpensive and easy to pump, making it the most suitable storage media for the analyzed TES facility.

TABLE XII: THERMAL CAPACITIES AT 68 °F OF SOME COMMON TES MATERIALS.

Material	Density	Specific Heat	Volumetric Thermal
	[kg/m^3]	[$J/kg K$]	Capacity [$10^6 J/m^3 K$]
Clay	1,458	879	1.28
Brick	1,800	837	1.51
Sandstone	2,200	712	1.57
Wood	700	2,390	1.67
Concrete	2,000	880	1.76
Glass	2,710	837	2.27
Aluminum	2,710	896	2.43
Iron	7,900	452	3.57
Steel	7,840	465	3.68
Gravelly Earth	2,050	1,840	3.77
Magnetite	5,177	752	3.89
Water	988	4,182	4.17

After having defined the type of storage used and its storage media, the operating temperature must be defined. The TES facility must be attached to a charge loop in order to accumulate thermal energy, and a discharge loop in which release the stored energy. The *Heat Recovery loop* has been selected as the charge loop, assuming an exhaust gas temperature between 850 °F and 950 °F. The maximum operating temperature of the storage tank was set at 200 °F. Reasonably, since the free surface of the water tank was considered being at atmospheric pressure, higher temperatures were not considered in order to avoid phase changes. The minimum operating temperature was fixed at 170 °F, the same operating temperature of the *Space Heating Hot Water loop*, which has been assumed to be the discharge loop.

Once the operating substance was decided (water at 185 °F: $\rho = 8.078 \text{ lb}_m/\text{gal}$, $c_p = 1.004 \text{ Btu}/\text{lb}_m\text{°F}$) and the maximum and minimum operating temperature were established, the capacity of the storage is a function only of its volume, as expressed in Equation 5.1. The various storage dimension considered throughout this thesis are mentioned in Table XIII. The last

TABLE XIII: DIFFERENT SIZES OF TES MODELS.

TES Model	Model 1	Model 2	Model 3	Model 4	Model 5	Model 6
Volume [gal]	11,800	14,000	20,000	26,500	39,500	53,000

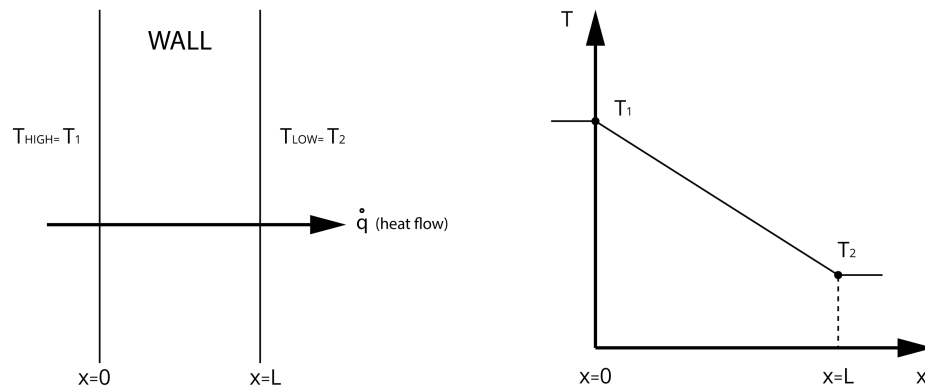


Figure 43: Temperature and heat flow during conductive heat transfer.

parameter needed to properly model the TES facility is the *Heat Loss Coefficient*.

A detailed set of instruction has been provided in Appendix C in order to properly define the implementation of the hot thermal storage.

5.4.1 Thermal Losses

Heat transfer processes are classified into three types: conduction, convection and radiation (the latter will not be discussed in this work because its not involved in the analyzed process).

Conduction is defined as a transfer of thermal energy through a solid affected by a temperature gradient without bulk motion of the matter (e. g. wall and insulation of the TES tank), as shown in Figure 43. Conductive heat transfer is a function of the different temperatures

involved in the process, and of the geometrical and thermal properties of the material [27]. The process can be defined using the one-dimensional form of *Fourier's law of heat conduction*:

$$\dot{q} = -k \frac{dT}{dx} \quad (5.2)$$

$$\dot{q} = \frac{\dot{Q}}{A} \implies \dot{Q} = -k A \frac{dT}{dx} = k A \frac{(T_{high} - T_{low})}{L} \quad (5.3)$$

- \dot{q} Heat flux;
- k Thermal conductivity;
- A Cross sectional area;
- L Thickness of the material;
- $(T_{high} - T_{low})$ Temperature difference across L .

The thermal conductivity is a well-tabulated property for a different number of materials, as shown in Table XIV.

TABLE XIV: THERMAL CONDUCTIVITY OF DIFFERENT MATERIALS.

Material	Steel	Water	Air	Brick	Wood	Rigid PU Foam
Th. Conductivity [Btu/h-ft-°F]	29.91	0.34	0.02	0.23	0.11	0.01

The second type of mechanism involved in the calculation of thermal losses from the TES system is the convective heat transfer, and it is referred as the transfer of thermal energy between a surface (e. g. external surface of the TES tank) and a moving fluid (e. g. air) at different temperature.

Convective heat transfer phenomena can be classified into three categories:

- Forced or assisted convection;
- Natural or free convection;
- Boiling or condensing processes (neglected for the purpose of this analysis).

Forced convection takes place when the fluid flow is caused by an external force, such as a pump or simply the wind.

Natural convection occurs when the fluid movement is triggered by buoyancy forces caused by a difference of density due to temperature variations in the fluid [28].

To better understand the convection process, the conditions of temperature and fluid velocity of a surface are schematically illustrated in Figure 44. The thickness δ' denominates the region of space attached to the surface in which the fluid velocity is very low ($c \sim 0$), therefore where most of the temperature difference occurs. Outside this layer, the temperature will assume a constant value $T = T_\infty$ (definition of δ'). The definition of the heat flux involved in the process is defined by the following equation:

$$\dot{q} = \frac{\dot{Q}}{A} \implies \dot{Q} = \frac{k(T_w - T_\infty)}{\delta'} \quad (5.4)$$

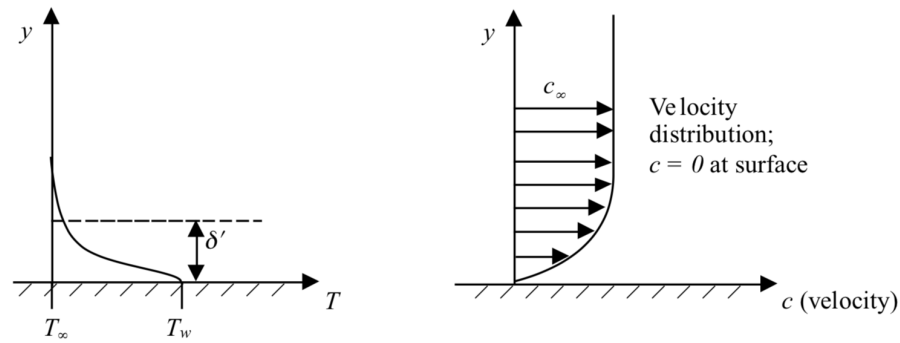


Figure 44: Temperature and velocity near a surface during convective heat transfer.

- \dot{q} heat flux;
- k thermal conductivity;
- A cross sectional area;
- δ' thickness of the layer;
- $(T_w - T_\infty)$ difference between the temperature reached and the one of the surface.

The thickness of the layer is not a fluid property and depends on various factors: velocity (Reynolds number), wall surface, pressure gradient and Mach number. Usually the quantity $\frac{k}{\delta'}$ is defined as well as the convective heat transfer coefficient (symbol h), that is calculated empirically. Equation 5.4 is referred as *Newton's law of cooling* and assumes the following definition:

$$\dot{Q} = Ah(T_w - T_\infty) \quad (5.5)$$

In the case of forced convection involving an air flow, the evaluation of h can be computed by the following experimental equation:

$$h = 10.45 - v + 10\sqrt{v} \quad (5.6)$$

where v is considered to be the relative speed between the object surface and the air (wind speed in [m/s]). The thermal losses involved in the TES tank are a combination of conductive and convective heat transfer process. The storage is assumed to have a cylindrical shape and to be located outdoors, in order to avoid space availability problems. Furthermore, the lower surface is considered to be in contact with the ground. This means that, for the sake of simplicity, only the upper and lateral surfaces are expected to loose heat.

A scheme of the tank's external surface has been depicted in Figure 45.

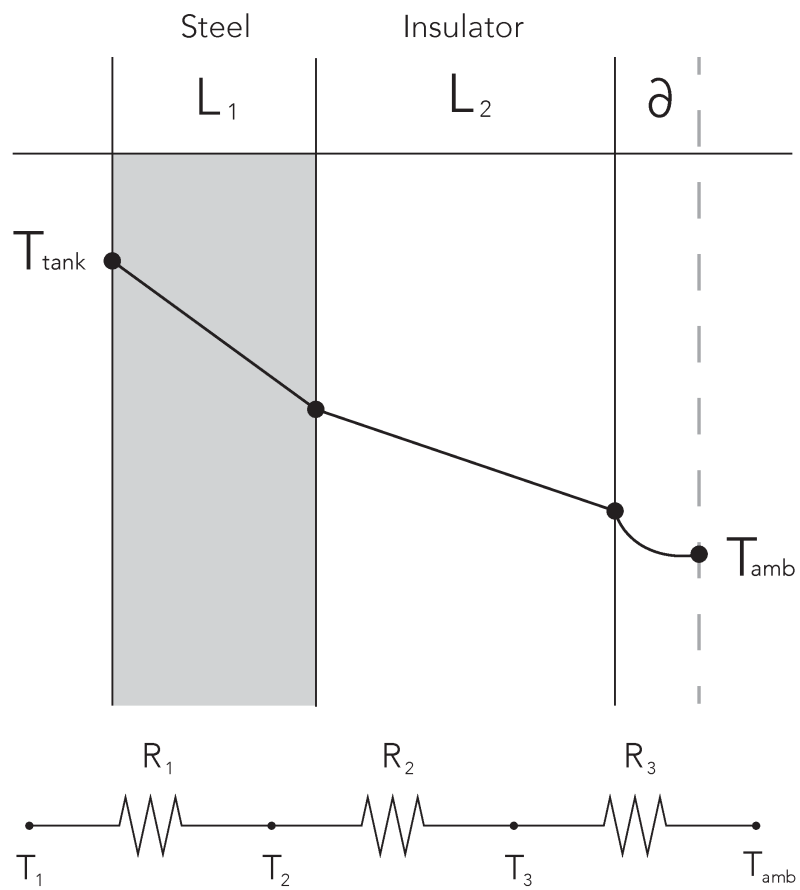


Figure 45: Surface of the TES affected by conductive and convective heat transfer.

The temperature of the internal surface (T_1) is assumed to be the same temperature of the fully mixed tank (T_{tank}), which varies between the minimum and maximum operating temperatures. Through the thickness of the steel surface (L_1) and the thickness of the insulation (L_2) the heat transfer is regulated by Equation 5.3:

$$\frac{\dot{Q}}{A} = k_{steel} \frac{(T_2 - T_1)}{L_1} \quad (5.7)$$

$$\frac{\dot{Q}}{A} = k_{ins.} \frac{(T_3 - T_2)}{L_2} \quad (5.8)$$

- T_1 Temperature of the tank;
- T_2 Temperature between the steel surface and the insulation (rigid PU foam);
- T_3 Temperature of the external surface;
- A Upper and lateral area of the storage;
- L_1 Thickness of the steel wall;
- L_2 Thickness of the insulation;
- k_{steel} Thermal conductivity of steel;
- $k_{ins.}$ Thermal conductivity of the insulation.

The convective heat transfer takes place between the external surface and the surrounding environment, according to Equation 5.4:

$$\frac{\dot{Q}}{A} = h (T_{amb} - T_3) \quad (5.9)$$

- T_{amb} Temperature of the external environment;
- h Convective heat transfer coefficient.

The convective heat transfer coefficient can be computed using Equation 5.6. The value of the wind speed and of the external temperature, as well as the temperature of the tank, are given by eQuest[®] on hourly basis.

The overall heat transfer process can be defined by the following equation:

$$\dot{Q} = \frac{(T_{amb} - T_1)}{R} \quad (5.10)$$

where R is defined as the total thermal resistance:

$$R = \frac{L_1}{A k_{steel}} + \frac{L_2}{A k_{ins.}} + \frac{1}{h A} \quad (5.11)$$

The *Heat Loss Coefficient* to input in eQuest[®] must be in BTU/h-F and it is equal to $1/R$. In Table XV are summarized the structural information on the different storage systems analyzed and the corresponding *Heat Loss Coefficient*. The information reported in Table XV were retrieved from *Advance Tank Co.*, a company specialized in the design and manufacturing of TES systems [29]. The material used for the insulation was Rigid PU foam ($k_{ins.} = 0.014$ BTU/h-ft-°F) and the one for the wall was steel ($k_{steel} = 29.912$ BTU/h-ft-°F).

TABLE XV: HEAT LOSS COEFFICIENTS FOR DIFFERENT TES MODELS.

TES Model	Height [ft]	Diameter [ft]	Wall Thickness [in]	Insulation Thickness [in]	Heat Loss Coefficient [BTU/h-°F]
Model 1	13.1	6.2	0.098	4.724	15.10
Model 2	13.1	6.8	0.098	4.724	17.15
Model 3	13.1	8.1	0.098	4.724	20.79
Model 4	13.1	9.3	0.098	4.724	24.79
Model 5	20.6	9.0	0.138	5.512	29.33
Model 6	26.2	9.3	0.197	5.905	34.55

5.4.2 Supply and Demand Mismatch

In order to evaluate the feasibility of implementing a TES facility into a CHP plant, the study of the supply and demand mismatch must be carried out [30]. In particular, the definition

of the Degree of Mismatch (DM) has been provided, which correlates the HPR of the system to the one required by the user.

Through the establishment of the DM, a relationship with the PRSEC has been evaluated. Considering the operating strategies and the loads of the CHP plant, this study has produced critical values of the DM above which the adoption of a TES-CHP system is considered feasible. To evaluate the maximum energy saving potential introduced by the storage system certain key assumptions were considered. It is assumed that all energy supply devices work steadily (e. g. gas turbine) under the rated condition, and that the TES device is an ideal one: negligible irreversible energy loss during the charging and discharging phase and sufficient tank's capacity to store the extra energy produced by the plant.

The definition of HPR was given in Equation 3.1, nevertheless it can be seen from two different prospective: from the demand side (indicated with d) or from the supply side (indicated with s):

$$HPR_d = \frac{\int_0^T \dot{Q}_d(t) dt}{\int_0^T \dot{E}_d(t) dt} = \frac{Q_d}{E_d} \leftarrow Q_d = H_d \quad (5.12)$$

$$HPR_s = \frac{\int_0^T \dot{Q}_s(t) dt}{\int_0^T \dot{E}_s(t) dt} = \frac{Q_s}{E_s} \quad (5.13)$$

- H_d Heating consumption of the building;
- Q_d Thermal energy consumption of the building (only heating);
- E_d Electric energy consumption of the building;
- Q_s Recoverable thermal energy from the plant;

- E_s Electric energy produced by the plant.

Accordingly, the DM can be defined by the following equation:

$$DM = \frac{HPR_d}{HPR_s} = \frac{Q_d}{Q_s} \cdot \frac{E_s}{E_d} \quad (5.14)$$

Based on the different operating strategies of the system the degree of mismatch can assume different meanings. However, since the plant is operating in FEL mode (as mentioned in section 3.1.2), the definition of the DM is the following:

$$E_s = E_d \implies DM = \frac{Q_d}{Q_s} \quad (5.15)$$

Its value can express three different situations:

- **DM=1:** supply precisely meets the consumption;
- **DM<1:** the heat load requested is satisfied, the extra heat produced by the system will be wasted;
- **DM>1:** the system does not produce enough heat to meet the demand, gas boilers will cover the lack of heat.

Even though this approach does not take into consideration the temporal supply-demand discrepancy, it takes into account the overall difference between the consumption and supply during the period under analysis.

The fulfillment of the demand represents a prerequisite in order to understand the feasibil-

ity of the TES-CHP system compared to conventional system. Obviously, the greater the gap between the DM and the unity, the greater will be the difference between supply and demand. This leads to the study of different scenarios, based on the different working conditions of the system.

In order to establish the potential energy saving deriving from the installation of TES over the *base model*, a correlation between the DM and the PRSEC must be evaluated.

The definition of the PRSEC has been already stated in Equation 3.7. In the *base model*, the electricity is purchased directly from the grid, while the heating load is satisfied using gas boilers.

So, having introduced the DM, the evaluation of the relationship between supply energy and consumption was summarized in Table XVI.

TABLE XVI: RELATIONSHIP BETWEEN CONSUMPTION AND SUPPLY FOR HEATING AND ELECTRICITY WORKING CONDITIONS.

System	Electricity Supply [E_s]	Thermal Supply [Q_s]
Base Model	E_d	$E_d \cdot HPR_s \cdot DM$
TES-CHP (FEL)	$DM \cdot E_d$	$E_d \cdot HPR_s \cdot DM$

Based on the values mentioned in Table XVI, it is possible to calculate the PRSEC with the following system, depending on the value of DM:

$$PRSEC = \begin{cases} 1 - \frac{\frac{1}{\eta_{grid}} + \frac{\eta_{GT}}{DM \cdot HPR_s}}{\frac{1}{\eta_{grid}} + \frac{\eta_{boiler}}{(DM-1)HPR_s}}, & \text{if } DM \leq 1 \\ 1 - \frac{\frac{1}{\eta_{GT}} + \frac{\eta_{boiler}}{DM \cdot HPR_s}}{\frac{1}{\eta_{grid}} + \frac{\eta_{boiler}}{DM \cdot HPR_s}}, & \text{if } DM > 1 \end{cases} \quad (5.16)$$

Based on the assumption that the gas turbine works steadily in the rated condition and does not have heat leakage ($\eta_{GT} = 33\% \implies HPR_s = 2$) and considering $\eta_{grid} = 50\%$ and $\eta_{boiler} = 82\%$ and an ideal heat exchanger ($\eta_{HE} = 100\%$) between the *Heat Recovery Loop* and the *Space*

Heating Hot Water Loop, it is possible to study the trend of the PRSEC depending on the DM, as illustrated in Figure 46.

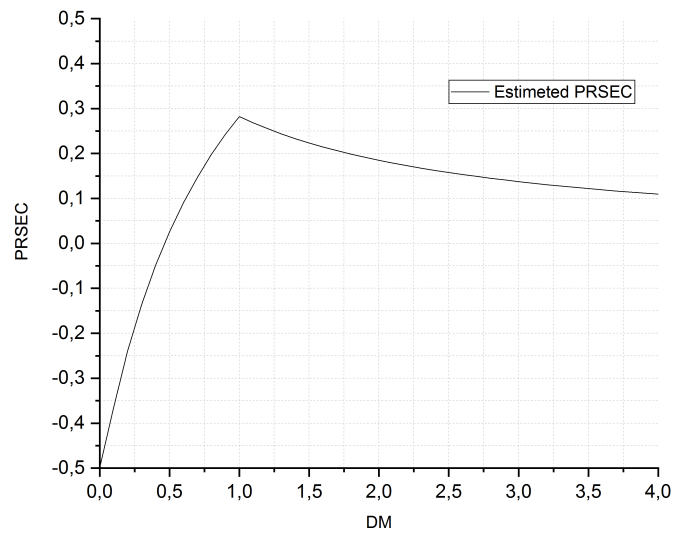


Figure 46: Trend of the PRSEC in function of the DM for a CHP system adopting FEL strategy.

As it is clear, the PRSEC is strongly related to the thermal performance of the energy supply devices. It is pointed out that that below a certain value of DM, which is called Critical Degree of Mismatch ($DM_{CRI} = 0.46$), the adoption of a TES-CHP system following FEL operation strategy doesn't seem appropriate. On the other hand, the maximum value of the PRSEC can

be obtained with $DM = 1$. This value corresponds to $PRSEC_{max} = 28.9\%$.

The values of the DM and the estimated PRSEC of the CHP system under consideration are reported in Table XVII. This feasibility study shows that the highest savings would be

TABLE XVII: VALUES OF DM AND ESTIMATED PRSEC FOR DIFFERENT SIZES OF CHP SYTEMS INTEGRATED WITH AND IDEAL TES FACILITY.

Size [kW]	DM	Estimated PRSEC
600	0.89	23.82%
700	0.88	23.39%
800	0.86	22.52%
900	0.86	22.52%
1,000	0.85	22.08%
1,100	0.85	22.08%
1,200	0.85	22.08%
1,300	0.84	21.63%

met by a 600 kW gas turbine, with an estimated PRSEC of 23.82%. Although, these values are just an idea of the convenience of adopting a CHP-TES system over a conventional one, in the case of a real system PRSEC values will be lower.

The main reasons why these values must not be taken for granted are the following:

- In this study, the FEL strategy assumes that the electrical consumption will be constantly met by the electrical supply ($E_d = E_s$) which is not always true. In matter of fact an undersized gas turbine can lead the facility to purchase the extra electricity needed during peak loads from the grid (section 3.3);
- During the analysis, the gas turbine was assumed to work at full load conditions, performing at the highest efficiency ($\eta_{GT} = 33\%$). On the contrary, in actual systems, the turbine would work under partial load conditions during small-load periods, which means a decrease in efficiency;
- The size of the TES tank was considered large enough to store all the *Recoverable Heat*, although in real plants that would be impossible. The TES has a limited size, which means a limited storage capacity. Furthermore, there is always a part of wasted energy during charge/discharge process and due to thermal losses.

Even if this study does not reflect the actual values of PRSEC, it was fundamental in the understanding the convenience of installing a TES facility.

5.4.3 Sizing of the TES

In order to find the optimal size of the TES, a multi-variable optimization process was adopted [31]. The free independent parameters under considerations were:

- The size of the gas turbine;
- The volume of the TES.

To perform the optimization process, the maximum of the *objective function* must be investigated by alternatively change the discrete values of the variable parameters. The objective function considered is the PRSEC value calculated through Equation 3.7.

The parametric analysis is repeated swapping the manipulated and the fixed variable: at each step, the optimal value of the previous stage is assigned to the fixed variable, while the manipulated variable is free to vary according to the constraints. By doing this, it is possible to reduce the multi-variable optimization analysis to a single-variable problem.

An iterative optimization analysis is necessary, since it is not possible to know a priori the expression of the objective multi-variable function. The analysis is stopped when two subsequent steps reach a satisfactory tolerance in terms of difference (when the same result is achieved during the following step). During the first step, a *Model 3* ($V=20,000$ gal) was introduced in the original CHP plant, meanwhile the size of the turbine was considered as a variable. The choice of starting from this size of storage was random. The results of the first step, leading to the optimal value of the engine size are reported in Table XVIII. The definition of the abbreviations appearing in the following tables is given in Appendix D.

TABLE XVIII: FIRST STEP OPTIMIZATION PROCESS, OPTIMAL ENGINE SIZE FOR A *MODEL 3* TES FACILITY IN A CHP FACILITY.

Size [kW]	F_B [MBTU]	F_{PM} [MBTU]	$Q_{rec.}$ [MBTU]	E_{PM} [MWh]	$E_{pur.}$ [MWh]	η_{CHP}	η_{FERC}	PRSEC	$PRSEC_{GT}$
600	13,253.1	59,922.0	26,095.0	5,200.0	4,815.0	73.2%	51.4%	19.5%	29.5%
700	10,901.9	69,909.5	28,329.2	6,066.2	3,949.0	70.1%	49.9%	20.3%	27.6%
800	10,167.1	79,978.0	30,339.5	6,906.0	3,109.0	67.4%	48.4%	19.9%	25.7%
900	9,281.2	90,321.0	31,838.3	7,630.0	2,385.0	64.1%	46.4%	18.6%	22.8%
1,000	8,222.6	100,585.0	32,706.3	8,266.0	1,749.0	60.6%	44.3%	16.8%	19.2%
1,100	7,716.4	110,781.0	33,096.7	8,788.0	1,227.0	56.9%	42.0%	14.0%	15.0%
1,200	7,511.5	120,718.0	33,285.7	9,220.0	795.0	53.6%	39.8%	10.5%	10.6%
1,300	7,310.8	130,642.0	33,446.9	9,495.0	520.0	50.4 %	37.6%	6.0%	5.4%

From the first step, the 700 kW turbine resulted having the highest PRSEC of 20.3%. As shown in Table XVIII, increasing the size of the engine resulted in an higher value of *Recovered Heat* ($Q_{rec.}$) with respect to the original CHP system thanks to the implementation of the TES (Table V). Although, the successful exploitation of the *Recovered Heat* can be registered only during those months where the thermal energy load is sufficiently high (cold months). During, the remaining part of the year (warm months), the TES system does not seem particularly useful, since the thermal supply from the CHP is much above the request from the hospital.

In the second step of the optimization process, the size of the turbine has been fixed to 700 kW, while the volume of the storage was varied. The results are shown in Table XIX.

TABLE XIX: SECOND STEP OPTIMIZATION PROCESS, OPTIMAL TES SIZE FOR A 700 KW GAS TURBINE IN A CHP FACILITY.

TES Model	Volume [gal]	F_B [MBTU]	F_{PM} [MBTU]	$Q_{rec.}$ [MBTU]	E_{PM} [MWh]	$E_{pur.}$ [MWh]	η_{CHP}	η_{FERC}	PRSEC	$PRSEC_{GT}$
Model 1	11,800.0	11,116.0	69,909.5	28,157.9	6,066.2	3,949.0	69.9%	49.7%	20.2%	27.5%
Model 2	14,000.0	10,992.2	69,909.5	28,257.0	6,066.2	3,949.0	70.0%	49.8%	20.3%	27.6%
Model 3	20,000.0	10,901.9	69,909.5	28,329.2	6,066.2	3,949.0	70.1%	49.9%	20.3%	27.6%
Model 4	26,500.0	10,859.9	69,909.5	28,362.8	6,066.2	3,949.0	70.2%	49.9%	20.4%	27.7%
Model 5	39,500.0	10,841.0	69,909.5	28,377.9	6,066.2	3,949.0	70.2%	49.9%	20.4%	27.7%
Model 6	53,000.0	10,830.5	69,909.5	28,386.3	6,066.2	3,949.0	70.2%	49.9%	20.4%	27.7%

The analysis has demonstrated very similar values of PRSEC among different TES sizes. For this reason, the TES efficiency parameter was introduced:

$$\eta_{TES} = \frac{TES \text{ Energy Discharge}}{TES \text{ Energy Charge}} \quad (5.17)$$

This parameter takes into account the thermal losses and the irreversibilities during the charge/discharge process of the tank [32]. The different values of the η_{TES} are shown in Table XX. The charge and discharge loads were obtained as eQuest[®] outputs.

TABLE XX: SECOND STEP OPTIMIZATION PROCESS, TES EFFICIENCY VALUES FOR A 700 KW GAS TURBINE IN A CHP FACILITY.

TES Model	Volume [gal]	TES Charge Energy [MBTU]	TES Discharge Energy [MBTU]	η_{TES}
Model 1	11,800.0	1,507.9	1,451.2	96.2%
Model 2	14,000.0	1,607.6	1,550.3	96.4%
Model 3	20,000.0	1,690.7	1,622.5	96.0%
Model 4	26,500.0	1,738.5	1,656.1	95.3%
Model 5	39,500.0	1,766.7	1,671.2	94.6%
Model 6	53,000.0	1,789.5	1,679.6	93.9%

As shown by the results, the higher the size of the storage, the lower will be its efficiency. The reason relies on the fact, that the TES tank will not be used for warmer months, therefore, larger tanks will be affected by larger thermal losses (section 5.4.1).

A *Model 2* TES (V=13,200 gal) appears to have the highest efficiency ($\eta_{TES} = 96.4\%$). Hence, this model was considered for the third step of the optimization as shown in Table XXI.

TABLE XXI: THIRD STEP OPTIMIZATION PROCESS, OPTIMAL ENGINE SIZE FOR A *MODEL 2* TES FACILITY IN A CHP FACILITY.

Size [kW]	F_B [MBTU]	F_{PM} [MBTU]	$Q_{rec.}$ [MBTU]	E_{PM} [MWh]	$E_{pur.}$ [MWh]	η_{CHP}	η_{FERC}	PRSEC	PRSEC _{GT}
600	13,259.1	59,922.0	26,090.0	5,200.0	4,815.0	73.1%	51.4%	19.5%	29.5%
700	10,992.2	69,909.5	28,257.0	6,066.2	3,949.0	70.0%	49.8%	20.3%	27.6%
800	10,528.6	79,978.0	30,039.5	69,06.0	3,109.0	67.0%	48.2%	19.7%	25.5%
900	10,486.0	90,321.0	30,838.3	7,630.0	2,385.0	63.0%	45.9%	17.8%	22.0%
1,000	9,547.9	100,585.0	31,606.3	8,266.0	1,749.0	59.5%	43.8%	16.0%	18.4%
1,100	9,041.7	110,781.0	31,996.7	8,788.0	1,227.0	55.9%	41.5%	13.1%	14.2%
1,200	8,836.8	120,718.0	32,185.7	9,220.0	795.0	52.7%	39.4%	9.7%	9.7%
1,300	8,756.6	130,642.0	32,246.9	9,495.0	520.0	49.5%	37.1%	5.1%	4.4%

This step concludes the sizing process, since the same result of the first step has been reached. The adoption of a 700 kW with the implementation of a *Model 2* TES (V=14,000 gal) has proved to be optimal. A PRSEC of 20.3% has been achieved.

5.4.4 Benefits to the CHP System

The introduction of an optimal TES size in the CHP system resulted in an overall improvement in the performance of the plant and in a reduction of source energy consumption. A comparison between the original cogeneration plant over the one adopting thermal storage is summarized in Table XXII. A definition of the abbreviations used in Table XXII is given in Appendix D.

TABLE XXII: COMPARISON OF CHP OVER TES-CHP IN TERMS OF EFFICIENCIES AND ENERGY CONSUMPTION.

Parameter	COGENERATION (700 kW)	COGENERATION (700 kW) + TES (14,000 gal)
F_B [MBTU]	12,921.9	10,914.8
$Q_{rec.}$ [MBTU]	26,707.3	28,314.5
η_{CHP}	67.8%	70.1%
η_{FERC}	48.7%	49.9%
$PRSEC$	19.0%	20.3%
$PRSEC_{GT}$	27.0%	27.6%

As a result, the $PRSEC$ value increased from 19.0% to 20.3%. This is due to the higher value of *Recovered Heat*: the original system recovered 26,707.3 MBTU, while the one with thermal storage was able to use 28,318.5 MBTU. Figure 47 offers a comparison between the monthly *Recovered Heat* of an optimal CHP layout with and without storage.

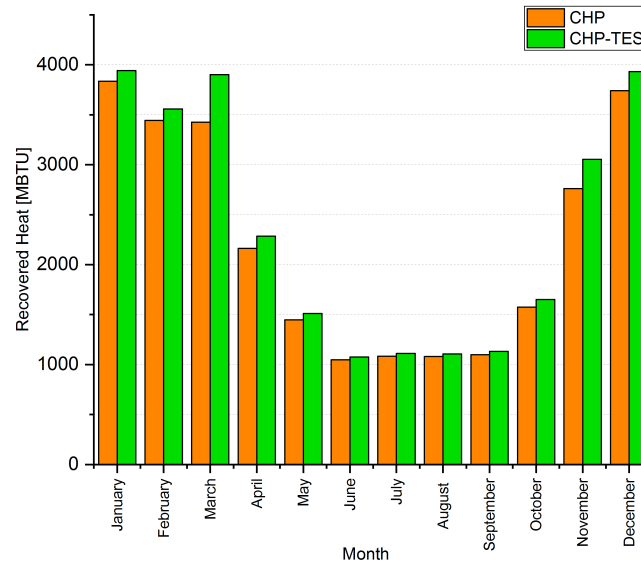


Figure 47: Comparison of the amount of *Recovered Heat* between CHP and TES-CHP system, both with a 700 kW turbine.

The advantage of an higher quantity of exploited heat, caused a decrease in the fuel consumption of the boilers, as shown in Figure 48. In fact, thanks to the use of TES during colder months, the need of thermal energy from the auxiliary boilers has been reduced. During peak thermal loads, the TES was able to discharge thermal energy into the *Space Heating Hot Water loop*, limiting the use of the boilers.

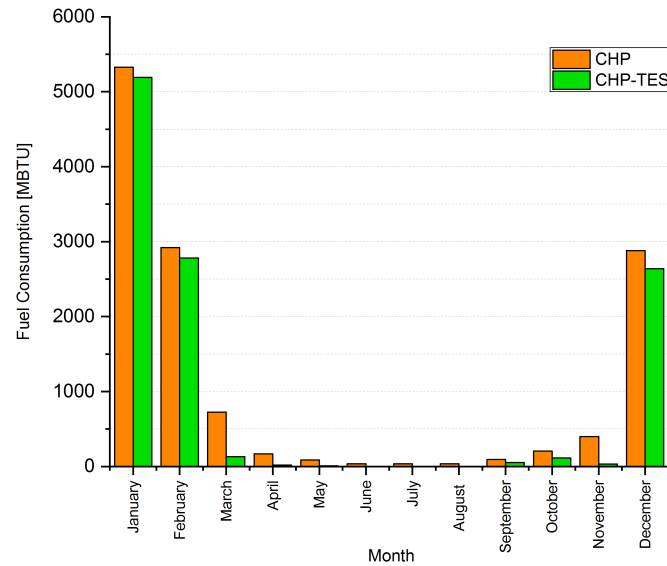


Figure 48: Comparison of boiler fuel consumption between CHP and TES-CHP system, both with a 700 kW turbine.

Nevertheless, the effects of the thermal storage were not of primary importance, since the thermal energy requested by the hospital was much below the recovered energy available from the engine. Therefore, the TES was mainly used only during half of the year.

Much different results will be obtained in the adoption of a TES facility attached to a trigeneration system, as shown in the following paragraphs.

5.5 Coupling TES to the CCHP system

The same considerations provided in Section 5.4 were assumed. A fully mixed TES water tank was implemented in the trigeneration plant, operating in the same temperature range of the previous case (170 °F - 200 °F).

Identical thermal storage capacities summarized in Table XIII were analyzed, therefore no change to the thermal loss model (Section 5.4.1) was made.

The introduction of a storage system, among other changes, levels out the peaks of WRH available for the operation of the absorption chiller. This means that a new sizing procedure for the correct installation of the absorption chiller must be carried out. The same procedure discussed in Section 4.4 was adopted. However, the estimation of the WRH produced by the cogeneration plant did not assume particular importance. This is connected to the fact that the introduction of TES brings an increment in the availability of heat used as an input by the chiller. This can only cause an increment of the size of the chiller compared to the case without the use of storage (Chapter 4). The installed sizes of the absorption chiller introduced in the original CCHP plant were listed in Table VII. Starting from those values, an iterative approach has been followed, increasing the size at every step until the boiler's fuel consumption exceeded its standard value.

As already mentioned in Section 4.4, a deviation from the original boiler's fuel consumption is a symptom of the oversizing of the chiller. The results are summarized in Table XXIII. It is shown that the larger the TES capacity, the larger the increment of the chiller's size, due to

TABLE XXIII: INSTALLED ABSORPTION CHILLER SIZES FOR THE CCHP PLANT WITH DIFFERENT TES CAPACITY.

Size [kW]	Inst. Chill. Cap. (with Model 1) [tons]	Inst. Chill. Cap. (with Model 2) [tons]	Inst. Chill. Cap. (with Model 3) [tons]	Inst. Chill. Cap. (with Model 4) [tons]	Inst. Chill. Cap. (with Model 5) [tons]	Inst. Chill. Cap. (with Model 6) [tons]
600	153	154	154	154	154	154
700	229	230	233	233	233	233
800	273	274	278	281	281	281
900	306	307	311	315	322	322
1,000	340	340	344	348	355	363
1,100	382	383	387	391	398	406
1,200	423	424	428	432	439	446
1,300	489	490	494	498	505	512

the major availability of *Recovered Heat*. Obviously, this expansion becomes more pronounced adopting larger turbines.

5.5.1 Supply and Demand Mismatch

The purpose of a trigeneration system is to simultaneously meet the demand of cooling, heating, and power. Therefore, the model elaborated in Section 5.4.2, must be updated in order to include the effect of the cooling demand required by the hospital.

The definition of the supply side, expressed through Equation 5.13, as well as the characterization and meaning of the DM (Equation 5.14) remained unchanged. On the contrary, the definition of the demand side represented by Equation 5.12, must include the heat required to operate the absorption chiller. Equation 5.12 will become:

$$HPR_d = \frac{\int_0^T \dot{Q}_d(t) dt}{\int_0^T \dot{E}_d(t) dt} = \frac{Q_d}{E_d} \leftarrow Q_d = H_d + \frac{C_d}{COP_{abs.}} \quad (5.18)$$

- H_d heating consumption of the building;
- C_d cooling consumption of the building;
- $COP_{abs.}$ average COP of the absorption chiller;
- Q_d overall thermal energy consumption of the building (heating and cooling);
- E_d electric energy consumption of the building.

A major simplification to the system has been made: the entire cooling load is assumed to be satisfied through the use of the absorption chiller, no electric chiller is contemplated. The reason relies in the fact that this preliminary study has the objective of understanding if the waste heat coming from the gas turbine is enough to satisfy the request of heat coming from both: the heating system, and the absorption chiller.

Therefore, the hypothesis of providing cold energy exclusively through an absorption chiller, results in an acceptable overestimation of the system. Moreover, in order to proceed with the analysis of the source energy savings, an additional parameter must be introduced named *accumulated heating load ratio* (r). It is defined as the ratio of the heating load to the overall thermal consumption:

$$r = \frac{\int_0^T \dot{Q}H_d(t)dt}{\int_0^T \dot{Q}_d(t)dt} = \frac{H_d}{Q_d} \quad (5.19)$$

Following the same approach used in the analysis of the cogeneration system (Section 5.4.2), the relationship between supply and consumption is illustrated in Table XXIV. Introducing this new definitions, implies a modification in Equation 5.16, which will become:

$$PRSEC = \begin{cases} 1 - \frac{\frac{1}{\eta_{GT}}}{\frac{1}{\eta_{grid}} + \frac{r \cdot DM \cdot HPR_s}{\eta_{boiler}} + \frac{(1-r) \cdot DM \cdot HPR_s \cdot COP_{abs.}}{\eta_{grid} \cdot COP_{elec.}}}, & \text{if } DM \leq 1 \\ 1 - \frac{\frac{1}{\eta_{GT}} + \frac{(DM-1)HPR_s}{\eta_{boiler}}}{\frac{1}{\eta_{grid}} + \frac{r \cdot DM \cdot HPR_s}{\eta_{boiler}} + \frac{(1-r) \cdot DM \cdot HPR_s \cdot COP_{abs.}}{\eta_{grid} \cdot COP_{elec.}}}, & \text{if } DM > 1 \end{cases} \quad (5.20)$$

TABLE XXIV: RELATIONSHIP BETWEEN CONSUMPTION AND SUPPLY FOR HEATING, COOLING AND ELECTRICITY WORKING CONDITIONS.

System	Electricity Supply [E_s]	Heating Supply [H_s]	Cooling Supply [C_s]
Base Model	E_d	$E_d \cdot HPR_s \cdot DM \cdot r$	$E_d \cdot HPR_s \cdot DM \cdot (1 - r) \cdot COP_{abs.}$
TES-CHP (FEL)	$DM \cdot E_d$	$E_d \cdot HPR_s \cdot DM \cdot r$	$E_d \cdot HPR_s \cdot DM \cdot (1 - r) \cdot COP_{abs.}$

Considering the same values stated in Section 5.4.2 in terms of equipment performance, it is possible to obtain the trend of the *PRSEC* in function of the DM and of the accumulated heating load ratio, as illustrated in Figure 49.

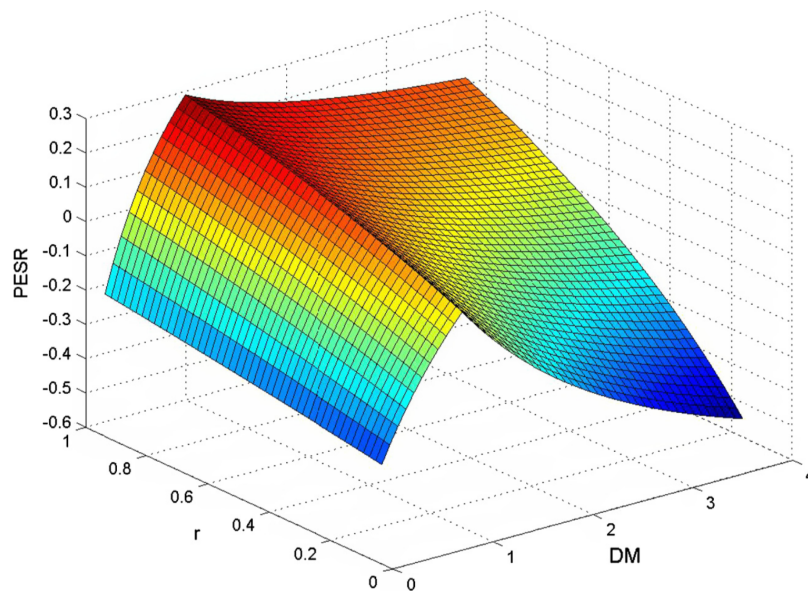


Figure 49: Trend of the PRSEC in function of the DM and r for a CCHP system adopting FEL strategy.

The calculation of DM_{CRI} is trivial, and it's merely influenced by the performances of the energy supply equipment, as well as by the value of r . The value can be expressed as follows:

$$DM_{CRI} = \begin{cases} \frac{\frac{1}{\eta_{GT}} - \frac{1}{\eta_{grid}}}{\frac{r \cdot HPR_s}{\eta_{boiler}} + \frac{(1-r) \cdot HPR_s \cdot COP_{abs.}}{\eta_{grid} \cdot COP_{elec.}}}, & \text{if } DM \leq 1 \\ \frac{\frac{1}{\eta_{GT}} - \frac{1}{\eta_{grid}} - \frac{HPR_s}{\eta_{boiler}}}{\frac{r \cdot HPR_s}{\eta_{boiler}} + \frac{(1-r) \cdot HPR_s \cdot COP_{abs.}}{\eta_{grid} \cdot COP_{elec.}} - \frac{HPR_s}{\eta_{boiler}}}, & \text{if } DM > 1 \end{cases} \quad (5.21)$$

From Equation 5.21 it is possible to understand the range of DM values for which the system is profitable. The range is given by the following:

$$DM = \left(\frac{\frac{1}{\eta_{GT}} - \frac{1}{\eta_{grid}}}{\frac{r \cdot HPR_s}{\eta_{boiler}} + \frac{(1-r) \cdot HPR_s \cdot COP_{abs.}}{\eta_{grid} \cdot COP_{elec.}}}, \frac{\frac{1}{\eta_{GT}} - \frac{1}{\eta_{grid}} - \frac{HPR_s}{\eta_{boiler}}}{\frac{r \cdot HPR_s}{\eta_{boiler}} + \frac{(1-r) \cdot HPR_s \cdot COP_{abs.}}{\eta_{grid} \cdot COP_{elec.}} - \frac{HPR_s}{\eta_{boiler}}} \right) \quad (5.22)$$

It is assumed that the performance of the boiler, the gas turbine, the heat exchangers and the grid remained unchanged compared to the cogeneration plant. Considering a $COP_{abs.} = 0.75$ and a $COP_{elec.} = 4$, the analysis of the critical DM value and estimated PRSEC was performed and showed in Table XXV.

TABLE XXV: VALUES OF DM AND ESTIMATED PRSEC FOR DIFFERENT SIZES OF CCHP SYSTEMS INTEGRATED WITH AN IDEAL TES FACILITY.

Size [kW]	r	DM	DM_{CRI}	Estimated PRSEC
600	0.58	1.52	1.99	7.40
700	0.58	1.52	1.99	7.40
800	0.58	1.49	1.99	7.97
900	0.58	1.48	1.99	8.12
1,000	0.58	1.48	1.99	8.22
1,100	0.58	1.47	1.99	8.32
1,200	0.58	1.47	1.99	8.36
1,300	0.58	1.47	1.99	8.36

The results appearing in Table XXV demonstrate the convenience of adopting a CCHP-TES system, in fact the values of DM are below the maximum limit of DM_{CRI} .

However, the estimated PRSEC values don't assume any significance for the analysis. This is because the system that was considered in this study is somehow different from the one in Chapter 4. In particular, in the aforementioned results, it was assumed that the entire cooling

load was satisfied by an absorption chiller. In the event that there wasn't enough waste heat to operate this device, a gas boiler would have provided hot water. This solution is not acceptable in terms of efficiency, as already demonstrated in Figure 41.

This different plant layout also justifies the fact that the PRSEC value increases with larger turbine sizes. Actually, bigger turbine's capacities produce a higher amount of waste heat which is used to drive the absorption chiller, without recurring to the use of the gas boiler.

In spite the fact that the values of PRSEC are not reliable, this study demonstrated that the implementation of a TES system into a CCHP facility is meaningful.

5.5.2 Sizing of the TES

The same multi-variable optimization process explained in Section 5.4.3 was considered [31]. The objective function under analysis is the PRSEC calculated through Equation 3.7. The free independent variables are the size of the turbine, and the capacity of the storage.

From Table XXVI to Table XXVIII are shown the three optimization steps that were performed in order to reach the most advantageous solution. The definition of the abbreviations appearing in those tables is given in Appendix D.

The value of $PRSEC_{GT}$ was evaluated using Equation 4.17. The $Q_{rec.}$ represents the *Recovered Heat* used by the heating system during colder months, while the $Q_{abs.}$ symbolizes the cooling load produced by the absorption chiller.

After the optimization process, it emerged how a *Model 5* TES tank ($V = 39,500$ gal), paired with a 900 kW gas turbine could allow the system to reach a 25.1% reduction in source energy consumption compared to a traditional system. With respect to the original trigeneration

TABLE XXVI: FIRST STEP OPTIMIZATION PROCESS, OPTIMAL ENGINE SIZE FOR A *MODEL 3* TES FACILITY IN A CCHP SYSTEM.

Size [kW]	F_B [MBTU]	F_{PM} [MBTU]	$Q_{rec.}$ [MBTU]	$Q_{abs.}$ [MBTU]	E_{PM} [MWh]	$E_{pur.}$ [MWh]	PRSEC	$PRSEC_{GT}$
600	13,256.2	59,922.0	26,092.4	8,093.3	5,200.0	4,222.1	23.5%	31.1%
700	10,936.0	69,807.0	28,300.9	8,175.2	6,059.3	3,357.0	24.4%	29.2%
800	10,203.7	79,171.9	30,309.2	9,116.9	6,845.1	2,502.8	24.5%	27.6%
900	9,319.5	88,577.0	31,806.5	11,641.7	7,507.7	1,655.0	24.6%	25.3%
1,000	8,516.7	97,744.1	32,379.2	11,669.0	8,065.1	1,095.2	22.9%	21.8%
1,100	8,015.1	107,178.9	32,765.7	11,682.7	8,534.0	625.6	20.2%	17.7%
1,200	7,812.5	115,790.2	32,952.8	11,696.0	8,870.1	288.3	16.9%	13.6%
1,300	7,613.8	123,899.9	33,112.4	11,697.0	9,020.9	138.1	12.8%	8.7%

TABLE XXVII: SECOND STEP OPTIMIZATION PROCESS, OPTIMAL TES SIZE FOR A 900 KW GAS TURBINE IN A CCHP SYSTEM.

TES	Volume [gal]	F_B [MBTU]	F_{PM} [MBTU]	$Q_{rec.}$ [MBTU]	$Q_{abs.}$ [MBTU]	E_{PM} [MWh]	$E_{pur.}$ [MWh]	η_{TES}	PRSEC	$PRSEC_{GT}$
Model 1	11,800.0	14,861.7	88,580.5	27,206.5	11,445.2	7,508.0	1,668.4	98.2%	23.2%	21.6%
Model 2	14,000.0	13,187.0	88,579.4	28,596.5	11,453.4	7,507.9	1,667.9	98.1%	23.6%	22.7%
Model 3	20,000.0	9,319.5	88,577.0	31,806.5	11,641.7	7,507.7	1,655.0	98.1%	24.6%	25.3%
Model 4	26,500.0	8,958.1	88,566.4	32,106.5	11,656.8	7,506.8	1,654.1	98.1%	24.9%	25.5%
Model 5	39,500.0	8,615.9	88,566.4	32,556.5	11,681.3	7,506.1	1,653.0	98.1%	25.1%	25.9%
Model 6	53,000.0	8,616.2	88,566.4	32,556.5	11,681.3	7,506.1	1,653.0	98.1%	25.1%	25.9%

TABLE XXVIII: THIRD STEP OPTIMIZATION PROCESS, OPTIMAL ENGINE SIZE FOR A *MODEL 5* TES FACILITY IN A CCHP SYSTEM.

Size [kW]	F_B [MBTU]	F_{PM} [MBTU]	$Q_{rec.}$ [MBTU]	$Q_{abs.}$ [MBTU]	E_{PM} [MWh]	$E_{pur.}$ [MWh]	PRSEC	$PRSEC_{GT}$
600	13,146.6	59,907.0	26,183.4	8,101.9	5,199.0	4,221.1	23.6%	31.2%
700	10,744.4	69,799.8	28,459.9	8,177.4	6,057.1	3,356.1	24.5%	29.3%
800	9,468.7	79,160.5	30,919.2	9,180.1	6,840.0	2,500.3	25.0%	28.0%
900	8,615.9	88,566.4	32,556.5	11,681.3	7,506.1	1,653.0	25.1%	25.9%
1,000	7,016.7	97,723.5	33,050.2	11,767.3	8,063.3	1,089.5	24.0%	22.3%
1,100	6,918.7	107,141.3	33,125.7	11,786.4	8,531.0	620.4	21.0%	18.0%
1,200	6,454.7	115,744.5	33,499.8	11,798.7	8,866.5	284.0	18.0%	14.0%
1,300	6,135.5	123,847.7	33,752.4	11,815.1	9,016.2	133.1	13.9%	9.3%

system studied in Chapter 4, the introduction of the storage enabled the adoption of a larger turbine and led to an increment in energy savings by 4.1%.

In the following section, a detailed review will be conducted on the effects brought by the by the introduction of hot thermal energy storage in a CCHP facility.

5.5.3 Benefits to the CCHP System

The major benefits introduced by the implementation of a TES system coupled to a trigeneration plant can be listed as follows:

- Minor decrease in the prime mover's fuel consumption;
- Decrease in the boiler's fuel consumption;
- Increase in the cooling load satisfied by the absorption chiller;
- Decrease in the overall electric consumption;
- Slight decrease in the electric peak demand.

Basically, introducing a thermal storage remarks the improvements in source energy consumption already provided by the trigeneration system and discussed in Section 4.5. Table XXIX summarizes the enhanced performance of the TES-CCHP system over the CCHP analyzed in Chapter 4. The comparison was carried out maintaining the same engine size of the optimal TES-CCHP system, which was a 900 kW gas turbine. The definition of the abbreviations adopted in Table XXIX is provided in Appendix D.

TABLE XXIX: COMPARISON OF CCHP OVER TES-CCHP IN TERMS OF PERFORMANCE AND ENERGY CONSUMPTION.

Parameter	TRIGENERATION (900 kW)	TRIGENERATION (900 kW) + TES (39,500 gal)
F_B [MBTU]	12,917.1	8,615.9
F_{PM} [MBTU]	88,695.4	88,566.7
$Q_{rec.}$ [MBTU]	28,914.3	32,556.5
$Q_{abs.}$ [MBTU]	10,455.4	11,681.3
E_{PM} [MWh]	7,630.3	7,506.1
$E_{pur.}$ [MWh]	1,851.6	1,653.0
$PRSEC$	21.0%	25.1%
$PRSEC_{GT}$	26.2%	25.9%

The reduction in the fuel consumption of the boiler can be explained by a combination of factors. The first one is the reduction in the heat produced by the boiler in order to satisfy the heat request during colder months. The introduction of the storage enables a better exploitation of the *Recoverable Heat*, and therefore a lower amount of *Wasted Recoverable Heat* during winter. The second reason is connected to the fact that the TES allows a more efficient operation of the absorption chiller. In the original trigeneration plant, the boiler occasionally had to provide the heat source for the operation of the chiller. In the TES-CCHP facility, this event is more uncommon due to the larger availability of *Recovered Heat*. The adoption of TES results in a reduction in the fuel burned by the prime mover. The explanation can be found in the lower amount of electricity produced due to higher amount of cooling load satisfied by the absorption chiller ($Q_{abs.}$), which implies a inferior usage of the electric chiller. Nonetheless, the decrease in the fuel consumption of the turbine is less evident then expected, being the performance of the equipment worse because of the increment in partial load operations (Section 2.2).

The reduction of the overall electricity consumption and peak demand are strictly related to a greater reliance of the absorption chiller, as demonstrated by the higher value of $Q_{abs.}$ in the TES-CCHP plant compared to the one without storage. Even though a minor reduction in electricity peak demand, that dropped from 1,13 MW to 1,127 MW, the total electric consumption declined by 3.4%, going from 9,481.9 MWh to 9,159.1 MWh.

These comprehensive improvements in the source energy usage enabled the system adopting

a TES device to reach a PRSEC of 25.1%, 4.1% higher than the one with no storage option (same layout 900 kW gas turbine).

CHAPTER 6

CONCLUSIONS

In this thesis a total of four plant layouts were analyzed:

- A combined heat and power plant;
- A combined heat and power plant with hot thermal storage;
- A combined cooling, heating, and power plant;
- A combined cooling, heating, and power plant with hot thermal storage.

A detailed performance analysis was performed in each case, focusing on the amount of *Recovered Heat* correctly exploited which prevented the loss of *Wasted Recoverable Heat*.

In the two different plant's layouts the introduction of TES resulted beneficial. In the case of a CHP system it resulted in an increase of PRSEC from 19.0% to 20.3%. In the cogeneration layout, the introduction of hot storage, did not affected the optimal size of the plant (700 kW in both cases). The reason relies in the fact that during warmer months, the heat load from the hospital was much lower than the *Recoverable Heat*, culminating in a significant amount of WRH. In this situation the use of storage was convenient only during colder months, discharging the accumulated energy during peak heating demand periods enabled a minor operation of the

gas boilers lowering their fuel consumption. Figure 50 summarizes the effect of the increasing volume size of the TES over the percentage of *Recovered Heat*, defined as follow:

$$\text{Perc. Recovered Heat} = \frac{\text{Recovered Heat}}{\text{Total Recoverable Heat}} = \frac{\text{Recovered Heat}}{(\text{Recovered Heat} + \text{WRH})} \quad (6.1)$$

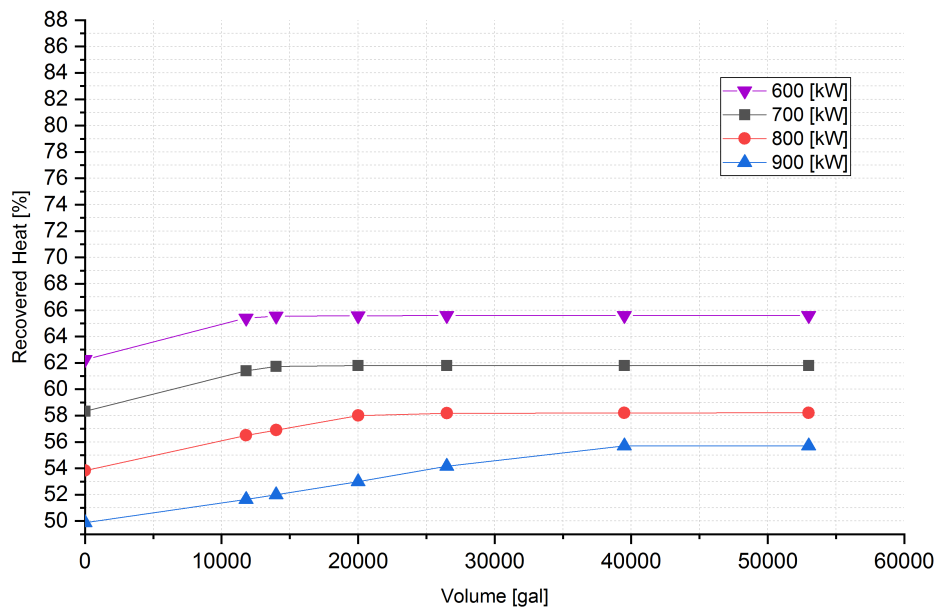


Figure 50: Influence of TES volume over percentage of *Recovered Heat* for different CHP sizes.

It is possible to see how improvements in the amount of exploited energy are more remarked for smaller engine capacities, in fact the steepness of the curve is higher for smaller layouts. Moreover, for bigger CHP systems the optimal size of the TES (maximum of the curve) is shifted to the right, enabling the utilization of larger tanks. The same information can be deduced from Figure 51, which illustrates the variation of the PRSEC in function of the TES volume, for different plants sizes.

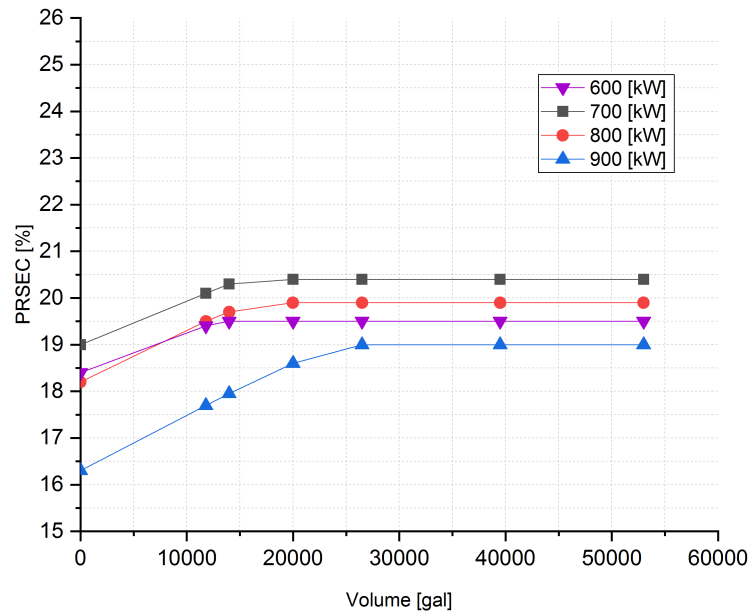


Figure 51: Influence of TES volume over PRSEC for different CHP sizes.

A much different picture was observed in the case of a CCHP layout. The introduction of the absorption chiller permitted a better exploitation of the *Recoverable Heat* throughout the entire year, resulting in higher performance values compared to a CHP layout. In this circumstance the implementation of a TES facility had a bigger impact on the overall management of the system. Not only allowing an increase of PRSEC of 2.4%, from 22.7% to 25.1%, but also causing an increment of the turbine's optimal capacity, from 800 kW to 900 kW. The TES had an impact on the overall fuel consumption, as well as the overall electricity request. Guaranteeing a constant source of heat for the operation of the absorption chiller, it limited the use of the electric chiller only to peak demand periods. This situation resulted in a reduced production of electricity by the turbine, therefore, a lower fuel consumption. A decrease in the fuel requested by the gas boilers was also noticed, due to the higher amount of *Recovered Heat* during colder months carried out by the TES.

In Figure 52 it is possible to understand the impact of the TES volume over the different CCHP layouts, especially in terms of percentage *Recovered Heat* (Equation 6.1). As in the case of a cogeneration plant, larger CCHP plants require a bigger tank. Furthermore, it can be noticed how the slope of the line decreases for greater CCHP capacities, due to the larger amount of total recoverable energy.

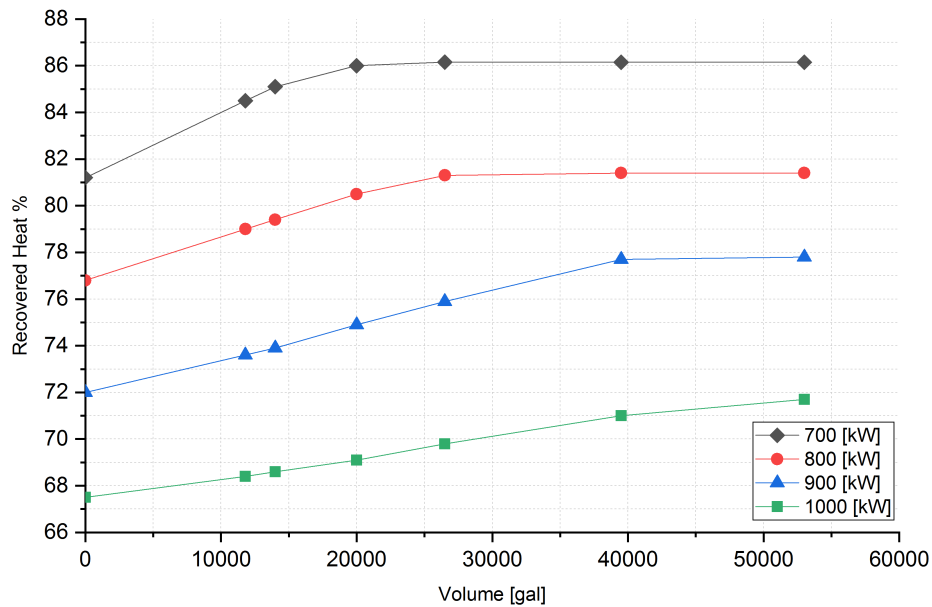


Figure 52: Influence of TES volume over percentage of *Recovered Heat* for different CCHP sizes.

A more detailed analysis on the effect of the storage is offered by study of the variation of the PRSEC (which includes the effect of recovered heat as well as the electricity production) in function of the plant's size and TES volume. Figure 53 demonstrates how the correct sizing of the TES could enable the operation of a larger gas turbine. In fact, a 900 kW CCHP layout results have the highest value of PRSEC.

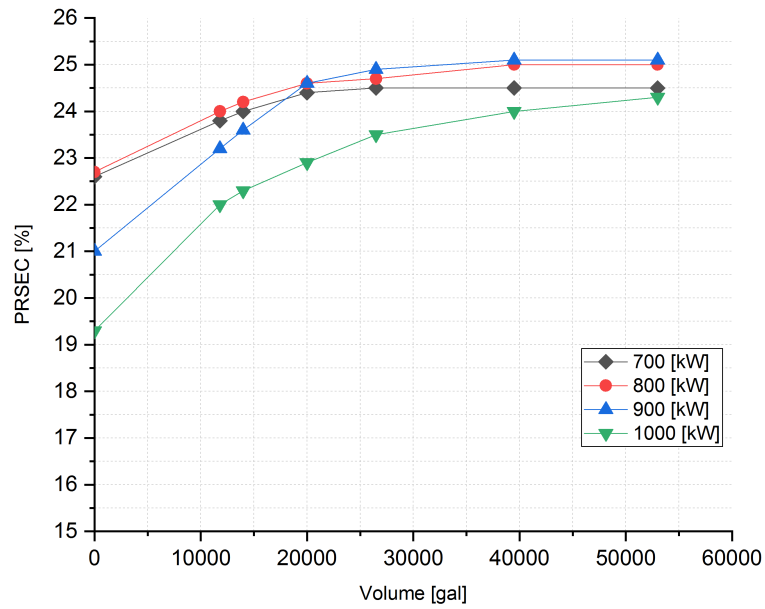


Figure 53: Influence of TES volume over PRSEC for different CCHP sizes.

Table XXX summarizes the comparison of the different optimal layouts in terms of recovered energy and PRSEC.

TABLE XXX: COMPARISON OF THE PERFORMANCE IN THE FOUR DIFFERENT OPTIMAL LAYOUTS.

Layout	Size [kW]	TES [gal]	$Q_{rec.}$ [MBTU]	$Q_{abs.}$ [MBTU]	PRSEC
CHP	700	-	26,707	-	19.0%
CHP-TES	700	14,000	28,318	-	20.3%
CCHP	800	-	28,099	10,577	22.7%
CCHP-TES	900	39,500	32,557	11,681	25.1%

APPENDICES

Appendix A

INSTRUCTIONS TO MODEL A CHP SYSTEM IN EQUEST®

STEP BY STEP INSTRUCTIONS FOR ADDING A CHP SYSTEM IN EQUEST:

- Open the original baseline building file, then go to *Building Creation Wizard* and on *WS1*, rename to identify the new model including the CHP system. Finish and save under the new name. This preserves the conventional building model in the original file for later use.
- Go to the "Mode" tab in the Toolbar and choose "Detailed Data Edit".
- At the top of the toolbar select "Water-Side HVAC" tab.

Input the electric generator (Gas Turbine):

- In the Component Tree (left side of the screen) right click on the folder named "*Electric Generators*" and then click on "*Create Electric Generator*" (left side of the screen).
- In the next screen set the "*Electric Generator Name*" and "*Electric Generator Type*". Choose "*Gas Turbine*".
- In the next screen specify the "*Generator Capacity*" in [kW].
- "*Required Electric Generator Data*" screen appears, and shows the "*Generator Capacity*" in [kW].
- Set the electric generator properties in "*Basic Specifications*" tab:

Appendix A (continued)

- In “*Meter Assignments*” preserve the default options.
 - In “*Equipment Capacity*” specify the “*Minimum Ratio*” as ratio of the minimum possible output to the full load output and “*Maximum Ratio*” as ratio of the maximum possible output to the full load output (if the generator is allowed to overload, “*Maximum Ratio*” is greater than 1.0). Use “*Minimum Ratio*”=0.1, and “*Maximum Ratio*”=1.0.
 - In “*Equipment Efficiency*” set the “*Heat Input Ratio*” as $\frac{1}{\text{Electrical Efficiency}}$ at maximum load. Do not use the eQuest default value. Use “*Heat Input Ratio*” = 3.39.
 - In “*Availability*” specify the “*Start-up Time*” as the equivalent amount of full-load run time necessary to bring the equipment up to operating conditions. Preserve the default eQuest value (0.17).
- Set the electric generator properties:
 - Switch to the “*Performance Curves*” tab Heat Input Ratio:
 - * Select “*Gas Turbine – HIR – fPLR*” under the Heat Input Ratio options.
 - * Select “*Gas Turbine – cap – fPLR*” under the Capacity options. Actually, this curve specifies the variation of the capacity with respect to the ambient temperature expressed in °F.
 - Select the “*Loop Attachments*” tab:
 - * Under “*Heat Recovery*” select “*Hot Water loop*” as the “*Exhaust Recovery Loop*”.

Appendix A (continued)

- Click “Done”.

Specify the performance curves.

Creating the Partial Load Ratio over Heat Input Ratio curve:

- In the component tree find and right click on the folder named “*Performance Curves*”, then select “*Create Curve Fit*”.
- Set “*Curve Fit Name*”, create from scratch and define the type of curve fit as *Quadratic*, hit OK.
- In the next screen, choose the way this new curve is going to be created, select “*Curve Coefficients*”.
- Insert coefficients data. A detailed representation of the curve is given in Section 2.3.1. The coefficients can be taken from Equation 2.11 ($a=0.1728$; $b=0.7784$; $c=0.0278$).
- The performance curve has been created and eQuest will display the Performance Curve Properties window. Hit Done.
- Go back to the component tree and double click on the created generator.
- Select the “*Performance Curve*” tab.
- On the left column, instead of the “*Gas Turbine – HIR – fPLR*” curve, select the curve previously created. Hit Done.

Creating the External Air Temperature over Capacity curve:

- In the component tree find and right click on the folder named “*Performance Curves*”, then select “*Create Curve Fit*”.

Appendix A (continued)

- Set "*Curve Fit Name*", create from scratch and define the type of curve fit as *Linear*, hit OK.
- In the next screen, choose the way this new curve is going to be created, select "*Curve Coefficients*".
- Insert coefficients data. A detailed representation of the curve is given in Section 2.3.2. The coefficients can be taken from Equation 2.14 ($a=114.6$; $b=-0.24$).
- The performance curve has been created and eQuest will display the "*Performance Curve Properties*" window. Hit Done.
- Go back to the component tree and double click on the created generator.
- Select the "*Performance Curve*" tab.
- On the right column, instead of the "*Gas Turbine – cap – fPLR*" curve, select the curve previously created. Hit Done.

Control the electric generator:

- In the component tree right click on "*Equipment Controls*" folder, then "*Create Equipment Control*".
- Create a control from scratch and select the type of control as "*Electrical*".
- Choose the meter the generator is tied to.
- Under the "*Load Range 1*" tab, go to the "*Generator Name*" drop down menu and look up for the generator that has been created. Input its capacity under "*Max Load*".

Appendix A (continued)

- Click Done.

Domestic hot water in the space heating hot water loop:

eQuest does not allow the user to attach multiple loops to the heat recovery loop of the power generator. For CHP, the user must assign the domestic hot water load to the hydronic hot water space heating loop and the hot water loop is created with a zero capacity water heater.

- At the top of the toolbar select “*Water-Side HVAC*” and double click on “*DHW plant 1 loop (1)*” in the component tree.
- In “*Process/DHW loads*” section, save the value of the “*Process Flow*” and click done.
- Select “*DHW plant 1 Wtr Htr (1)*” in the “*DHW plant 1 loop (1)*” section of the component tree, set 0 [MBTU/h] to the “*Equipment Capacity*” and click done.
- Select “*Process/DHW loads*” in the “*Hot water loop*” section. Using the equation Equation 3.2 is possible to compute the “*Process Load*” where G is the “*Process Flow*” saved previously, ρ is water density, c is water specific heat, and ΔT is the difference temperature between the inlet and outlet of the “*Process Flow*”, taking into account $T_{in} = 45 F$ and $T_{out} = 125 F$.
- Insert the “*Process Load*” calculated and the “*Process Flow*” saved.
- In “*Process Load Schedule*” choose “*DHW Eqp NRes Sch*”.
- Click Done

Appendix B

INSTRUCTIONS TO MODEL A CCHP SYSTEM IN EQUEST[®]

Input the absorption chiller:

- In the component tree (left side of the screen) right click on the folder named "*Project: 'Project Name'*" and then click on "*Create Chiller*".
- In the next screen, select the option to create the chiller from scratch (default), set the "*Chiller Name*" and "*Chiller Type*". Choose "*1-stage absorption chiller*".
- In the next screen specify the loops to which the chiller is connected: select "*Chilled Water loop*", "*Hot Water loop*", "*Condenser Water loop*".
- The "*Chiller Properties*" screen will appear, select the "*Basic Specification*" tab:
 - In "*Equipment Efficiency*" set as the the *Heat Input Ratio* 1.33 and in "*Equipment Capacity*" input the values suggested Table VII. Make sure you select the proper "*Equipment Capacity*" based on the "*Electric Generator Capacity*".
 - In "*Design Conditions*" vs "*Rated Conditions*" preserve the default options.
- Now select the "*Performance Curves*" tab:
 - In the drop down menu next to the "*Absor-1-HIR-fCHWT & ECT*" select "*Create Curve*". Make sure to select the proper curve type, in this case: "*Biquadratic in T*".

Appendix B (continued)

Input as curve coefficients the following: $a=0.3012$; $b=0$; $c=0$; $d=0$; $e=0$; $f=0$. Hit OK.

– In the drop down menu next to the "*Absor-1-HIR-fPLR*" select "*Create Curve*".

Make sure to select the proper curve type, in this case: "*Quadratic*". Input as curve coefficients the following: $a=1.2703$; $b=-0.0079$; $c=0.000054$. Hit OK.

– In the drop down menu next to the "*Absor-1-Cap-fCHWT & ECT*" select "*Create Curve*". Make sure to select the proper curve type, in this case: "*Biquadratic in T*".

Input as curve coefficients the following: $a=1.9327$; $b=0$; $c=0$; $d=-0.0152$; $e=0.00005$; $f=0$. Hit OK.

- Click Done.

Control the absorption chiller.

In order to properly control the absorption chiller and be sure that it satisfy the cooling loads of the building until its maximum capacity is reached, an equipment control is needed. Otherwise eQuest would just cover the cooling consumption with the electric chillers, using the absorption chiller only during the peak hours.

- In the component tree right click on "*Equipment Controls*" folder, then "*Create Equipment Control*".
- Create a control from scratch and select the type of control as "*Cooling*".
- Choose the circulation loop the equipment is tied to: "*Chilled Water loop*".

Appendix B (continued)

- Under the *"Load Range 1"* tab, on *"Seq 1"* go to the *"Chiller Name"* drop down menu and look up for the absorption chiller that has been created. Input its capacity under *"Max Load"*.
- Under the *"Load Range 1"* tab, on *"Seq 2"* go to the *"Chiller Name"* drop down menu and look up for the electric chiller. Input its capacity under *"Max Load"*.
- Click Done

Appendix C

INSTRUCTIONS TO MODEL A HOT THERMAL STORAGE SYSTEM IN EQUEST[®]

Insert a hot thermal storage tank:

- In the component tree (left side of the screen) right click on the folder named "*Project: 'Project Name'*" and then click on "*Create Thermal Storage*".
- In the next screen, select the option to create the storage from scratch (default), set the "*Thermal Storage Name*" and "*Thermal Storage Type*". Choose "*Hot Water Tank*".
- In the next screen specify the loops to which the storage is connected: select the "*Exhaust Heat Recovery loop*" as charge loop, and the "*Hot Water loop*" as discharge loop. under "*Schedule*" select "*Hourly Report Schedule*". Hit OK.
- The "*Thermal Storage Properties*" window will appear:
 - Under the "*Loop Assignment*" column, leave the eQuest default options.
 - Under the "*Charge/Discharge Operations*" column, leave the eQuest default options.
 - Under the "*Equipment Capacity*" column, input the desired capacity.
 - Under the "*Losses*" column, input the values of "Loss Coefficient" specified in Table XV. Leave the default location of the tank (outdoor).
 - Under the "*Operating Temperatures*" column, input as "*Base Temperature*" 200 °F, and in "*Temp. Range*" input 30 °F.

Appendix C (continued)

- Hit Done.

Remember, in the case of a hot thermal storage coupled to a trigeneration system, the absorption chiller capacity must be correctly selected based on the "*Electric Generator Capacity*" and on the "*Thermal Storage Capacity*". The user could use the values provided in Table XXIII.

Appendix D

LIST OF SYMBOLS

Symbol	Definition
F_B	Boiler fuel consumption
F_{PM}	Prime mover (gas turbine) fuel consumption
$Q_{rec.}$	Recovered heat
$Q_{abs.}$	Cooling load satisfied by the absorption chiller
E_{PM}	Electricity produced by the prime mover
$E_{pur.}$	Electricity purchased
η_B	Efficiency of the boiler
COP	Coefficient of performance of the electric chiller
η_{CHP}	CHP efficiency
η_{CCHP}	CCHP efficiency
η_{FERC}	FERC efficiency standard
η_{TES}	TES efficiency
PRSEC	Percentage Reduction Source Energy Consumption
PRSEC_{GT}	Percentage Reduction Source Energy Consumption - Gas Turbine

CITED LITERATURE

1. Haefke, C. and Cuttica, J.: *Market sector fact sheet: Combined heat and power in hospitals*. US DOE CHP Technical Assistance Partnership, 2013.
2. Bourgeois, T., Dillingham, G., Panzarella, I., and Hampson, A.: *Combined heat and power: Enabling resilient energy infrastructure for critical facilities*. ICF International Paper, 2013.
3. Svico, N.: *Simulation of cogeneration system with a molten carbonate fuel cell*. Master's thesis, Politecnico di Torino, 2017.
4. Ciccirella, F.: *Simulation of Emerging Smaller-Scale Tri-Generation Systems* Master's thesis, Politecnico di Torino, 2015.
5. Galli, P.: *Simulation of a Small Scale Co-generation System Using a Microturbine*. Master's thesis, Politecnico di Torino, 2014.
6. Bonnema, E., Studer, D., Parker, A., Pless, S., and Torcellini, P.: *Large hospital 50% energy savings: Technical support document*. National Renewable Energy Laboratory, 2010.
7. ANSI/ASHRAE: *Standard 90.1-2004, standard methods of determining, expressing and comparing building energy performance and greenhouse gas emissions*. American Society of Heating, Refrigerating and Air-Conditioning Engineers, Inc, 2010.
8. ASHRAE: *Standard 169-2006, weather data for building design standards*. American Society of Heating, Refrigerating and Air Conditioning Engineers, Inc., 2006.
9. Hirsch, J. and et al.: *eQuest[®] user manual: topics*. Building Energy Use and Analysis Program, 3, 2006.
10. Solar turbine: *Turbomachinery systems for oil and gas application*. Retrived from <https://mysolar.cat.com> on 02/20/2018, 2011.
11. Solar turbines: *Solar turbine - product support*. Retrived from <https://mysolar.cat.com> on 02/20/2018, 2011.

CITED LITERATURE (continued)

12. ISO International Organization for Standardization: *Iso 3977-2: Gas turbines-part 2: Standard reference conditions and ratings*. 1997.
13. Darrow, K., Tidball, R., and Hampson, A.: *Catalog of CHP Technologies*. Retrieved from <https://www.epa.gov> on 02/02/2018, 2017.
14. Haefke, C.: *Combined Heat and Power (CHP) for Healthcare*. US DOE CHP Technical Assistance Partnership, 2016.
15. Babus' Haq, R., Probert, S., and O' Callaghan, P.: *Assessing the prospects and commercial viabilities of small-scale chp schemes*. *Applied energy*, 31(1):19–30, 1988.
16. Al-Sulaiman, F. A., Hamdullahpur, F., and Dincer, I.: *Trigeneration: a comprehensive review based on prime movers*. *International journal of energy research*, 35(3):233–258, 2011.
17. Maurstad, O.: *An overview of coal based integrated gasification combined cycle (IGCC) technology*. MIT - Laboratory for Energy and the Environment, 2005.
18. YORK: *Millennium yia single-effect absorption chillers*. Retrieved from <http://www.johnsoncontrols.com/> on 02/20/2018, 2012.
19. YORK: *Isoflow single-effect absorption chillers*. Retrived from <http://www.johnsoncontrols.com/> on 02/20/2018, 2012.
20. Standard, ARI: *550/590-2003. Performance rating of water-chilling packages using the vapor compression cycle*. Air-conditioning and Refrigeration Institute, 2003.
21. Jackson, T.: *CHP Installation Keeps Hospital Running During Hurricane Harvey*. Retrieved from <https://www.energy.gov> on 01/18/2018, 2017.
22. ASHRAE: *Standard 105-2004, energy standard for buildings except low rise residential buildings*. American Society of Heating, Refrigerating and Air-Conditioning Engineers, Inc, 2010.
23. Dincer, I., and Rosen, M. A.: *Thermal Energy Storage : Systems and Applications*. Wiley, 2011.
24. Schmidt, F. W., and Willmott., A. J.: *Thermal energy storage and regeneration*. Hemisphere Pub. Corp., 1981.

CITED LITERATURE (continued)

25. Beckmann, G. , and Gilli, P.V.: *Thermal energy storage : basics-design-applications to power generation and heat supply*. Springer-Verlag, 1984.
26. Tomlinson, J.J., and Kannberg,L.D.: *Thermal energy storage*. Mechanical Engineering, 1990.
27. Spakovszky, Z.S.: *Thermodynamics and Propulsion*. Retrieved from <http://web.mit.edu> on 02/10/2018, 2002.
28. Engineering ToolBox: *Convective Heat Transfer*. Retrieved from <https://www.engineeringtoolbox.com> on 02/10/2018, 2003.
29. Advance Tank: *Thermal Energy Storage systems for industrial applications. 2017 Advance Tank Catalog*. Retrieved from <http://advancetank.com> on 02/01/2018, 2017.
30. Zhang, Y., Wang, X., Zhuo, S., and Zhang, Y.: *Pre-feasibility of building cooling heating and power system with thermal energy storage considering energy supply–demand mismatch*. *Applied Energy* 167, 125–134, 2016.
31. Sieniutycz, S., and Jezowski, J.: *Energy Optimization in Process Systems*. Elsevier Science [Imprint], 2009.
32. Tehrani S., M., Saffar-Avval, M., Kalhori, S., B., Mansoori, Z., and Sharif, M.: *Hourly energy analysis and feasibility study of employing a thermocline TES system for an integrated CHP and DH network*. *Energy Conversion and Management* 68, 281–292, 2013.

VITA

NAME Luca Romano

EDUCATION

Master of Science in Mechanical Engineering,
University of Illinois at Chicago, USA, August 2018

Master of Science in Energy and Nuclear Engineering,
Polytechnic of Turin, Italy, September 2018

Bachelor of Science in Mechanical Engineering,
Polytechnic of Milan, Italy, September 2016

SCHOLARSHIPS Thesis under request scholarship, 2017-2018
